UNIVERSITY OF OKLAHOMA

GRADUATE COLLEGE

CONTEMPORARY DROUGHT MONITORING WITH THE STANDARDIZED PRECIPITATION INDEX: EVALUATING THE EFFECT OF NONSTATIONARY PRECIPITATION REGIMES IN THE CONTIGUOUS UNITED STATES ON THE CHARACTERIZATION OF DROUGHT

A DISSERTATION

SUBMITTED TO THE GRADUATE FACULTY

in partial fulfillment of the requirements for the

Degree of

Doctor of Philosophy

By

DANIELA MARIA SPADE
Norman, Oklahoma
2024

CONTEMPORARY DROUGHT MONITORING WITH THE STANDARDIZED PRECIPITATION INDEX: EVALUATING THE EFFECT OF NONSTATIONARY PRECIPITATION REGIMES IN THE CONTIGUOUS UNITED STATES ON THE CHARACTERIZATION OF DROUGHT

A DISSERTATION APPROVED FOR THE
DEPARTMENT OF GEOGRAPHY AND ENVIRONMENTAL SUSTAINABILITY

BY THE COMMITTEE CONSISTING OF

Dr. Mark Shafer, Chair

Dr. Yang Hong

Dr. Renee McPherson

Dr. Todd Fagin

Dr. Michael Wimberly

ACKNOWLEDGEMENTS

I would like to sincerely thank my family and friends who supported and encouraged me over the past several years. Especially my dad, David Spade, and my dear friend and mentor, Kris Bowline. You two saw me across the finish line and refused to give up on me. Finishing this degree would not have happened without you two in my corner. Thank you as well to my mom, Maria, and my brother and sisters – Alex, Emilia, and Roxy, who have always been supportive and encouraging throughout my time in school. And a giant hug and thank you to Seth for your endless patience with my hectic schedule and for believing in and encouraging me, no matter the challenge I am facing.

I would also like to thank all my supportive cycling friends, especially Greg and Jackie Grosshans, my teammate Lori Boren Mayse, Dr. Brian Johnson, Dr. Billy Lee Crynes, Dr. Michelle Busch, and Dr. Karelia LaMarca. Thank you all so much for your enduring encouragement and support!

Thank you as well to my current and previous advisors who mentored me throughout this process. Especially Dr. Kirsten de Beurs and Dr. Mark Shafer, who took me under their wing and provided the guidance I needed to complete my dissertation research. I have learned so much from you both and am grateful for your mentorship. I would also like to thank my committee – Drs. Renee McPherson, Michael Wimberly, Todd Fagin, and Yang Hong – for their insight and patience throughout my time as a student. Thank you as well to the Department of Geography and Environmental Sustainability for giving me this opportunity and for remaining my advocate throughout my tenure as a graduate student. Thank you as well to Dr. Jay (Joshua) Wimhurst, who was very generous with their time and helped me through my coding roadblocks.

Finally, I would like to thank my employer, the Center for Spatial Analysis, for funding the completion of this degree and for showing unwavering patience and support over the past few years. Thank you especially to Dr. Jeffrey Widener for ensuring my degree funding, Leah Nash for never pressuring me and always remaining encouraging and supportive, and Dr. Todd Fagin, who encouraged me to finish after I was set on leaving the program. A huge thank you as well to my coworker, Candace Perry. Watching you complete your degree while remaining a powerhouse in the office has been immensely inspirational!

TABLE OF CONTENTS

ABSTRACT

This dissertation examines the impact of shifting climatic conditions on the accuracy and reliability of drought characterization in the contiguous United States using the Standardized Precipitation Index (SPI). Each chapter employs climate divisional precipitation data from the U.S. Climate Divisional Database to investigate the dynamics of drought and pluvial events using various 30- to 60-year climatological reference periods.

Chapter 2 investigates discrepancies found in NOAA's Climate Divisional SPI Dataset, revealing significant over- and underestimations of drought frequency, suggesting the presence of bias towards drought or pluvial conditions in certain regions. Chapter 3 explores how the choice of climatological reference period influences the SPI's characterization of drought and pluvial occurrence and severity, highlighting the sensitivity of drought indices to their underlying climatological reference periods.

Chapter 4 expands on the operational drought monitoring implications of transitioning between reference periods with differing precipitation regimes. Through comprehensive analyses and comparisons against various climatological reference periods, this dissertation uncovers critical insights into the SPI's performance and its dependence on precipitation regimes. The results of this dissertation emphasize the need for adaptive strategies in drought monitoring against the backdrop of a changing climate.

CHAPTER 1: INTRODUCTION

Droughts are among the most damaging and costly natural disasters, posing a major threat to agricultural industries, socio-economic development, and the environment. Drought vulnerability in the United States is increasing due to numerous factors such as population growth and shifting populations to water scarce regions, land-use changes, increased water demand, and a changing global climate (Wilhite et al., 2014). Further, droughts are among the most complex of natural hazards, because unlike other natural hazards such as hurricanes or tornadoes, droughts do not have a definitive onset or ending, their emergence and recession tend to be very slow, their effects manifest in a multitude of ways that impact every aspect of the hydrologic cycle, and they are regionally subjective. A drought in the northeastern U.S. would likely still yield above average precipitation values in the desert southwest, for example. Thus, despite the seemingly straightforward nature of drought, its complexities render the phenomenon as one of the most difficult natural hazards to monitor, notably as it pertains to operational drought monitoring.

The complexity of drought is further illustrated by the vast network of indicators, indices, and monitoring systems currently used to evaluate its effects on key components of the hydrologic cycle. For instance, not only are there over 150 conceptual definitions of drought identified in the scientific literature (Wilhite and Gantz, 1985), but the World Meteorological Organization (WMO) and Global Water Partnership's (GWP) handbook describing "some of the most commonly used" operational drought monitoring indices and indicators in use today provides an overview of 50 different monitoring tools (WMO and GWP, 2016). Further, Niemeyer (2008) identified over 150 drought indices in use, and Zargar et al. (2011) reviewed 74 drought indices to provide researchers with a comprehensive description of select drought monitoring tools. Undoubtedly, drought indices are indispensable both operationally and in the research setting as

they provide quantitative measures of drought onset, recession, and severity, but should the list of indices be this extensive? Is it helpful to have such a large selection of tools that are all geared toward the common goal of quantifying differing characteristics of drought? The complexity of drought as well as the wide range of economic sectors impacted partially explains the many quantitative measures of drought (Heim, 2002). Nonetheless, a percentage of indices published in scientific literature appear more closely aligned with academic pursuit rather than with the practitioner in mind.

Niemeyer (2008) argues that the "market of drought indices is slowly saturating", stating that most progress in the development of new indices is related to the emerging availability of novel remote sensing information such as development of single new sensors and the combination of different sensors. Zargar et al. (2011) came to a similar conclusion, attributing the ever-increasing number of published drought indices to technological development, notably in the field of remote sensing. Nonetheless, attempting to develop or identify a universal drought index is as fruitless as attempting to develop a universal conceptual definition of drought.

Heim's review of twentieth century drought indices suggests that the count of indices has increased both with the availability of new data sources and in response to an improved understanding of drought (Heim, 2002). As it pertains to the latter, the continued development of new drought indices is logical. However, the present study argues that, rather than investing resources in the continued development of additional drought indices as new datasets become available, the drought monitoring and research community should instead focus on improving the most pervasive operational drought indices in accordance with our improved understanding of drought and our climate system. For example, Wells et al. (2004) improved upon the Palmer

Drought Severity Index (PDSI) by replacing the empirical constants in the PDSI's computation with dynamically calculated values, thereby making the index (named the self-calibrating PDSI or sc-PDSI) spatially comparable. Vicente-Serrano et al. (2010) offered an improvement in the sc-PDSI in their development of the Standardized Precipitation Evapotranspiration Index (SPEI). Like the sc-PDSI, the SPEI also involves a climatic water balance, however unlike the sc-PDSI, the SPEI is multi-scalar which is imperative in operational drought monitoring.

More recently, studies have begun to contend with the issue of stationarity, or the lack thereof, in the realm of drought monitoring. Stationarity is the assumption that environmental variables fluctuate within a static envelope of variability and can be modeled with a time-invariant probability density function that is estimated from the instrumental record (Milly et al., 2008). The assumption of stationarity is readily apparent in indices such as the Standardized Precipitation Index (SPI), which is a key tool used for operational drought monitoring (Svoboda et al., 2002; NOAA NCEI, 2024) and one which references a pre-defined and climatically representative base period.

The SPI was developed by McKee et al. (1993) and is based on the probability of accumulating a given amount of precipitation over a specified timeframe, relative to the base period. The SPI is essentially a z-score, thus moisture anomalies are defined in terms of the number of standard deviations either above or below the base period's average – an SPI value of zero signifies the average precipitation amount, and the index becomes more negative (positive) as drought (pluvial) conditions become more severe. Since its development in the early 1990s, the SPI has been adopted as a key tool for operational drought monitoring (Svoboda et al., 2002; NOAA NCEI, 2024).

The SPI is well established not only as an operational tool but also in the research setting. From investigating the effect of timescale on the spatial patterns of drought frequency and duration (Kangas and Brown, 2007), to constructing a global drought frequency dataset (Spinoni et al., 2014) or exploring the spatiotemporal variabilities of drought severity (Livada and Assimakopoulos, 2007), the SPI has proven to be a statistically robust research tool. Wu et al. (2007) investigated how regional climatologies impact the underlying statistics of the SPI, while Wu et al. (2005) investigated whether the length of record of the underlying base period impacts the SPI. Guttman (1999) and Quiring (2009) investigated the effect that the probability density function used for normalizing precipitation has on the SPI.

In the context of climate non-stationarity, the impact that the underlying base period has on the characterization of drought according to the SPI has been investigated. Thomas et al. (2023) found that updating the base period from 1981-2010 to 1991-2020 resulted in fewer but more severe precipitation extremes. Cammalleri et al. (2022) evaluated the impact of transitioning from the 1981-2010 base period to the 1991-2020 base period on the value of the SPI, finding that drought classification changed in accordance with changing the base period.

Other studies have addressed the impact of a nonstationary climate on drought monitoring through adjusting the computational approach of the SPI. Stagge and Sung (2022), for example, used Bayesian splines to develop a nonstationary SPI model that could measure drought relative to a changing climate. However, novel approaches such as that suggested by Stagge and Sung (2022) would necessitate a significant change in the established drought monitoring practices. For this reason, other studies have advocated for the continued use of the 30-year moving window approach as it simultaneously captures climate non-stationarity while also leveraging the

existing infrastructure for drought monitoring (Hoylman et al., 2022).

This study investigates the dynamic nature of drought monitoring with the SPI within the context of nonstationary precipitation regimes. Specific research questions in this study include the following:

- How do operational SPI databases, such as those maintained by the National Centers for Environmental Information (NCEI), compare to research SPI databases?
- Does the choice of base period alter the severity and frequency of drought and pluvial events captured by the SPI?
- How does transitioning between base periods with overlapping precipitation data impact contemporary drought characterization?

The SPI is calculated using monthly average precipitation data at the climate division scale from the U.S. Climate Divisional Dataset. This dataset was selected because it offers a long-term, serially complete record of precipitation data for the contiguous U.S., with data spanning from 1895 – present. The nClimDiv dataset is also spatially coherent, making it an optimal tool to study large scale features such as drought. Chapter 2 provides a comprehensive overview of the SPI computational procedure and explores inconsistencies uncovered in the NOAA/NCEI SPI database. Chapter 3 delves into the effect that a changing climate has on the SPI by leveraging a series of 30-year moving windows to characterize modern-day drought conditions. The precipitation regimes for the six regions of the contiguous United States are deconstructed in order to elaborate on the base period's impact on the characterization of drought by the SPI. Chapter 4 investigates the operational impacts of transitioning between base periods with differing precipitation regimes. The study concludes in Chapter 5 with a summary of key

findings, a discussion of this study's limitations, and recommendations for future work and best practices based on the results of this study.

References

Cammalleri, C., J. Spinoni, P. Barbosa, A. Toreti, and J. V. Vogt, 2022: The effects of non-stationarity on SPI for operational drought monitoring in Europe. Int. J. Climatol., 42, 3418–3430, https://doi.org/10.1002/joc.7424.

——, 1999: Accepting the standardized precipitation index: A calculation algorithm. J. Amer. Water Resour. Assoc., 35, 311–322, https://doi.org/10.1111/j.1752-1688.1999.tb03592.x.

Heim, R. R., 2002: A Review of Twentieth-Century Drought Indices Used in the United States. Bull. Amer. Meteor. Soc., 83, 1149–1166, https://doi.org/10.1175/1520-0477-83.8.1149.

Hoylman, Z.H., R.K. Bocinsky, K.G. Jencso, 2022: Drought assessment has been outpaced by climate change: Empirical arguments for a paradigm shift. Nature Communications, 13, p. 2715

Kangas, R., and T. Brown, 2007: Characteristics of US drought and pluvials from a high-resolution spatial dataset. Int. J. Climatol., 27, 1303–325, https://doi.org/10.1002/joc.1473.

Livada, I., and V. D. Assimakopoulos, 2007: Spatial and temporal analysis of drought in Greece using the standardized precipitation index (SPI). Theor. Appl. Climatol., 89, 143–153, https://doi.org/10.1007/s00704-005-0227-z.

McKee, T. B., N. J. Doesken, and J. Kleist, 1993: The relationship of drought frequency and duration to time scales. Eighth Conf. on Applied Climatology, Anaheim, CA, Amer. Meteor. Soc., 179–186. Svoboda, M., and Coauthors, 2002: The Drought Monitor. Bull. Amer. Meteor. Soc., 83, 1181–1190, https://doi.org/10.1175/1520-0477-83.8.1181.

Milly, P. C. D. et al., 2008: Stationarity Is Dead: Whither Water Management? Science 319, 573-574 DOI:10.1126/science.1151915

Niemeyer, S., 2008: New drought indices. Options Méditerranéennes. Série A: Séminaires Méditerranéens, 80, pp.267-274.

NOAA National Centers for Environmental Information, Monthly Drought Report for July 2023, published online August 2023, retrieved on March 18, 2024 from https://www.ncei.noaa.gov/access/monitoring/monthly-report/drought/202307

Quiring SM., 2009: Developing objective operational definitions for monitoring drought. J Appl Meteorol Climatol. 48: 1217–29. http://journals.ametsoc.org/doi/abs/10.1175/2009JAMC2088.1.

Spinoni, J., Naumann, G., Carrao, H., Barbosa, P., and Vogt, J., 2014: World drought frequency, duration, and severity for 1951–2010. Int. J. Climatol., 34 (8), 2792-2804.

Stagge, J. H., and K. Sung, 2022: A Nonstationary Standardized Precipitation Index (NSPI) Using Bayesian Splines. J. Appl. Meteor. Climatol., 61, 761–779, https://doi.org/10.1175/JAMC-D-21-0244.1.

Svoboda, M., LeComte, D., Hayes, M., Heim, R., Gleason, K., Angel, J., Rippey, B., Tinker, R., Palecki, M., Stooksbury, D., Miskus, D., and Stephens, S., 2002. The Drought Monitor. *Bull. Amer. Meteor. Soc.*, **83**, 1181-1190. https://doi.org/10.1175/1520-0477- 83.8.1181.

Thomas, N. P., Marquardt Collow, A. B., Bosilovich, M. G., & Dezfuli, A., 2023: Effect of baseline period on quantification of climate extremes over the United States. Geophysical Research Letters, 50, e2023GL105204. https://doi.org/10.1029/2023GL105204

Vicente-Serrano, S. M., Beguería, S. & López-Moreno, J. I, 2010: A multiscalar drought index sensitive to global warming: the standardized precipitation evapotranspiration index. J. Clim. 23, 1696–1718.

Wells, N., Goddard, S. and Hayes, M.J., 2004: A self-calibrating Palmer drought severity index. Journal of climate, 17(12), pp.2335-2351.

Wilhite, D.A. and Glantz, M.H., 1985: Understanding: the drought phenomenon: the role of definitions. Water international, 10(3), pp.111-120.

——, Sivakumar, M.V. and Pulwarty, R., 2014: Managing drought risk in a changing climate: The role of national drought policy. Weather and climate extremes, 3, pp.4-13.

World Meteorological Organization (WMO) and Global Water Partnership (GWP), 2016: Handbook of Drought Indicators and Indices (M. Svoboda and B.A. Fuchs). Integrated Drought Management Programme (IDMP), Integrated Drought Management Tools and Guidelines Series 2. Geneva.

Wu, H., M. J. Hayes, D. A. Wilhite, and M. D. Svoboda, 2005: The effect of length of record on the standardized precipitation index. Int. J. Climatol., 25, 505–520, https://doi.org/10.1002/joc.1142.

——,M. D. Svoboda, M. J. Hayes, D. A. Wilhite, and F. Wen, 2007: Appropriate application of the standardized precipitation index in arid locations and dry seasons. Int. J. Climatol., 27, 65–79, https://doi.org/10.1002/joc.1371.

Zargar, A., Sadiq, R., Naser, B., and Khan, F., 2011: A review of drought indices. Environmental Reviews. 19 (NA): 333-349. https://doi.org/10.1139/a11-013

CHAPTER 2: MAJOR OVER- AND UNDERESTIMATION OF DROUGHT FOUND IN NOAA'S CLIMATE DIVISIONAL SPI DATASET

Abstract: Evaluation of the standardized precipitation index (SPI) dataset published monthly in the National Oceanic and Atmospheric Administration/National Centers for Environmental Information (NOAA/NCEI) climate divisional database revealed that drought frequency is being mischaracterized in climate divisions across the United States. The 3- and 6-month September SPI values were downloaded from the database for all years between 1931 and 2019; the SPI was also calculated for the same time scales and span of years following the SPI method laid out by NOAA/NCEI. Drought frequency is characterized as the total number of years that the SPI fell below 21. SPI values across 1931–90, the calibration period cited by NOAA/NCEI, showed regional patterns in climate divisions that are biased toward or away from drought, according to the average values of the SPI. For both time scales examined, the majority of the climate divisions in the central, Midwest, and northeastern United States showed negative averages, indicating bias toward drought, whereas climate divisions in the western United States, the northern Midwest, and parts of the Southeast and Texas had positive averages, indicating bias away from drought. The standard deviation of the SPI also differed from the expected value of 1. These regional patterns in the NCEI's SPI values are the result of a different (sliding) calibration period, 1895–2019, instead of the cited standardized period of 1931–90. The authors recommend that the NCEI modify its SPI computational procedure to reflect the best practices identified in the benchmark papers, namely, a fixed baseline period.

2.1 Introduction

a. Overview

The standardized precipitation index (SPI) is a probability-based moisture index designed to measure whether moisture conditions are normal, abnormally dry, or abnormally wet, relative to a predefined calibration, or base, period. The SPI was developed by McKee et al. (1993) to address the need for a drought index that had few data requirements and that accommodated for the fact that our key usable water sources (soil moisture, groundwater, snowpack, streamflow, and reservoir storage) respond to moisture deficits and the eventual arrival of precipitation on a distinct time scale. The SPI is based on the probability of accumulating a given amount of precipitation in a specified period of time, ranging from 1 to 24 months, relative to a predefined base period. The acquired cumulative probability values associated with each precipitation value are converted to the standard normal random variable Z, which allows for the estimation of both dry and wet conditions. Because the SPI is based on the standard normal distribution, an SPI value of zero signifies the average precipitation amount, relative to the base period, and the index becomes more negative or positive as dry or wet conditions, respectively, become more severe (Svoboda et al. 2012).

Despite its computation, the SPI can be nonnormally distributed. For example, the SPI becomes lower bounded and therefore nonnormally distributed when there is a high frequency of no precipitation (i.e., values of zero) because this reduces the size of the dataset used to construct the SPI (Wu et al. 2007). The size of the dataset is a key limitation in the ability of the SPI to accurately portray drought/wet conditions because it is a probability-related index; the parameters of the SPI's underlying probability distribution are sensitive to the length of record, particularly if the precipitation pattern changes between lengths of record (Guttman 1994; Wu et al. 2005). Hence, in arid climates or those climates with a distinct seasonality to the precipitation

regime, the SPI is prone to erroneous results and must be used with caution. Nonetheless, the SPI offers several advantages for operational use, including the fact that it requires only precipitation data to be computed, it can be calculated at various time scales, enabling it to capture both short and long-term drought and abnormal wetness, and it is normalized with respect to location, allowing it to be comparable across regions with different climates (Keyantash and NCAR Staff 2018). For these reasons, the SPI is widely used operationally in the United States. For example, it is one of the key drought indicators used by the U.S. Drought Monitor (USDM), which is considered to be the standard for operational drought monitoring in the United States (Svoboda et al. 2002). Similarly, the National Centers for Environmental Information (NCEI), formerly called the National Climatic Data Center, releases monthly State of the Climate Reports that provide detailed drought discussions according to what is indicated by the climate divisional SPI and Palmer drought index, among other drought indicators, available through the NOAA/NCEI climate divisional database (nClimDiv; Vose et al. 2014a). Furthermore, in 2011 the SPI was recommended through the Lincoln Declaration on Drought as the internationally preferred index to be used by all national meteorological and hydrological services to characterize meteorological droughts (Hayes et al. 2011). Modest data requirements and temporal flexibility of the SPI make it also popular in a research setting. Kangas and Brown (2007) used the SPI at various accumulation periods to investigate the effect of time scale on the spatial patterns of drought frequency and duration. Spinoni et al. (2014) used the 12-month SPI to construct a global drought frequency dataset, with the 12-month accumulation period accommodating the various precipitation regimes around the world. Using the 3-, 6-, and 12-month SPI, Livada and Assimakopoulos (2007) explored the spatiotemporal variability of drought intensity and duration in Greece. Furthermore, the temporal flexibility of the SPI also helped Guttman (1999) clarify

the time scale associated with the Palmer drought index. The objectives of this study stem from an analysis of drought frequency according to the USDM dataset. During the analysis of the SPI, which is one of the drought indicators examined by the authors of the USDM to construct the weekly USDM maps, inconsistencies were identified between the theoretical drought frequency values for a normalized index and the drought frequency values obtained from the NCEI's SPI dataset, prompting a careful examination of the dataset across its 1931–90 calibration period (see the NCEI document found online at ftp://ftp.ncdc.noaa.gov/pub/data/cirs/climdiv/divisional-readme.txt). Specifically, the objectives of this study are to demonstrate that the NCEI's SPI dataset is not in agreement with the standard normal distribution across the calibration period according to the average and standard deviation of each climate division's SPI value across that period. This was found to impact the characterization of drought frequency throughout the contiguous United States across the base period. Consultation with the point of contact for the NCEI's drought datasets revealed that the NCEI's SPI values do not align with the standard normal distribution because the NCEI uses a sliding calibration period, 1895–2019, instead of the cited standardized period of 1931–90. The following subsection provides background information on the SPI; sections 2 and 3 are dedicated to this study's data and methods, respectively; section 4 provides the results and section 5 documents studies that have utilized the NOAA/NCEI SPI dataset in recent years. Section 6 provides a brief summary of the results and conclusions.

b. Background on the SPI

The SPI is a Z-score-like measurement of accumulated precipitation, identifying the number of standard deviations above or below the mean (precipitation) of the base period. Positive SPI values indicate greater than average precipitation and negative values indicate less than average

precipitation. Figure 1 illustrates the relationship of the SPI to the standard normal distribution and following the statistical theory of the normal distribution, it demonstrates that a location is expected to be on the dry end of the spectrum 16% of the time and on the wet end of the spectrum 16% of the time. Note that an SPI value between -1 and 1 is considered neutral; a value less than -1 is considered to be dry; a value greater than 1 is considered to be wet.

[Figure 1]

Because precipitation frequency distributions typically are not normally distributed, several statistical procedures are used to transform accumulated precipitation values to an SPI. The basic workflow first involves the selection of a precipitation accumulation period, which is directly relevant to the type of drought one is interested in identifying. For instance, the 3-month SPI is a viable accumulation period in the analysis of agricultural or soil moisture drought (Svoboda et al. 2012). The 3-month SPI calculated for the month of May utilizes the total accumulated precipitation for March, April, and May. Next is the selection of a base period, which is a comparison period used to establish whether current conditions are normal, abnormally dry, or abnormally wet. The base period should ideally contain at least 30 years of continuous data that includes one long-term drought and one long-term wet period (Karl 1986; McKee et al. 1993; Edwards and McKee 1997). Guttman (1994) recommended that up to 80 years of data be used for reliable results in the estimation of extreme events. Following the selection of the accumulation and base periods, a probability density function is chosen that best fits the long-term precipitation dataset. The cumulative probability of each precipitation value is calculated using the estimated parameters associated with the probability density function for each time scale of interest (1-, 3-, 6-month, etc.). Last, an equiprobability transformation is made in order to convert the cumulative probability to the standard normal random variable Z with a mean of

zero and standard deviation of 1, yielding the SPI.

2.2 Data

NCEI SPI and precipitation

The contiguous United States consists of 344 climate divisions, with boundaries constructed through considerations of drainage basins, crop districts, climatic conditions, and county lines; each state contains between 3 and 10 climate divisions (Guttman and Quayle 1996). Divisional values of temperature and precipitation, from which the drought indices published in nClimDiv are derived, are estimated from area-weighted averages of grid point estimates that are interpolated from station data (Vose et al. 2014b). Climate divisional dataset files are available for download in ‘‘TXT,’’ ‘‘MAP,’’ and ‘‘KMZ’’ file formats.

SPI datasets were downloaded at 3- and 6-month time scales for the 48 contiguous United States from nClimDiv for all years from 1931 to 2019. The 3- and 6-month SPI time scales were selected for their relevance in capturing the short- and medium-term drought conditions (i.e., agricultural and meteorological drought) that impact the United States, and also because they are among the time scales used by NOAA/NCEI (hereinafter NCEI) to issue monthly State of the Climate Reports. The SPI at each time scale was downloaded using September as the ending period for the moving-total precipitation. September was selected to investigate end-of-water-year drought conditions.

Precipitation data were downloaded for each climate division to calculate the 3- and 6-month September SPI. The NCEI cites a base period of 1931–90 for all drought data posted in the nClimDiv database and this base period is also used in the calculated SPI dataset for consistency.

2.3 Methods

a. SPI computational procedure

The NCEI precipitation data are used to calculate the SPI. The NCEI fits monthly climate

division precipitation data to the Pearson type-III (PE3) probability density function for all precipitation values x > 0:

$$f(x) = \frac{(x-\xi)^{\alpha-1} exp-(x-\xi)/\beta}{\beta^{\alpha}\Gamma(\alpha)} \quad (1)$$

for $\gamma > 0 \; and \; \xi \leq x < \infty$

and

$$f(x) = \frac{(\xi-x)^{\alpha-1} exp-(\xi-x)/\beta}{\beta^{\alpha}\Gamma(\alpha)} \quad (2)$$

for

$\gamma \; < \; 0 \; and \; -\infty < x \leq \xi$

where α, β, and ξ are the shape, scale, and location parameters, respectively, and are respectively given by

$$\alpha = \frac{4}{\gamma^2}, \quad (3)$$

$$\beta = 12\sigma|\gamma| \quad (4)$$

and

$$\xi = \mu - 2\sigma/\gamma \quad (5)$$

The Γ(α) in Eqs. (1) and (2) denotes the gamma function (GAM). The method of L-moments is used by the NCEI for estimation of the PE3's location, shape, and scale parameters. The Fortran computer program SPICOMPUTE by N. Guttman outlines the computational procedure used to obtain the NCEI SPI values and can be found online (http://www1.ncdc.noaa.gov/pub/data/software/palmer/spi.f). Here, the same probability density function and SPI computational procedure outlined in SPICOMPUTE are applied. See appendix B for a thorough description of the SPI computational procedure using the PE3 distribution and

the method of L-moments for parameter estimation.

While the SPI is unbounded in theory, Guttman (1999) recommends truncating the cumulative probabilities from 0.001 to 0.999, which bounds the SPI between ±3.09. The estimation of extreme probabilities based on sample sizes < 100 may not be reliable. These bounds are enforced in the SPICOMPUTE FORTRAN code and are also applied in this study's method for consistency.

The ability of the PE3 probability distribution to accurately model the precipitation time series was evaluated using a two-sample Kolmogorov–Smirnov test and Pearson's chi-squared test, with a null hypothesis that the data comes from the normal probability distribution, at a significance level of 0.05.

b. Evaluation of the NCEI SPI against the derived PE3 SPI

To understand how the downloaded SPI values compared with the PE3-calculated SPI values based on the NCEI's precipitation data, several different experiments were designed.

1.) Comparison of the average and standard deviation of SPI

At each time scale and for each climate division, the average and standard deviation of the downloaded and calculated SPI values are taken across the base period. These values are expected to come out to 0 and 1, respectively, in accordance with the standard normal distribution. These criteria are used to determine whether or not a climate division's SPI time series agrees with the standard normal distribution. Average values below −0.01 are considered to be negatively biased, and values above 0.01 are considered to be positively biased. Likewise, a standard deviation below 0.99 represents a precipitation regime with a narrower distribution than the standard normal distribution, whereas a value above 1.01 is a wider distribution. This study compares the average and standard deviation of the NCEI SPI and the calculated SPI, based on

the PE3 distribution, for all climate divisions. Note that the expectation is that all means are 0 and all standard deviations are 1. In addition, it is expected that the NCEI SPI and the PE3 SPI values be identical because of the reported NCEI SPI calculation method.

The impact on drought detection of a climate division with a negative average SPI value across the base period is that the climate division is biased toward indicating drought conditions. In contrast, a positive average SPI value indicates the climate division is biased away from drought, meaning it is more difficult for the index to detect genuine drought in that climate division (Figs. 2a, b, respectively). The impact on drought detection of a climate division with a wider distribution than the standard normal distribution (i.e., a standard deviation greater than 1) is that it is more difficult for the index to move between levels of drought than it would be if the distribution was truly normal (Fig. 2c). Likewise, the impact on drought detection of having a standard deviation below 1 is that it is overly easy for the index to move between levels of drought intensity (Fig. 2d). In statistical terminology, these adjustments to the distribution width represent changes to the kurtosis of the distribution.

[Figure 2]

2.) Comparison of NCEI SPI and PE3 SPI by climate division across time

Three scatterplots were created using the 6-month NCEI SPI dataset plotted against the calculated 6-month SPI dataset. A scatterplot was created for a climate division with a negative average, a climate division with a positive average and a climate division with an average of 0 across the base period. Each scatterplot consists of 120 points, 60 for each dataset. A regression analysis was performed with a significance level of 0.05 to determine a relationship between the two datasets. The purpose of this analysis was to determine how the NCEI dataset compares with the calculated dataset across the entire range of SPI values comprising the base period. For

brevity, these results focus on the 6-month SPI as the 3-month SPI results were effectively identical.

From the standard normal distribution (Fig. 1), it is expected that approximately 9 drought years occur (16% of the time) across the 60-yr base period for each climate division. The same is expected for abnormally wet conditions.

To quantify the differences between the SPI values downloaded from the nClimDiv database (hereinafter referred to as NCEI3 for the 3-month SPI and NCEI6 for the 6-month SPI) and the calculated SPI values (abbreviated Calc3 and Calc6), the difference is taken between the total number of dry or wet years among the two datasets:

$$NCEI3 - Calc3 \quad (6)$$

and

$$NCEI6 - Calc6 \quad (7)$$

A negative or positive value respectively indicates that more dry or wet years were estimated by the Calc SPI dataset, and a value of zero indicates that there is no difference between the two datasets.

2.4 Results

a. Goodness of fit

Goodness-of-fit tests were performed to confirm the normality of the Calc3 and Calc6 datasets. The goodness-of-fit tests were the Kolmogorov–Smirnov and Pearson's chi-squared tests. Hypothesis tests for these two approaches produced p values of 1 for every climate division and in every time scale analyzed, indicating the PE3 probability distribution successfully transforms the original precipitation time series into a normal distribution.

b. 1931–90 average and standard deviation of the SPI

If the NCEI3 data behave as expected, average SPI values should equal 0 with a standard

deviation of 1 for each climate division. Instead, this study found that 114 (33.1%) of the 344 climate divisions across the conterminous United States had a positive average SPI across the base period. The bulk of these climate divisions are concentrated across the western United States, with smaller groups of positive average values appearing along the Gulf Coast and Midwest (Fig. 3a). The same pattern is also shown by the NCEI6 data, although to a lesser extent, with 75 (21.8%) climate divisions showing a positive average (Fig. 3e). More climate divisions with negative averages were found across the base period [200 (56.1%) climate divisions in NCEI3 and 232 (67.4%) climate divisions in NCEI6]. The spatial pattern of negative averages is the same in both datasets—the majority of the climate divisions in the central and northeastern United States showed negative averages to varying extents.

[Figure 3]

The western United States shows the greatest grouping of positive averages whereas spatial grouping of negative averages is prevalent in the south-central, Midwest, and northeastern United States according to the NCEI3 and NCEI6 datasets.

Although the Calc3 and Calc6 datasets also contain climate divisions with averages that are different from 0 (Figs. 3c and 3g, respectively), the spatial patterns seen in NCEI3 and NCEI6 could not be replicated at either time scale. Rather, only 16 (4.7%) climate divisions with positive and 3 (0.9%) climate divisions with negative averages appear in the Calc3 dataset with 3 (0.9%) and 7 (2.0%) in the Calc6 dataset, when following the PE3 methodology. The spatial distribution of the climate divisions with averages different from zero according to the Calc3 and Calc6 datasets appears to be random, with some grouping of positive averages for climate divisions in Northern California and eastern Oregon.

Spatial grouping of standard deviations of the SPI values different from 1 across the base period

is also evident in the NCEI3 and NCEI6 datasets (Figs. 3b and 3f, respectively). In total, 107 (31.1%) climate divisions have distributions wider than the standard normal distribution and 196 (57.0%) have distributions narrower than the standard normal distribution according to the NCEI3 dataset. Similarly, 108 (31.4%) have distributions wider than the standard normal distribution and 201 (58.4%) climate divisions have distributions narrower than the standard normal distribution in the NCEI6 dataset. So, the two datasets exhibit very similar biases in the shapes of the SPI distributions, seemingly independent of the time scale. In both datasets, the standard deviation is above 1 in climate divisions in the western and midwestern United States. Interestingly, the northeastern United States switches between a standard deviation above 1 in the NCEI3 dataset to a value below 1 in the NCEI6 dataset, suggesting a seasonal component to the distributions. This is also seen in a group of climate divisions in Nevada, Utah, Idaho, and Oregon. Although not shown here, examination of the NCEI3 dataset for March and June also revealed a seasonal component in the spatial patterns of averages and standard deviations. This suggests that, according to the NCEI dataset, whether a climate division will be biased toward or away from drought is dependent on the ending period for the moving-total precipitation.

For many climate divisions across the United States in the Calc3 and Calc6 datasets, the standard deviation of SPI values also differs from 1, although to a greater degree in the NCEI datasets (Figs. 3d and 3h, respectively). In total this study found 54 (15.7%) climate divisions with a standard deviation wider and 164 (47.7%) with a standard deviation narrower than the standard normal distribution in Calc3; this study found 53 (163) climate divisions with a standard deviation wider (narrower) than the standard normal distribution in Calc6. As was the case for the mean SPI computations, the proportion of standard deviations above and below the reference value (i.e., 1) were very similar across the 3- and 6-month SPI periods. Thus, it does not appear

that the averaging period is responsible for the fluctuations. This is addressed further in the appendix. Nonetheless, regional patterns in the standard deviations above or below 1 are not seen in the Calc3 or Calc6 results.

c. Relationship between NCEI6 and Calc6, 1931–90

Figure 4 plots NCEI6 against the Calc6 dataset for climate divisions that have a negative average (Fig. 4a), positive average (Fig. 4b) and an average of zero (Fig. 4c) according to the NCEI6 dataset shown in Fig. 3a. The selected climate divisions are shown in bold in the map insets.

[Figure 4]

Figures 4a and 4b show disagreements between the NCEI6 and Calc6 datasets along the entire range of SPI values. There is a nearly 1:1 relationship between the two dataset values (correlation coefficient squared $R^2 = 0.99$), but the intercept is below (Fig. 4a) and above (Fig. 4b) zero with a slope less than 1. The fact that there is not a lot of variation along the regression lines indicates that the two SPI datasets were derived from the same underlying precipitation dataset, otherwise there would be more variation along the line. For the climate division in Nebraska (Fig. 4a), the intercept is −0.29 with a slope of 0.96, which is notably lower than 1. In terms of drought and wet events, this indicates that NCEI6 is underestimating the magnitude of precipitation events and overestimating the magnitude of drought events. For the climate division in Nevada (Fig. 4b), the intercept is 0.13 with a slope of 0.90, which is significantly lower than 1. In terms of drought and wet events, this indicates that NCEI6 is underestimating the magnitude of dry events and overestimating the magnitude of wet events. In contrast, the climate division in Oregon (Fig. 4c) shows a 1:1 relationship ($R^2 = 1$) with a regression line centered over zero and a slope equal to 1, indicating that NCEI6 and Calc6 are estimating dry and wet events at the same magnitude.

d. 1931–90 total number of dry and wet years

Climate divisions in the central, Midwest, and northeastern United States are dry biased with standard deviations greater than 1 according to the NCEI3 and NCEI6 datasets, making it more difficult for the SPI to detect wet conditions relative to the standard normal distribution. The effects of the dry bias in these regions are shown in Fig. 5a, which illustrates the total number of dry years that occurred across the 1931–90 base period according to the NCEI6 dataset. Unsurprisingly, each of the three regions exhibits a greater number of dry years than expected.

[Figure 5]

Climate divisions in the western, southeastern, and northern Midwest parts of the United States are biased away from drought (and toward wet conditions) with standard deviations less than 1 according to the NCEI6 dataset, making it more difficult for the SPI to detect dry conditions relative to the standard normal distribution. The effects of the wet bias in these regions are shown in Fig. 5d, which shows the total number of wet years that occurred across the 1931–90 base period according to the NCEI6 dataset. A greater number of wet years than would be expected is observed in many regions.

Because the SPI is a standardized index, each climate division should theoretically contain the same number of dry or wet years. According to the statistical theory of the standard normal distribution, each climate division should be on the dry end of the spectrum 16% of the time and on the wet end of the spectrum 16% of the time. This was found to be the case for the majority of the climate divisions based on the Calc6 dataset across the 1931–90 time period (Figs. 5b,e), wherein 219 climate divisions across the United States experienced dry conditions for the expected total of 8–10 dry years and 221 climate divisions experienced wet conditions for the expected total of 8–10 wet years across the 60-yr period. Although not shown here, 199 and 220

climate divisions contained the expected total number of dry and wet years, respectively, according to the Calc3 dataset. Figures 5c and 5f elucidate spatial differences between the total number of dry and wet years estimated by the two datasets (NCEI6–Calc6), and these differences arise in climate divisions with averages different from zero shown in Fig. 3e. Climate divisions with negative average values, such as those in the Midwest and southeast United States, estimated far more dry years than the Calc6 dataset; the northern Great Plains in particular estimated between 7 and 9 additional dry years (Fig. 5c). The same regions estimated far fewer wet years than the Calc6 dataset (Fig. 5f).

These results demonstrate the cumulative effect that the biased average and standard deviations in the NCEI6 dataset had on drought detection across the base period.

2.5 Discussion

Consultation with the point of contact for the nClimDiv database revealed that the NCEI's SPI values are dry/wet biased in this study's results because the dataset is in fact calibrated using the full period of record (here, 1895–2019) and not 1931–90. This moving-window approach to calibrating the data means that there is no fixed baseline associated with the dataset, the calibration period is updated every year. The lack of a baseline makes NCEI's SPI data unusable as a research dataset because the baseline is updated continuously as new data become available; consequently, it is impossible to accurately compare across studies as they each may be comparing against different historical records. Therefore, it becomes impossible to use the dataset to identify changes in frequency of occurrence or intensity of drought. For example, studies typically compare present anomalies with an established baseline to assess change, such as departure from 20th-century average (e.g., IPCC, National Climate Assessment, and NCEI State of the Climate Report).

Another concern is that calculating the SPI in such a fashion violates the formulation originally proposed by McKee et al. (1993), who recommended a recent climatic history as the basis for comparison to derive the SPI. Further, a fixed base period was used by Edwards and McKee (1997), who recommend a fixed calibration period containing at least one dry spell and one wet spell. The NCEI's approach does not follow this standard and users are not aware of the discrepancy because the online metadata associated with the product indicate that "all drought data are calibrated using the period 1931–1990." Consequently, the 1931–90 period was used to compare against the NCEI's SPI formulations in this study, which revealed the inconsistencies. However, other studies that did not conduct a validation of the NCEI dataset for the base period would be unaware that it lacks a fixed baseline.

A review of the literature identified several studies that have used the NCEI SPI dataset in recent years. Cumbie-Ward and Boyles (2016) used the climate divisional NCEI SPI dataset at various time scales and for all months across a 10-yr period ending in 2015 to make an objective analysis of the performance of an experimental high-resolution SPI dataset. Lu et al. (2019) used the NCEI SPI (1-, 2-, 3-, 6-, 9-, and 12-month time scales) as well as the NCEI Palmer drought indices in the derivation of an experimental monthly agricultural drought index across the 1895–2013 time period. In addition to product calibration and validation, the climate divisional SPI dataset has also been used in recent years to link groundwater levels with drought in the central United States (Whittemore et al. 2016; Leelaruban et al. 2017). Despite the fact that each of these studies downloaded the same datasets from the same data source, the authors are all analyzing a different set of SPI values because the calibration period is not fixed. For example, in 1934 climate division 2503 in Nebraska has a 6-month September SPI value of −1.35 based on a 1931–90 base period, −1.62 based on an 1895–2009 base period, and −1.58 based on an 1895–

2019 period. Thus, the only way for various research studies to be comparable would be if the respective authors happened to publish simultaneously.

2.6 Recommendations

The authors recommend that the NCEI modify its SPI computational procedure to reflect the best practices identified by McKee et al. (1993) and Edwards and McKee (1997), namely, the use of a fixed baseline period. Further, the NCEI should go back through its SPI database and recompute the entire SPI archive using a fixed baseline period, presumably 1931–90. This will allow the authors of previous studies that have incorporated the NCEI SPI dataset to reevaluate their previous conclusions using the revised NCEI SPI dataset.

2.7 Conclusion

Because the SPI is based on the standard normal distribution, it should have a mean of zero and a standard deviation of 1 across the base period. Our results indicate inconsistencies between the NCEI's divisional SPI datasets and the standard normal distribution. Examination of the NCEI's 3- and 6-month September SPI datasets across the cited 1931–90 base period indicates climate divisions in the western United States, parts of the southeastern United States, and the northern Midwest are biased away from drought; climate divisions throughout the central to northern plains, Midwest, Northeast, and parts of the Southwest were found to be biased toward drought (Fig. 3). Consultation with the NCEI dataset's point of contact revealed that these biases appeared in the dataset over the 1931–90 time period because the dataset is in fact calibrated using a moving window, in contrast to what is stated in the online metadata associated with the product.

The NCEI must make it clear that the dataset in its current form cannot be used to identify changes in frequency of occurrence or intensity of drought because the SPI values for any given

climate division evolve over time as the calibration period continually expands. Further, the current dataset should not be used in research settings, as results become impossible to reproduce given that the dataset values change over time. The authors strongly recommend that the NCEI modify its SPI computational procedure from a moving window to a fixed baseline approach and republish the entire SPI archive using this fixed baseline period.

2.7.1 APPENDIX A

Calc3 and Calc6 Average and Standard Deviation

On the basis of the average of the Calc3 SPI values across the base period, 19 climate divisions have an SPI that does not follow a standard normal distribution (i.e., nonzero average). Seventeen of these climate divisions are in the western United States and, based on the Level III Ecoregion data provided by the EPA, all but four of these climate divisions reside in either a Mediterranean climate or desert climate (western Idaho, eastern Oregon, and southwest Wyoming). The remaining two climate divisions reside in non-arid climates. Likewise, according to the Calc6 average SPI across the base period, 10 climate divisions have an SPI that does not follow a standard normal distribution across the base period. Eight of these climate divisions are in the western United States, with the majority residing in either a Mediterranean or desert climate. The remaining two climate divisions reside in non-arid climates; see Table A1. Wu et al. (2007) demonstrated that the SPI can become nonnormally distributed whenever there is a high probability of zero values in the dataset and advised caution when applying the SPI to study drought in arid climates or climates with a distinct seasonality to the precipitation. Therefore, the nonzero averages in Calc3 and Calc6 in this study are attributed to the high probability of zero values in the datasets, because the climate divisions with SPI values not following the standard normal distribution reside in regions with a distinct seasonality in the precipitation regime. Thus, we should be cognizant that the nonzero averages of the SPI in these calculations may be an

indicator that the SPI is not fully valid for these climate divisions.

[Table 1]

The standard deviations differ from 1 in the Calc3 and Calc6 datasets. This study attributes this to the method of L-moments used to calculate the parameters of the PE3 distribution. L-moments are the expectations of linear combinations of order statistics, measuring the same aspects of a distribution as the central moments. Hosking (1990) gives a comprehensive description of the theory of L-moments, which are defined for continuous probability distributions, but in practice they often must be estimated from a finite sample (Hosking 1996). To verify the effect of L-moments on the standard deviation of SPI values in the Calc3 and Calc6 datasets, the climate division precipitation data was fit to the two-parameter GAM (Thom 1958), which was used by McKee et al. (1993) in the original development of the SPI. For this analysis, the parameters were calculated via maximum likelihood estimation (Venables and Ripley 2002) instead of the method of L-moments. Following this approach, only 12 (3.5%) of the climate divisions were found to have standard deviations in disagreement with the standard normal distribution for the GAM-derived Calc3 and Calc6 datasets, respectively.

2.7.2 APPENDIX B

SPI Computational Procedure via Method of L-Moments

Integrating Eqs. (1) and (2) from section 3a over the range of precipitation values yields the cumulative distribution function:

$$F(x) = G\left(\alpha, \frac{x-\xi}{\beta}\right)\Gamma(\alpha) \qquad \text{(B1)}$$

for $\gamma > 0$ and

$$F(x) = 1 - G(\alpha, \frac{\xi-x}{\beta})/\Gamma(\alpha) \qquad \text{(B2)}$$

for $\gamma < 0$,

where G(α, x) denotes the incomplete gamma function:

$G(\alpha, x) = \int_0^x t^{\alpha-1} e^{-t} dt$ (B3)

The L-moments are the expectations of linear combinations of order statistics, measuring the same aspects of a distribution as the central moments. Hosking (1990) gives a comprehensive description of the theory of L-moments and L-moment ratios. The latter are computed for higher order L-moments (r ≥ 3):

$tr = \ell r/\ell 2$ (B4)

where

$\ell r = n^{-1} \sum_{j=1}^{n} w_{j:n}^{(r)} x_{j:n}$ (B5)

$w_{j:n}^{(1)} = 1$ (B6)

$w_{j:n}^{(2)} = \frac{2(j-1)}{n-1} - 1$ (B7)

$(r-1)(n-r+1)w_{j:n}^{(r)} = (2r-3)(2j-n-1)w_{j:n}^{(r-1)} - (r-2)(n+r-2)w_{j:n}^{(r-2)}$

for $r \geq 3$ (B8)

Given the L-moments above, the parameters of the PE3 distribution are calculated following Hosking and Wallis (1997). If $0 < |t3| < 1/3$, then $z = 3\pi t_3^2$

and

$a \approx \frac{1+0.2906z}{z+0.1882z^2+0.0442z^3}$ (B9)

If $1/3 \leq |t3| < 1$, then $z = 1 - |t3|$ and

$a \approx \frac{0.36067z - 0.59567z^2 + 0.25361z^3}{1 - 2.78861z + 2.56096z^2 - 0.77045z^3}$ (B10)

Following the estimation of α, the parameters of the PE3 distribution are calculated as

$\gamma = 2\alpha^{-1/2} sign(t3)$

$\sigma = t_2 \pi^{1/2} \alpha^{1/2} \Gamma(\alpha)/\Gamma(\alpha + \frac{1}{2})$

and

$$\mu = t_1 \qquad \text{(B11)}$$

Cumulative probability values are obtained after plugging the values of Eq. (B11) into Eqs. (B1) and (B2).

2.8 References

Carbone, G.J., Lu, J. and Brunetti, M., 2018. Estimating uncertainty associated with the standardized precipitation index. *Int. J. Climatol.*, **38** (S1), 607–616.

Cumbie-Ward, R.V. and Boyles, R.P, 2016. Evaluation of a High-Resolution SPI for Monitoring Local Drought Severity. *J. Appl. Meteor. Climatol.*, **55**, 2247-2262, doi: 10.1175/JAMC-D-16-0106.1.

Edwards, D.C. and McKee, T.B., 1997. Characteristics of 20th Century Drought in the United States at Multiple Time Scales. Climatology Report 97-2, Department of Atmospheric Science, Colorado State University, Fort Collins, CO, 155pp.

Guttman N.B., 1994. On the sensitivity of sample L moments to sample size. *J. Climate.* **7**: 1026–1029.

Guttman, N.B. and Quayle, R.G., 1996. A Historical Perspective of U.S. Climate Divisions. *Bull. Amer. Meteor. Soc.*, **77**, 2 293-304. https://doi.org/10.1175/1520-0477(1996)077%3C0293:AHPOUC%3E2.0.CO;2

Guttman N.B., 1999. Accepting the standardized precipitation index: a calculation algorithm. *JAWRA* **35** (2): 311–322.

Hayes, M., Svoboda, M., Wall, N. and M. Widhalm, 2011. The Lincoln Declaration on Drought: Universal meteorological drought index recommended. *Bull. Amer. Meteor. Soc*., 92, 485–488.

Hosking, J. R. M., 1990, 'L-moments: Analysis and estimation of distributions using linear combinations of order statistics', *J. R. Statist. Soc.* B **52**, 105–124.

Hosking, J.R.M., 1996, FORTRAN routines for use with the method of L-moments: Version 3, IBM Research Report RC20525, T.J. Watson Research Center, Yorktown Heights, New York.

Kangas, R. and Brown, T., 2007. Characteristics of US drought and pluvials from a high-resolution spatial dataset. *Int. J. Climatol.*, **27** (10), 1303–1325. doi: 10.1002/joc.1473.

Karl, T.R., 1986. The sensitivity of the Palmer Drought Severity Index and Palmer's Z- index to their calibration coefficients including potential evapotranspiration. *J. Appl. Meteor. Climatol.* **25** 77–86.

Keyantash, John & National Center for Atmospheric Research Staff (Eds). Last modified 07 Aug 2018. "The Climate Data Guide: Standardized Precipitation Index (SPI)." Retrieved from https://climatedataguide.ucar.edu/climate-data/standardized- precipitation-index-spi

Leelaruban, N., Padmanabhan, G., Oduor, P., 2017. Examining the relationship between drought indices and groundwater levels. *Water*, **9**, 82. doi: 10.3390/w9020082

Livada, I. and Assimakopoulos, V.D., 2007. Spatial and temporal analysis of drought in Greece

using the Standardized Precipitation Index (SPI). *Theor. Appl. Climatol.* **89**, 143-153. doi: 10.1007/s00704-005-0227-z

Lu, J., Carbone, G.J., and Gao, P., 2019. Mapping the agricultural drought based on the long-term AVHRR NDVI and North American Regional Reanalysis (NARR) in the United States, 1981 - 2013. *Appl. Geogr.* **104**, 10-20. doi: 10.1016/j.apgeog.2019.01.005.

McKee, T.B., Doesken, N.J. and Kleist, J., 1993. The relationship of drought frequency and duration to time scales. Eighth Conference on Applied Climatology, American Meteorological Society, Jan 17-23, 1993, Anaheim CA, 179-186.

NDMC (2018) SPI Generator. Available at https://drought.unl.edu/droughtmonitoring/SPI/SPIProgram.aspx. Accessed December 2018.

Svoboda, M., LeComte, D., Hayes, M., Heim, R., Gleason, K., Angel, J., Rippey, B., Tinker, R., Palecki, M., Stooksbury, D., Miskus, D., and Stephens, S., 2002. The Drought Monitor. *Bull. Amer. Meteor. Soc.*, **83**, 1181-1190. https://doi.org/10.1175/1520-0477- 83.8.1181.

Venables, W.N. and Ripley, B.D., 2002. Modern applied statistics with S. Springer, New York, pp. 435 - 446.

Vose, R.S., Applequist, S., Squires, M., Durre, I., Menne, M.J., Williams, C.N., Jr., Fenimore, C., Gleason, K., Arndt, D., 2014a. NOAA's Gridded Climate Divisional Dataset (CLIMDIV). NOAA National Climatic Data Center. doi:10.7289/V5M32STR

Vose, R.S., Applequist, S., Squires, M., Durre, I., Menne, M.J., and Coauthors, 2014b. Improved historical temperature and precipitation time series for U.S. climate divisions. *J. Appl. Meteor. Climatol.,* **53**, 1232-1251. doi: 10.1175/JAMC-D-13-0248.1

Wang, H., Chen, Y., Pan, Y., Chen, Z., and Ren, Z., 2019. Assessment of Candidate Distributions for SPI/SPEI and Sensitivity of Drought to Climatic Variables in China. *Int. J. Climatol.* doi: 10.1002/joc.6081

Whittenmore, D., Butler, J., and Wilson, B., 2016. Assessing the major drivers of water- level declines: new insights into the future of heavily stressed aquifers. *Hydrol. Sci. J.* **61**, 134-145 https://doi.org/10.1080/02626667.2014.959958z

World Meteorological Organization, 2012. Standardized Precipitation Index User Guide (M. Svoboda, M. Hayes and D. Wood). (WMO-No. 1090), Geneva.

Wu, H., Svoboda, M.D., Hayes, M.J., Wilhite, D.A., and Wen, F., 2007. Appropriate application of the Standardized Precipitation Index in arid locations and dry seasons. *Int. J. Climatol.* **27**, 65-79. doi: 10.1002/joc.1371

Wu, H., Hayes, M.J., Wilhite, D.A. and Svoboda, M.D., 2005. The Effect of Length of Record on the Standardized Precipitation Index. *Int. J. Climatol.* **25**, 505-520. doi: 10.1002/joc.1142

2.9 Figures and Tables

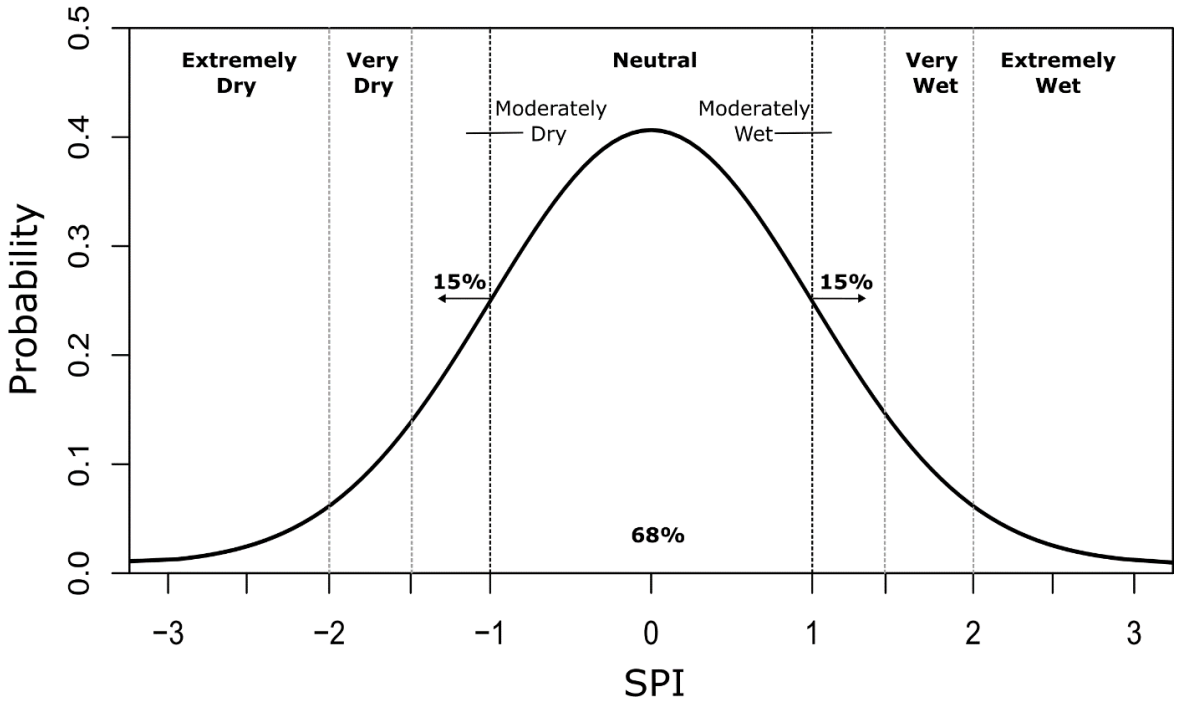

Figure 1: Standard normal distribution with the SPI.

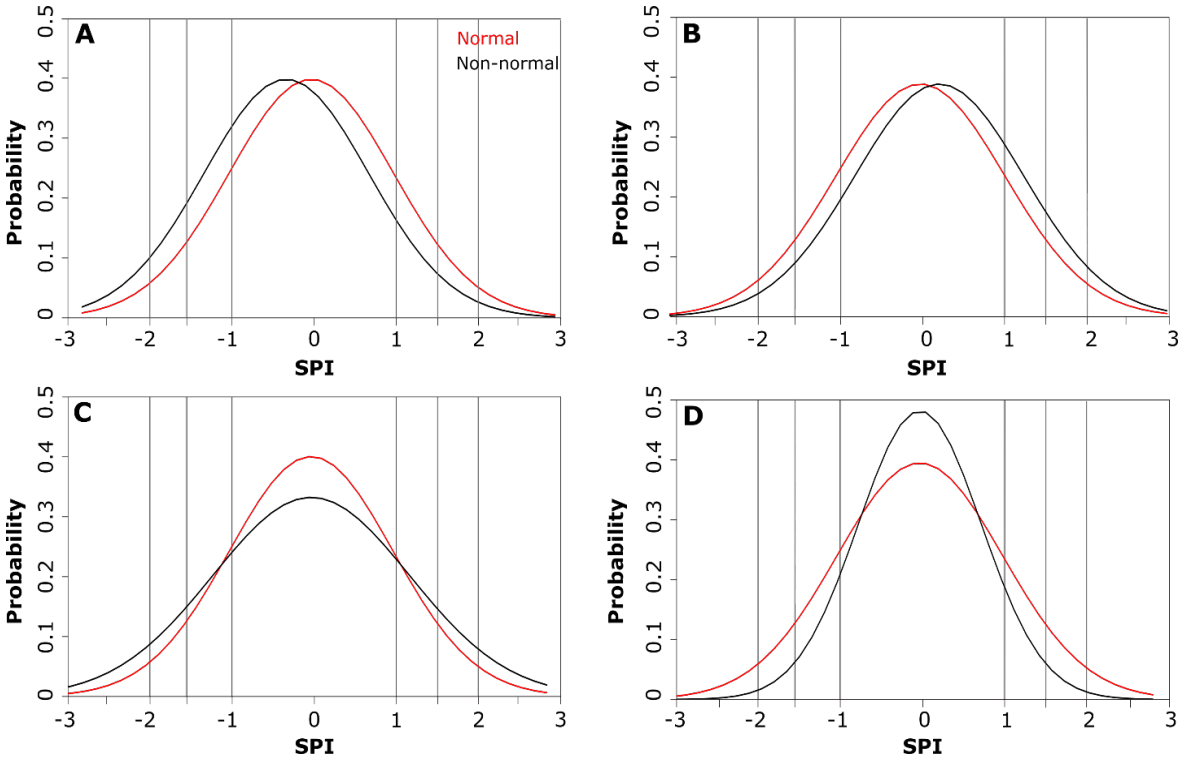

Figure 2: Standard normal distribution (red curve) overlaid (black curves) with (a) a negatively-biased distribution, (b) a positively-biased distribution, (c) a distribution with a standard deviation greater than 1 (leptokirtic), and (d) a distribution with a standard deviation less than 1(platykurtic).

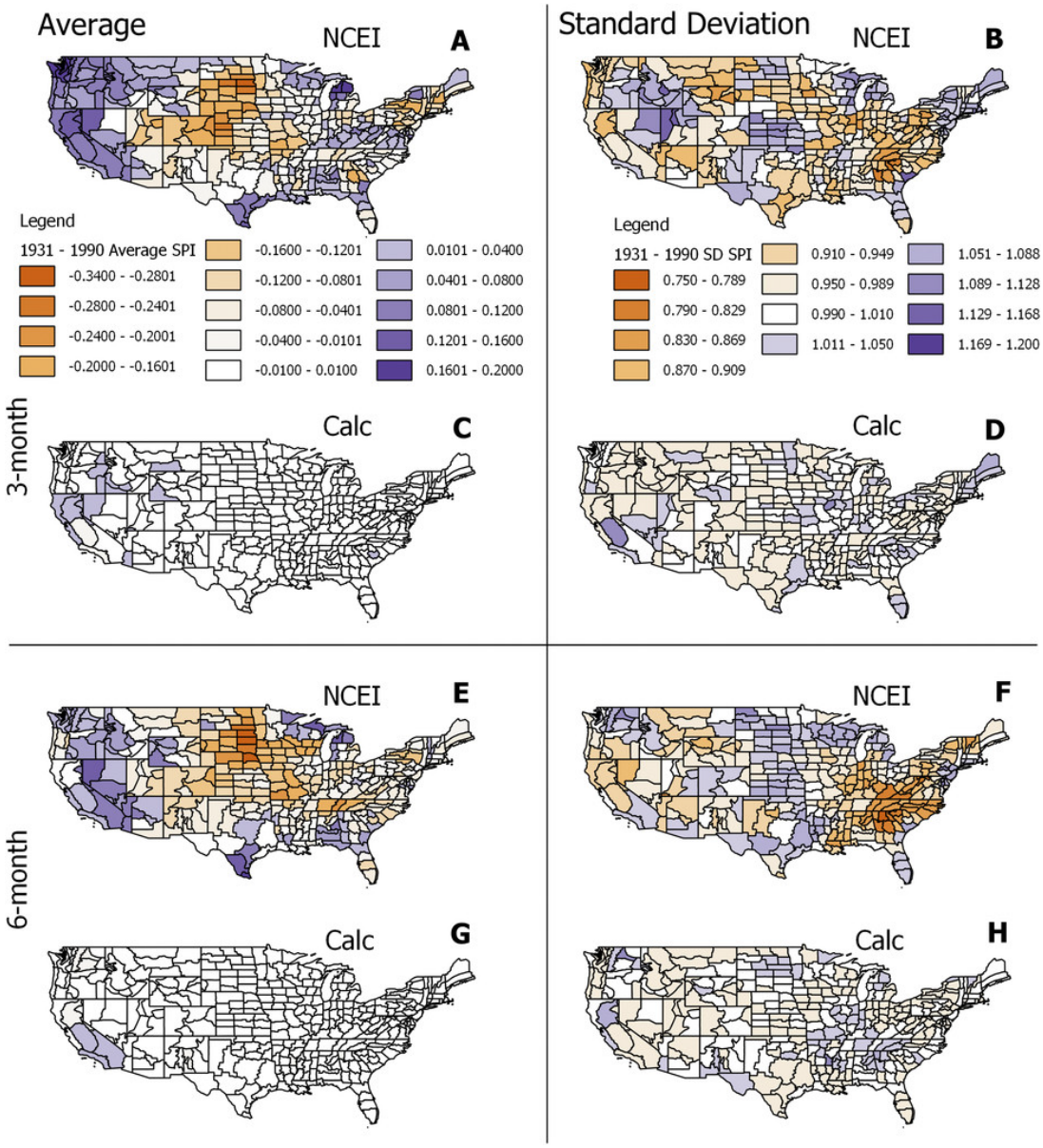

Figure 3: The 1931–90 (left) average and (right) standard deviation of September SPI values according to the (a), (b) NCEI3, (c), (d) Calc3, (e), (f) NCEI6, and (g), (h) Calc6.

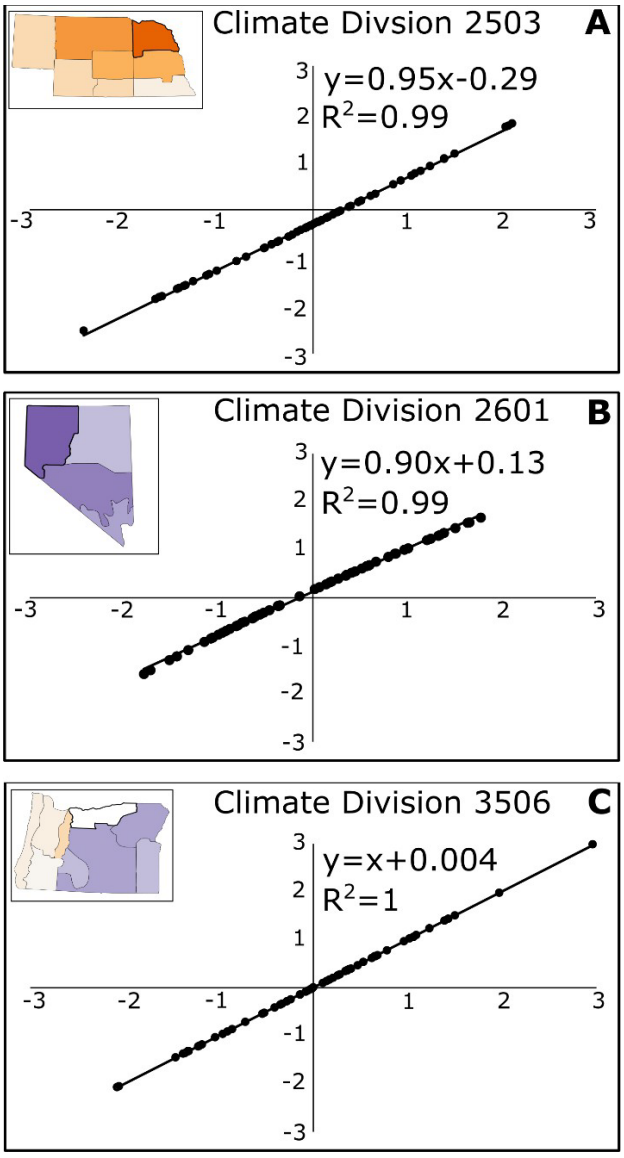

Figure 4: The 1931–90 September NCEI6 values plotted against the Calc6 values for (a) a climate division with a negative average value across that time period according to the NCEI6, (b) a climate division with a positive average value, and (c) a climate division with an average value of 0.

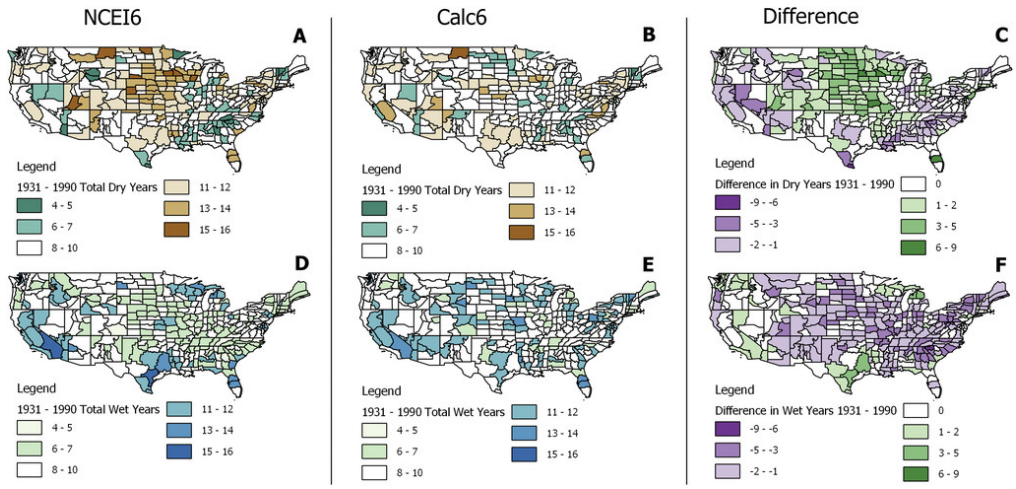

Figure 5: Total number of (a), (b) dry and (d), (e) wet years across the 1931–90 time period according to the (left) NCEI6 and (center) Calc6 datasets, along with the difference in the total number of (c) dry and (f) wet years between the two datasets (i.e., NCEI6 − Calc6).

Table A1. Climate type associated with the climate divisions that had SPI values in disagreement with the standard normal distribution according to the Calc3 and Calc6 datasets.

Calc3		Calc6	
Climate division	Climate type	Climate division	Climate type
205	Warm deserts	309	Southeastern U.S. plains
401	Western cordillera	402	Western cordillera
402	Western cordillera	405	Mediterranean California
403	Western cordillera	406	Mediterranean California
404	Mediterranean California	407	Warm deserts
405	Mediterranean California	901	Ozark–Ouachita–Appalachian forests
406	Mediterranean California	2906	South-central semiarid prairies
1005	Cold deserts	4506	Western cordillera
1006	Cold deserts	4507	Cold deserts
1007	Cold deserts	4508	Cold deserts
1103	Southeastern U.S. plains		
2405	West-central semiarid prairies		
2601	Cold deserts		
3508	Western cordillera		
3509	Cold deserts		
3806	Southeastern U.S. plains		
4202	Warm deserts		
4510	Cold deserts		
4803	Cold deserts		

CHAPTER 3: THE IMPACT OF CLIMATOLOGICAL BASE PERIOD ON DROUGHT AND PLUVIAL CHARACTERIZATION IN THE CONTIGUOUS UNITED STATES USING THE STANDARDIZED PRECIPITATION INDEX

Abstract: This study investigates the impact of varying climatological base periods on the Standardized Precipitation Index (SPI) and its characterization of drought and pluvial conditions across the contiguous United States over the 2000-2020 time period. Using climate divisional precipitation data from the U.S. Climate Divisional (nClimDiv) database, the SPI is calculated at the 3-, 6-, and 12-month timescales using eight different climatological base periods. The results indicate that the choice of base period alters the value of drought and pluvial severity yielded by the SPI, and this is due to variability in the precipitation frequency distributions amongst base periods, including the median and mean value, standard deviation, and skewness of each distribution. The resultant variability in drought and pluvial values amongst base periods underscores the sensitivity of the SPI to its underlying base period.

3.1 Introduction

The Standardized Precipitation Index (SPI) was developed by McKee et al. (1993) as a probability-based moisture index designed to determine whether moisture conditions are normal, abnormally dry, or abnormally wet, relative to a pre-defined base period. Since that time, the SPI has been recognized as the internationally preferred index for use by all national meteorological and hydrological services to characterize meteorological droughts (Hayes et al., 2011) due in large part to its minimal data requirements, simple computational procedure, and its ability to track precipitation deficiencies across various timescales. By comparing the accumulated precipitation for a particular timescale with the historical average at that timescale, the SPI captures precipitation anomalies on either end of the moisture spectrum. Further, because the index expresses precipitation magnitudes as a standardized departure from a probability distribution function, comparisons of SPI values across space and time are possible.

The SPI characterizes the moisture status on a standardized scale and is therefore spatially and temporally invariant, thus its use as a tool to discern various characteristics of drought and even other drought monitoring products has been well established in the research literature. One of the more prominent of these studies by Guttman (1998) compared historical SPI timeseries with the corresponding Palmer Drought Severity Index (PDSI) timeseries to determine if the PDSI could also be considered spatially and temporally invariant. The author found that the PDSI was spatially variant and temporally fixed at 12-months. Since that time, the SPI has been used to develop regional drought climatologies (Lloyd-Hughes and Saunders, 2002), as a tool to evaluate global drought response to a changing climate (Jenkins and Warren, 2014), and as a foundational tool for other standardized drought metrics that standardize temperature as well as precipitation (Vicente-Serrano et al., 2010).

Despite its popularity, the SPI does have shortcomings that researchers must contend with, such as the sensitivity of the index to the normalization procedure used (Quiring et al., 2009) and the length of record used in standardizing the precipitation data, with a longer record length providing more data and therefore less uncertainty when deriving the underlying parameters associated with the SPI (Wu et al., 2005). More recently, however, studies have shown that another shortcoming of the SPI is its dependence on the climatologically representative base period because of the implicit assumption of a stationary climate (Stagge and Sung, 2022). For this reason, contemporary approaches to drought monitoring with the SPI have used either a quasi-stationary reference period (Hoylman et al., 2022), such as the 30-year periods used by the World Meteorological Organization or have opted to use the entire period of record as a base period (Vose et al., 2014a), however Hoylman et al. (2022) used empirical data to illustrate that long-term base periods introduced dry and wet biases in the SPI. Furthermore, Stagge and Sung (2022) point out that using the full period of record to calculate the SPI ignores climate nonstationarity as the implicit assumption is that all observations within the dataset can be characterized by the same distribution, thereby ignoring long-term trends. The authors went on to develop a more statistically complex solution to the issue of nonstationarity via the use of Bayesian splines (Stagge and Sung, 2022). In recognizing the complex nature of some of these more statistically robust solutions to nonstationarity, other studies have evaluated the ability of SPI values derived from static base periods to reproduce the values generated by non-stationary SPI values (Cammalleri et al., 2022), and Thomas et al. (2023) investigated the impact that switching between two consecutive 30-year base periods had on the value of percentile-based climate indices including the SPI.

Regardless of the approach taken to account for climate variability in drought monitoring, non-

stationarity presents a significant challenge, and if not accounted for by standardized drought indices such as the SPI, misleading results can occur. The purpose of this study is to determine the extent to which the severity and frequency of drought and pluvial occurrences are impacted by the underlying base period used as the reference climatology in the contiguous U.S. The analysis is performed using climate divisional precipitation data to compute the SPI over the 2000 – 2020 time period using a series of eight different 30-year base periods.

3.2 Data

The SPI is calculated using monthly average precipitation data at the climate division scale from the U.S. Climate Divisional Dataset (nClimDiv). This dataset was selected because it offers a long-term, serially complete record of precipitation data for the contiguous U.S., with data spanning from 1895 – present. The nClimDiv dataset is also spatially coherent, making it an optimal tool to study large scale features such as drought. This study used data from 1920 to 2020.

There are a total of 344 climate divisions across the contiguous U.S., with each state subdivided into anywhere between 1 and 10 divisions, depending on the size of the state. Divisional boundaries within each state are reflective of various considerations, including climatic conditions, drainage basins, and crop and river districts (Guttman and Quayle, 1996). nClimDiv is maintained by the National Centers for Environmental Information (NCEI) and is utilized by the National Oceanic and Atmospheric Administration (NOAA) National Climatic Data Center (NCDC) to issue monthly State of the Climate Reports that summarize recent and long-term trends in temperature and precipitation conditions (NOAA NCEI, 2023). Divisional temperature and precipitation data are derived from a 5kmx5km gridded instance of the Global Historical Climatology Network-Daily (GHCN- Daily) dataset. In total, there are 14,702 precipitation

stations and 10,325 temperature stations utilized in the construction of the grid point estimates. Vose et al. (2014b) provide a comprehensive overview of the climatologically aided interpolation technique employed to transform this station data into gridded values.

3.3 Methods

The SPI was developed by McKee et al., (1993) as a means of evaluating drought conditions at specific timescales. For this study, the 3-, 6-, and 12-month SPI is calculated for the contiguous United States using climate divisional precipitation data and for a study period of 2000 - 2020. At each timescale, the SPI is calculated for January, April, July, and October using eight distinct 30-year climatological base periods (Table 1).

[Table 1]

Table 1 indicates that base periods beginning in 1950 or earlier are classified as antiquated and base periods beginning in 1960 or later are classified as contemporary.

Fundamentally, the SPI is the transformation of a precipitation time series into the standard normal distribution, with a mean value of 0 and a standard deviation of 1 over the region's climatically representative base period (Spade et al., 2020). The value of the SPI (which generally ranges between -3 and 3) indicates how many standard deviations a precipitation value is above or below the base period's average value (McKee et al., 1993). The sections below summarize the process of retrieving SPI values from a precipitation time series at both the climate division and regional scale, respectively.

3.3.1 SPI Computational Procedure

The precipitation time series of the climate division's base period is fit to the 2-parameter Gamma distribution, given by:

$$g(x) = \frac{1}{\beta^{\alpha}\Gamma(\alpha)} x^{\alpha-1} e^{\frac{-x}{\beta}} \text{ for } x > 1 \qquad (1)$$

where:

- x is the precipitation amount ($x > 0$)
- α is the shape parameter ($\alpha > 0$)
- β is the scale parameter ($\beta > 0$), and

$\Gamma(\alpha)$ is the gamma function, given by:

$$\Gamma(\alpha) = \int_0^\infty x^{\alpha-1} e^{-x} dx \quad (2)$$

The shape and scale parameters are estimated through the maximum likelihood estimation (MLE) method:

$$\alpha = \frac{1}{4A}\left(1 + \sqrt{1 + \frac{4A}{3}}\right) \quad (3)$$

$$\beta = \frac{\bar{x}}{\alpha} \quad (4)$$

$$A = \ln(\bar{x}) - \frac{\sum \ln(x)}{n} \quad (5)$$

where:

- n = number of precipitation observations
- $\bar{x}$ = the average precipitation value of the dataset

The shape and scale parameters were calculated for each of the three timescales and months described above, yielding a total of 96 α and β_{rate} values, respectively, for each climate division. Note that β_{rate} is the rate parameter and is simply the inverse of the scale parameter.

The cumulative probability of each precipitation value of interest was then calculated by integrating the precipitation time series over the complete range of precipitation values, using the α and β parameters associated with each base period:

$$G(x) = \int_0^x g(x)dx = \frac{1}{\beta^\alpha \Gamma(\alpha)} \int_0^x x^{\alpha-1} e^{\frac{-x}{\beta}} dx \quad (6)$$

$$H(x) = q + (1 - q)G(x) \quad (7)$$

Equation 6 is modified to account for the probability of zeros in the precipitation dataset, and this modification is given by Equation 7, where:

- q = m/n
- m = number of zeros in the dataset

The cumulative probability of the 2000 – 2020 precipitation time series for all 344 climate divisions is calculated using the α and β parameters associated with each base period (Table 1). The inverse of the cumulative probability is taken, yielding the SPI with a mean of 0 and a standard deviation of 1 over the base period, in accordance with the standard normal distribution. The process outlined above is accomplished using the *fitdistrplus* package and its associated functions in R (Delignette-Muller and Dutang, 2015; R Core Team, 2022).

3.3.2 Regional SPI

In this study, the contiguous U.S. is divided into six regions: High Plains, Midwest, Northeast, Southeast, Southern, and Western, matching those used by the U.S. Drought Monitor (Figure 1). To calculate the SPI at the regional scale, each climate division's precipitation value was scaled by area to yield the area-weighted precipitation. This was accomplished by first dividing the area of each climate division by the total area of its associated region. This value is then multiplied by that climate division's precipitation values. The weighted values are then added together to retrieve a precipitation total for the region. Once these values are calculated, the procedure outlined in section 3.1 is applied at the regional scale.

[Figure 1]

3.3.3 Comparison of Base Periods

The SPI values at each timescale are plotted for the 2000 – 2020 timeframe to visualize the range

of SPI values yielded by each base period. These plots are created for each accumulation period and ending month to determine if there is a seasonal component to the changes identified. To quantify the effect of differing base periods on the value of the SPI at each month and timescale over the study period, the range of SPI values yielded by all base periods was calculated annually. This involved taking the absolute value of the difference between the largest SPI value and the smallest SPI value yielded by the eight base periods for each year of the 2000-2020 study period, resulting in a total of 21 values per month.

3.3.4 Drought and Pluvial Totals

This study retrieved the total number of drought years captured by each base period at each month and timescale and for each region by getting the count of the number of times the SPI was less than or equal to -1 according to each base period. After these values were retrieved for each month and timescale, the average was taken over all the months so that the average number of drought events yielded by each base period could be retrieved for the three timescales. The same process was used to retrieve the total number of pluvial years after getting the count of the number of times the SPI was greater than or equal to +1 according to each base period. Note that values between -1 and +1 are considered neutral conditions (Edwards and McKee, 1997).

3.4 Results

3.4.1 Impact of Base Period on Characterization of Drought

The non-stationary base periods yielded unique SPI values throughout the study period for each region considered. Depending on the region or climate division, timescale, and month, the antiquated base periods tended to yield higher absolute SPI values for pluvial and drought conditions, as well as during neutral conditions. This suggests that current day drought conditions (i.e., from 2000 to present) are perceived as less severe according to the antiquated base periods (base periods 1, 2, 3, and 4) and more severe according to the contemporary base

periods (base periods 5, 6, 7, and 8). In contrast, pluvial conditions are perceived as more (less) severe according to the antiquated (contemporary) base periods. Exceptions to this generalization were identified in certain regions and climate divisions, as detailed in the following subsections. Climate divisions discussed below were selected because they are representative of the results of the remaining climate divisions within the climate division's region.

3.4.11 High Plains

A wide range of SPI values are apparent at all months and accumulation periods within the High Plains region, and in general, the value of this range increases as the accumulation period increases (Tables 2 and 3). For instance, in 2019 the 12-month July SPI has a range of 1.15 (Table 3) while the 3-month July range for the same year was only 0.67 (not shown in the table). Nonetheless, a large range of values also occurred at the 3-month timescale, notably in October 2012 where base period 2 yielded an SPI of -1.59 (severely dry) and base period 7 a value of -3.09 (extremely dry), yielding a range of 1.5 (Table 3).

[Table 2]
[Table 3]

An average of 12.5 drought events occurred over the study period between all months and timescales in the High Plains; the greatest number of drought events were captured by base periods 6, 7 and 8 (Table 4). Conversely, an average of 18.5 pluvial events occurred over the study period between all months and timescales; the greatest number of pluvial events were captured by base periods 2 and 4 (Table 5).

Climate divisions within the High Plains region also showed a large range in SPI values at each timescale**.** For instance, the 6-month July SPI for climate division 0501 in southeast Colorado was -2.74 (extremely dry) in 2012 according to base period 6 and -1.58 (severely dry) according to base period 8 (Figure 2). Similarly, climate division 1405 in central Kansas was assigned an

SPI of -0.56 (neutral conditions) according to base period 2 and an SPI of -1.53 (severely dry) according to base period 8 (Figure 2).

[Figure 2]

The increase in the range of SPI values with increasing accumulation period seen at the regional scale was not consistently shown at the climate division scale. For example, climate divisions sampled in Colorado, Kansas, and South Dakota (not shown) indicated a general increase in the range of SPI from the 3- to 12-month timescale, although this was not the case for climate divisions sampled in Wyoming or North Dakota (not shown).

[Table 4]
[Table 5]

3.4.12 Midwest

With a few exceptions, the results of the Midwest region indicate that the antiquated base periods yielded higher absolute SPI values than the contemporary base periods during times of drought and pluvial conditions, as illustrated in Figure 3 which provides the 6-month results. In 2012, for instance, the 6-month October SPI has a value of -2.00 (extreme drought) according to base period 8 and -0.70 (neutral) according to base period 2. Similarly, in 2004 the 3-month July SPI was 2.20 (extreme pluvial) according to base period 4 and 0.50 (neutral) according to base period 8 (not shown).

[Figure 3]

Out of all six regions, the fewest number of drought events occurred in the Midwest and Northeast regions, with an average count of 6.3 between all months, timescales, and base periods (Table 4). In the Midwest region, the greatest number of drought events were captured by base period 8 and the fewest number of drought events were captured by base periods 1 and 2 (Table 4). Conversely, an average of 28.3 pluvial events were observed over the study period between

all months and timescales; the greatest number of pluvial events were captured by base periods 3 and 4 and the fewest number of pluvial events were captured by base period 8 (Table 5). Similar to the High Plains region, the range of SPI values increases as the accumulation period increases for all months except July, which had a similar range in values at each timescale (Table 3). Climate divisional results mirrored those at the regional scale with respect to the increasing range of SPI values with increasing timescale, however the results of the antiquated and contemporary base periods are more dynamic than the regional results. For instance, at the 6-month timescale climate division 1503 in northern Kentucky diverges from the regional results for all months except January and October where the antiquated base periods consistently yielded higher SPI values than contemporary base periods for drought, pluvial, and neutral conditions. In contrast, the April and July results indicate that base periods 5, 6, and 7 had the highest SPI values for each of the 4 (7) pluvial years in April (July; Figure 4). Similarly, the 6-month April SPI for climate division 2102 in northern Minnesota indicates base periods 4 and 5 had the lowest SPI values for each of the 6 drought events; likewise base periods 7 and 8 consistently had the highest SPI values during the 6 pluvial events. The 6-month October SPI for the same climate division more closely mirrors the regional results with the antiquated base periods consistently yielding higher SPI values than the contemporary base periods for drought, pluvial, and neutral conditions (Figure 4).

[Figure 4]

3.4.13 Northeast

In the Northeast region, the greatest number of drought events were captured by base period 8 and the fewest number of drought events were captured by base period 3 (Table 4). Out of all six regions, the Northeast region captured the greatest number of pluvial events, with an average of

28.8 events between all months, timescales, and base periods; the greatest number of pluvial events were captured by base periods 1 and 3 and the fewest number of pluvial events were captured by base period 8 (Table 5).

Regardless of the moisture status, the antiquated base periods consistently yielded higher absolute SPI values than those associated with the contemporary base periods, and in many instances the difference in values are impactful to the characterization of drought. In 2001, for example, the 12-month October SPI was -1.18 (moderate drought) according to base period 3 and -2.09 (extreme drought) according to base period 8. Similarly, in 2006 the SPI was 2.58 (extremely wet) according to base period 1 and 1.10 (moderately wet) according to base period 8. Further, an increasing range of SPI values was also seen as the accumulation period increased (not shown). For instance, the maximum difference in SPI values for the April 3-month timescale was 0.86, while at the 12-month timescale this difference was 1.48.

Climate divisions sampled in the Northeast region had results similar to the regional scale's results, notably in terms of the ratio of the number of pluvial events to drought events. Climate divisions 3605 (central PA) and 4602 (central WV), however, deviated from the pattern of larger SPI values yielded by the antiquated base periods compared with the contemporary base periods. In Pennsylvania, the 6-month July SPI had four drought events over the study period and base period 3 yielded the lowest SPI value for each of these events (Figure 5). Similarly in West Virginia, the 6-month January SPI had four pluvial events over the study period and the contemporary base periods yielded the highest SPI values for each of these events (Figure 5).

[Figure 5]

3.4.14 Southeast

The results of the Southeast region deviate from the other regions in two ways. First, the size of

the range in SPI values is similar across all timescales (Tables 2 and 3). Second, the antiquated base periods frequently yielded the lowest SPI values during times of drought and the highest absolute SPI values during pluvial years, as shown by the 6-month results (Figure 6). Further, out of all six regions, the Southeast experienced the greatest number of drought events, with an average of 18.25 events captured over the study period between all months, timescales, and base periods. The greatest number of drought events were captured by base periods 3, 5, and 8 and the fewest were captured by base period 7 (Table 4). Conversely, an average of 18.2 pluvial events were observed over the study period between all months, timescales, and base periods; the greatest number of pluvial events were captured by base periods 2, 3, and 5 and the fewest number of pluvial events were captured by base periods 6 and 8 (Table 5). Note that at every July timescale and the 6- and 12-month April timescales, the antiquated base periods yielded the lowest values during drought events and the highest values during pluvial events (Tables 4 and 5).

[Figure 6]

For climate divisions sampled in central Florida (0804) and central Georgia (0905), the results were similar to what was seen at the regional scale, with the antiquated base periods yielding lower SPI values during times of drought and the contemporary base periods yielding higher SPI values during pluvial conditions (Figure 7). In contrast, climate divisions sampled in North and South Carolina (3107 and 3806, respectively) and Alabama (0107) only reflected the regional results for the month of July (not shown).

[Figure 7]

3.4.15 Southern

An average of 12.83 drought events occurred over the study period between all months,

timescales, and base periods in the Southern region; the greatest number of drought events were captured by base periods 7 and 8 and the fewest number by base periods 2, 3, and 4 (Table 4). Conversely, an average of 20 pluvial events occurred over the study period between all months, timescales, and base periods; the greatest number of pluvial events were captured by base periods 2, 3, and 4 and the fewest number were captured by base period 8 (Table 5).

With a few exceptions, the antiquated base periods yielded higher absolute values during drought and pluvial events throughout most months and timescales considered. A clear distinction in the values yielded by the contemporary and antiquated base periods is clear during the four drought events of the 12-month January timescale, for example. A similar distinction is seen for the pluvial events of the 12-month April timescale. Nonetheless, certain antiquated base periods yielded lower SPI values for drought and pluvial events at the 3-month April, 6-month July and October, and the 12-month October timescales. Similar to other regions, the range of SPI values increased as the accumulation period increased in the Southern region (Tables 2 and 3).

Climate divisions sampled in the Southern region showed mixed results. In climate division 1609 (southern Louisiana), the antiquated base periods yielded lower SPI values during drought years, notably in April and July (Figure 8), however in central Mississippi, the Oklahoma Panhandle, and central Tennessee, the opposite is true (not shown). Results for climate divisions in north and south Texas (divisions 4103 and 4109, respectively) were variable. In north Texas, the antiquated base periods generally yielded higher SPI values during drought and pluvial events, however there were exceptions in July and October. In south Texas, some of the antiquated base periods yielded lower SPI values during drought and higher absolute values during pluvial years, similar to the results of the Southeast region. In April, base period 1 yielded lower SPI values than all other base periods throughout the majority of the study period (Figure 9).

[Figure 8]
[Figure 9]

3.4.16 Western

An average of 17.08 drought events occurred over the study period between all months, timescales, and base periods in the Western region; the greatest number of drought events were captured by base periods 3 and 6 and the fewest number by base periods 1 and 8 (Table 4). Conversely, an average of 11.25 pluvial events occurred over the study period between all months, timescales, and base periods; the greatest number of pluvial events were captured by base periods 1 and 2 and the fewest number were captured by base periods 5 and 6 (Table 5). With a few exceptions, the Western region's results tended to mirror the results of the Southeast region wherein the antiquated base periods yielded higher SPI values during pluvial years and lower SPI values during drought years, as shown by the 6-month results in Figure 10. For instance, the 3-month April and 6-month July results reflect what was shown in the High Plains, Midwest, Northeast, and Southern regions, wherein the antiquated base periods yielded higher SPI values than the contemporary base periods for both drought and pluvial events. In contrast, at the 3-month July, 6-month April and October, and 12-month January through October timescales, the antiquated base periods yielded higher SPI values during pluvial years and lower SPI values during drought years than what was yielded by the contemporary base periods. The 6- and 12-month October results show lower SPI values yielded by the antiquated base periods than the contemporary base periods during the drought years of the early 2000s. Similarly, the 6- and 12-month April results show higher SPI values yielded by the antiquated base periods than the contemporary base periods during the 2017 pluvial event.

[Figure 10]

Similar to the regional results, at the climate divisional scale the results are variable. For

instance, in division 4508 (eastern Washington), the antiquated base periods yielded higher SPI values for drought and pluvial events in April and July but the reverse was true in October (Figure 11). In contrast, in climate division 2906 (central New Mexico), the antiquated base periods yielded higher SPI values for drought and pluvial years at every month (Figure 11). In northern California (division 402), the antiquated base periods yielded higher absolute values during pluvial years and lower values during drought years (Figure 12).

[Figure 11]
[Figure 12]

3.5.1 Changing Precipitation Regimes

A large (small) range of SPI values yielded by the same precipitation event is the result of differing (similar) underlying precipitation frequency distributions amongst base periods, which in turn have differing (similar) cumulative probabilities assigned to precipitation events. Because the SPI is simply a z-score, or the inverse of the cumulative probability, each precipitation event from 2000-2020 was assigned a range of SPI values in accordance with the distinct cumulative probabilities yielded by each base period. This concept is demonstrated in Figures 13 and 14, which illustrate the 3- and 12-month July precipitation regimes, respectively, for the Southern region at each base period. The precipitation regimes are illustrated by the precipitation frequency distributions (Figure 13A and 14A), each regime's fitted gamma curve (Figures 13B and 14B), and each regime's CDF (Figure 13C and 14C). At the 3-month timescale, the Southern region's SPI results were similar amongst base periods (Tables 2 and 3) and Figure 13A indicates that the small range of values is attributed to the similar precipitation regimes of each base period. The median precipitation value of each base period hovers between 10.46 and 11.57 inches and the skew of each distribution is positive, indicating an asymmetric distribution extending toward larger precipitation values.

In contrast, Figure 14A illustrates a higher degree of variability amongst the precipitation regimes associated with each base period. The median precipitation value of each base period ranges between 35.85 and 39.72 inches and the skewness of each distribution oscillates between positive and negative values. The variability in the sign of each base period's skew value indicates that the precipitation regimes are not consistently skewed toward larger or smaller precipitation values, as was the case at the 3-month timescale, but rather switch between the two. While base periods 1, 7, and 8 are skewed toward smaller precipitation values, base periods 4, 5, and 6 are skewed toward larger precipitation values. In contrast, base periods 2 and 3 have a skew of nearly 0, indicating a higher degree of symmetry in the distribution.

[Figure 13]
[Figure 14]

Despite the similarities in the 3-month accumulated precipitation regimes of each base period, there are key differences illustrated by Figure 13B and 13C. Figure 13B shows that from base period 1 to base period 8, the distribution has flattened, becoming slightly wider, with the standard deviation increasing from 1.80 at base period 1 to 2.34 at base period 8. Figure 13A illustrates that the wider range of values is associated with more data in the tails of the distribution, suggesting a higher occurrence of precipitation extremes on both ends of the moisture spectrum. Further, Figure 13C indicates a shift toward greater precipitation values when transitioning from antiquated to contemporary base periods. For instance, the 50^{th} percentile of base period 1 is 10.7 inches compared with 11.3 inches for base period 8. Similar differences are shown in Figure 14B and 14C. Figure 14B illustrates that from base period 1 to base period 8, the precipitation distribution also flattened, becoming wider. The standard deviation increased from 4.27 for base period 1 to 5.55 for base period 8. Similar to the 3-month results, Figure 14A

indicates that the wider range of values is associated with more data in the tails of the distribution, indicative of a higher occurrence of precipitation extremes. Figure 14C shows a distinct shift to the right toward larger precipitation values when moving from antiquated to contemporary base periods. The 50th percentile of base period 1 is 37.4 inches compared with 39.4 inches for base period 8. Thus, both the 3- and 12-month July precipitation regimes shifted toward greater precipitation values for the contemporary base periods compared with the antiquated base periods, although the shift was more pronounced at the larger timescale. Additionally, both timescales demonstrated an increase in the frequency of precipitation extremes, both on the dry and wet end of the moisture spectrum.

Table 6 summarizes the 6-month median, standard deviation and the 25th and 75th percentile values of base periods 1 and 8 for each region. The base period with the largest values of each statistic is shown in bold, and regions with mixed results between the two base periods are shown in grey. As shown in Table 6, the results of the Northeast region indicate that base period 8 has the larger median, standard deviation, and percentile values for each month while the other regions show mixed results between base periods.

Shown in Table 6 is that in January and April, the Western region became drier from base period 1 to base period 8 at the 6-month timescale, and in July, the Southeast region became drier from base period 1 to base period 8 at the 6-month timescale. These results are in contrast to the results of the other regions shown in Table 6, which became wetter from base period 1 to base period 8. The impact of a changing precipitation regime on the characterization of drought and pluvial events by the SPI is evident when reviewing Figures 3, 6, and 10. In Figure 3, the 2000-2020 6-month SPI timeseries shown for the Midwest region shows that the contemporary base periods depict drought events as more severe and pluvial events as less severe, relative to the

antiquated base periods. As shown in Table 6, the precipitation regime of the Midwest region is becoming wetter as the base periods move closer to present day. In contrast, regions that are becoming drier as the base periods transition closer to the present day depict drought events as less severe, relative to the antiquated base periods, as shown in the Southeast region's 6-month July results (Figure 6) and the Western region's 6-month April and October results (Figure 10).

[Table 6]

3.5.2 Impact of Base Period on Drought and Pluvial Totals

Apart from in the Southeast, each region's results indicated that the antiquated base periods generally yielded fewer (more) drought (pluvial) events than the contemporary base periods, as illustrated in Figure 15. In Figure 15, each timescale's average drought and pluvial count per base period are shown. As discussed in the previous subsection, the larger number of drought events detected by the contemporary base periods is attributed to the higher average precipitation values of the contemporary base periods compared to the antiquated base periods, as demonstrated at the 6-month timescale in Table 6 and which was also observed at the 3- and 12-month timescales (not shown). Additionally, the antiquated base periods' lower average precipitation values accounts for the higher occurrence of pluvial events during those periods compared to the contemporary periods.

[Figure 15]

In contrast, the Southeast region's average precipitation did not consistently trend toward increasing values for the contemporary base periods, as was the case for other regions. Rather the Southeast region's 30-year average precipitation fluctuated between trending upward and trending toward to lower values when progressing from antiquated to contemporary base periods, depending on the month and timescale. For instance, the Southeast region's 30-year average

precipitation trended toward decreasing values during the contemporary base periods at the 3-month April and July timescale, respectively, as well as at the 6-month July timescale. Figure 6 illustrates that the antiquated base periods yielded the lowest SPI values during drought periods in these months. Further, a declining 30-year average precipitation was observed from base period 6 to base period 7 throughout the entire 12-month timescale, and the antiquated base periods yielded the lowest SPI values during times of drought at this timescale (not shown).

In the Western region, the 30-year average precipitation has increased overall from the start of base period 1 to the start of base period 8, hence the higher (lower) drought (pluvial) count by the contemporary base periods. Nonetheless, the region's 30-year average precipitation has been on a decreasing trend from about 1970 to 2020 at most months and timescales (not shown), and based on the results of this study, this suggests that the drought count will likely begin to decrease for future 30-year base periods as the region's climate continues to trend toward lower values. This paradoxical outcome would technically be accurate based on the underlying computational procedure of the SPI.

3.5 Discussion

The results of each region examined in this study oscillated between small and large ranges of SPI values yielded by each of the eight base periods, and as illustrated by Figures 13 and 14, a large (small) range of SPI values is the result of differing (similar) precipitation regimes amongst base periods, which in turn yield differing (similar) gamma distributions. Wu et al., (2005) came to the same conclusion in their study investigating the impact of base period length on the value of the SPI using data derived from weather stations in Nebraska. The authors emphasized the role of the gamma distribution's underlying shape and scale parameters, noting that if the precipitation regimes amongst base period lengths are similar (different), then the shape

parameters, scale parameters, and, by extension, the gamma distributions, are also similar (different) and will yield similar (differing) SPI values.

Further, the results of this study indicated that the range of SPI values yielded by each base period generally increased as the accumulation period increased, regardless of region or month (Tables 2 and 3), suggesting that the impact of differing base periods on the SPI is more pronounced for larger accumulation periods. This was also found to be the case in a study by Cammalleri et al., (2022), wherein the effect of transitioning from one base period to another on the temporal consistency of the SPI was quantified in a few different ways. One approach was to extract the precipitation value from the earlier base period that yielded an SPI of -1; using this precipitation value, they computed the SPI according to the later base period. The authors then took the difference between the SPI value yielded by the later base period and the initial value of -1, allowing them to quantify the impact of the change in base period on that dryness level via the mean absolute deviation and the mean bias deviation. The authors found that the shorter-term SPI values (i.e., 1-month SPI) were only marginally impacted by the change in base period whereas the differences in the longer-term values (i.e., 12-month SPI) were more pronounced. Further, the results of this study indicate that as the average precipitation decreases, drought events will decrease as well because the SPI is less likely to detect drought. Thomas et al., (2023) came to a similar conclusion in their study investigating the impact of updating the base period from 1981- 2010 to 1991-2020 on the quantification of climate extremes such as drought in the U.S. The authors found that because the latter base period was warmer than the first base period, fewer warm extremes were detected, and more cold extremes detected when using the latter period. Additionally, the authors found that there were fewer but heavier precipitation extremes using the latter base period.

Based on the findings of Thomas et al. (2023), it is reasonable to deduce that incorporating the entire period of record as the base period rather than a moving 30-year window addresses the issue of differing SPI values yielded depending on the base period. However, this approach introduces new complexities to the issue, namely that present day SPI values would be influenced by climate regimes that are no longer representative of the present climate. For instance, Hoylman et al. (2022) conducted a study of the SPI across the U.S. and found substantial differences in the SPI values calculated using the most recent 30 years of data versus those calculated using the period of record (70+ years of data). The authors found that the period of record SPI values indicated a dry bias in the southwestern and southeastern U.S., meaning that drought conditions were characterized as more severe than what is realistic for modern-day precipitation regimes. Likewise, the authors found wet biases introduced in the Pacific Northwest and Midwest, wherein drought was characterized as less severe than what is realistic for modern-day precipitation regimes in the area. Thus, there is a trade-off that must be contended with. That is, one can opt to calculate the SPI using the entire period of record, which would result in consistent SPI values, although these values may be unrealistic for the present-day climate. Crucial to dataset consistency, however, the period of record must have a definitive ending year rather than taking the sliding scale approach used by the NCEI (see Chapter 2). Alternatively, one can calculate the SPI using a 30-year moving window approach, as demonstrated in the present study. This approach results in SPI values that are representative of modern climate regimes, however the SPI values will differ depending on the base period, which is symptomatic of a changing precipitation regime.

3.6 Conclusion

This study investigated the impact of base period on the value of the SPI at various timescales in

the contiguous U.S. at the climate divisional and regional scale over the 2000-2020 time period. The purpose of the study was to determine the extent to which drought and pluvial severity and total occurrences of each differed depending on the base period used as the reference climatology.

Results indicated that the base period impacts the characterization of drought and pluvial conditions in accordance with the distinct precipitation regimes associated with each base period. Additionally, the range of SPI values yielded by each base period generally increased as the accumulation period increased. In every region except for the Southeast, the antiquated base periods yielded more pluvial events and fewer drought events than the contemporary base periods, reflective of the drier climate conditions associated with the antiquated base periods. This study also found that the 30-year precipitation averages are on a decreasing trend when transitioning from antiquated to contemporary base periods within the Western and Southeast regions, suggesting that the number and severity of drought events captured by the SPI in these regions will likely begin to decrease in accordance with the drying climate.

3.7 References

Cammalleri, C., J. Spinoni, P. Barbosa, A. Toreti, and J. V. Vogt, 2022: The effects of non-stationarity on SPI for operational drought monitoring in Europe. Int. J. Climatol., 42, 3418–3430, https://doi.org/10.1002/joc.7424.

Delignette-Muller, M.L. and Dutang, C., 2015: fitdistrplus: An R Package for Fitting Distributions. Journal of Statistical Software, 64(4), 1-34. URL: http://www.jstatsoft.org/v64/i04/.

Edwards, D.C. and McKee, T.B., 1997: Characteristics of 20th Century Drought in the United States at Multiple Time Scales. Climatology Report 97-2, Department of Atmospheric Science, Colorado State University, Fort Collins, CO, 155pp.

Guttman N.B., 1994. On the sensitivity of sample L moments to sample size. J. Climate. 7: 1026–1029.

Guttman, N. B, 1998: Comparing The Palmer Drought Index And The Standardized Precipitation index ties of the PDSI and its variations have been the referenced studies show that the intended, J. Am. Water Resour. Assoc., 34, 113–121, https://doi.org/10.1111/j.1752-1688.1998.tb05964.x.

Guttman, N.B. and Quayle, R.G., 1996. A Historical Perspective of U.S. Climate Divisions. Bull. Amer. Meteor. Soc., 77, 2 293-304. https://doi.org/10.1175/1520-0477(1996)077%3C0293:AHPOUC%3E2.0.CO;2

Hayes, M., Svoboda, M., Wall, N. and M. Widhalm, 2011. The Lincoln Declaration on Drought: Universal meteorological drought index recommended. Bull. Amer. Meteor. Soc., 92, 485–488.

Hoylman, Z.H., R.K. Bocinsky, K.G. Jencso, 2022: Drought assessment has been outpaced by climate change: Empirical arguments for a paradigm shift. Nature Communications, 13, p. 2715

Jenkins, K., and Warren, R., 2015: Quantifying the impact of climate change on drought regimes using the Standardised Precipitation Index. Theor. Appl. Climatol. 120, 41–54. https://doi.org/10.1007/s00704-014-1143-x.

McKee, T. B., N. J. Doesken, and J. Kleist, 1993: The relationship of drought frequency and duration to time scales. Eighth Conf. on Applied Climatology, Anaheim, CA, Amer. Meteor. Soc., 179–183.

NOAA National Centers for Environmental Information, Monthly Drought Report for July 2023, published online August 2023, retrieved on March 18, 2024 from https://www.ncei.noaa.gov/access/monitoring/monthly-report/drought/202307

Quiring SM., 2009: Developing objective operational definitions for monitoring drought. J Appl Meteorol Climatol. 48: 1217–29. http://journals.ametsoc.org/doi/abs/10.1175/2009JAMC2088.1.
R Core Team, 2023: _R: A Language and Environment for Statistical Computing_. R Foundation for Statistical Computing, Vienna, Austria. <https://www.R-project.org/>.

Spade D., Beurs K., Shafer M., 2020: Major over- and underestimation of drought found in NOAA's climate divisional SPI dataset. J Appl Meteorol Climatol 59:1469–1480

Stagge, J. H., and K. Sung, 2022: A Nonstationary Standardized Precipitation Index (NSPI) Using Bayesian Splines. J. Appl. Meteor. Climatol., 61, 761–779, https://doi.org/10.1175/JAMC-D-21-0244.1.

Thomas, N. P., Marquardt Collow, A. B., Bosilovich, M. G., & Dezfuli, A., 2023: Effect of baseline period on quantification of climate extremes over the United States. Geophysical Research Letters, 50, e2023GL105204. https://doi.org/10.1029/2023GL105204

Vicente-Serrano, S. M., Beguería, S. & López-Moreno, J. I, 2010: A multiscalar drought index sensitive to global warming: the standardized precipitation evapotranspiration index. J. Clim. 23, 1696–1718.

Vose, R.S., Applequist, S., Squires, M., Durre, I., Menne, M.J., Williams, C.N., Jr., Fenimore, C., Gleason, K., Arndt, D., 2014a. NOAA's Gridded Climate Divisional Dataset (CLIMDIV). NOAA National Climatic Data Center. doi:10.7289/V5M32STR

Vose, R.S., Applequist, S., Squires, M., Durre, I., Menne, M.J., and Coauthors, 2014b: Improved historical temperature and precipitation time series for U.S. climate divisions. J. Appl. Meteor. Climatol., 53, 1232-1251. doi: 10.1175/JAMC-D-13-0248.1

Wu, H., Hayes, M.J., Wilhite, D.A. and Svoboda, M.D., 2005: The Effect of Length of Record on the Standardized Precipitation Index. Int. J. Climatol. 25, 505-520. doi: 10.1002/joc.1142

Wu, H., Svoboda, M.D., Hayes, M.J., Wilhite, D.A., and Wen, F., 2007. Appropriate application of the Standardized Precipitation Index in arid locations and dry seasons. Int. J. Climatol. 27, 65-79. doi: 10.1002/joc.1371

3.8 Figures and Tables

Table 1: Base periods and the associated classifications

Base Period	Year Range	Classification
1	1920 – 1950	Antiquated
2	1930 – 1960	Antiquated
3	1940 – 1970	Antiquated
4	1950 – 1980	Antiquated
5	1960 – 1990	Contemporary
6	1970 – 2000	Contemporary
7	1980 – 2010	Contemporary
8	1990 – 2020	Contemporary

Figure 1: The 344 climate divisions of the contiguous United States were subdivided into six regions: the High Plains, Midwest, Northeast, Southeast, Southern, and Western regions.

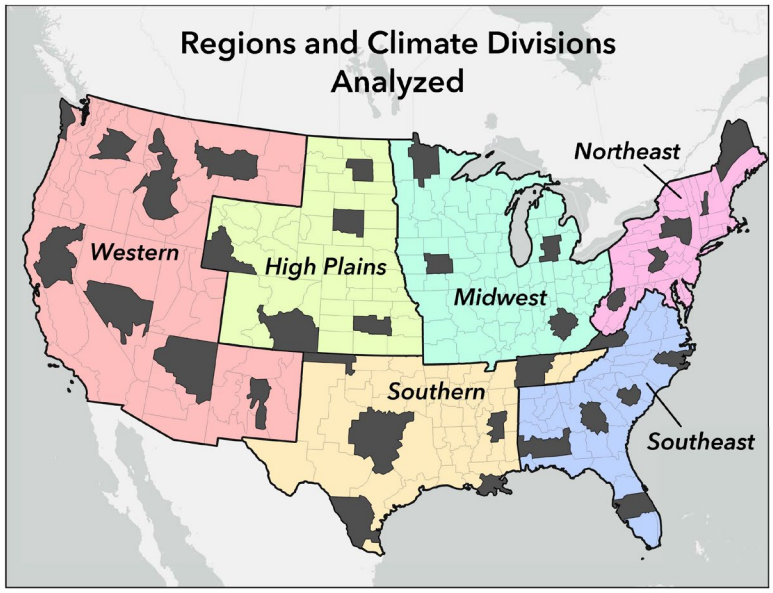

Table 2: Maximum range of January and April SPI values yielded by the eight base periods at each timescale for each region. Note that in columns 2 (3) and 6 (7) provide the maximum (minimum) SPI values yielded by the base periods listed next to those values (denoted by mW). For example, in the first row of column 2, the maximum SPI value is 1.96 and this value was yielded by base period 2. The same row in column 3 shows that the minimum SPI value is 1.17 and this value was yielded by base period 6. Columns 4 and 8 provide the absolute value of the difference between the maximum and minimum SPI values, and columns 5 and 9 provide the year associated with the maximum range in values.

	3-month January				3-month April			
Region	**Max SPI | mW**	**Min SPI | mW**	**Range**	**Year**	**Max SPI | mW**	**Min SPI | mW**	**Range**	**Year**
HP	1.96 | mW2	1.17 | mW6	0.79	2016	2.19 | mW4	1.46 | mW1, 6	0.73	2016
MW	-1.37 | mW3	-2.37 | mW8	0.99	2003	-0.81 | mW2	-1.72 | mW8	0.90	2010
NE	-1.51 | mW5	-2.46 | mW8	0.95	2002	3.09 | mW5	2.23 | mW8	0.86	2011
SE	-1.26 | mW2	-1.98 | mW6	0.72	2018	-1.65 | mW7	-2.46 | mW2	0.80	2007
S	-1.39 | mW4	-2.03 | mW1	0.65	2000	-0.82 | mW5	-1.35 | mW8	0.54	2011
W	1.53 | mW1	0.73 | mW4	0.80	2006	2.46 | mW3	1.83 | mW6	0.63	2017
	6-month January				**6-month April**			
Region	**Max SPI | mW**	**Min SPI | mW**	**Range**	**Year**	**Max SPI | mW**	**Min SPI | mW**	**Range**	**Year**
HP	-1.76 | mW2	-2.88 | mW7	1.12	2013	2.65 | mW4	1.76 | mW6	0.89	2016
MW	-1.20 | mW3	-3.09 | mW7	1.88	2000	-1.44 | mW1, 2	-2.41 | mW8	0.97	2003
NE	3.09 | mW3	1.42 | mW8	1.66	2004, 2006	2.65 | mW1	1.61 | mW6	1.04	2019
SE	2.88 | mw4	1.90 | mW8	0.98	2010	1.75 | mW2	1.08 | mW6	0.66	2019
S	-2.14 | mW4	-3.09 | mW5	0.95	2000	-1.14 | mW4	-1.83 | mW8	0.70	2011
W	2.26 | mW1	1.40 | mW6	0.86	2017	2.51 | mW3	1.34 | mW6	1.17	2017
	12-month January				**12-month April**			
Region	**Max SPI | mW**	**Min SPI | mW**	**Range**	**Year**	**Max SPI | mW**	**Min SPI | mW**	**Range**	**Year**
HP	-1.76 | mW2	-2.88 | mW7	1.12	2013	-2.23 | mW2	-3.09 | mW6-8	0.86	2013
MW	-0.51 | mW2	-1.71 | mW8	1.19	2000	3.09 | mW3	1.62 | mW8	1.47	2011
NE	2.58 | mW3	1.26 | mW8	1.31	2004	2.58 | mW3	1.09 | mW8	1.48	2005
SE	-1.81 | mW7	-2.65 | mW6	0.84	2001	2.75 | mW4	1.85 | mW8	0.90	2019
S	-1.21 | mW3	-2.37 | mW6	1.15	2006	3.09 | mW2	1.98 | mW8	1.11	2016
W	-1.83 | mW2	-2.51 | mW4	0.69	2014	2.87 | mW1	1.58 | mW6	1.30	2017

Table 3: Maximum range of July and October SPI values yielded by the eight base periods at each timescale for each region. Note that in columns 2 (3) and 6 (7) provide the maximum (minimum) SPI values yielded by the base periods listed next to those values (denoted by mW). For example, in the first row of column 2, the maximum SPI value is 2.37 and this value was yielded by base period 1. The same row in column 3 shows that the minimum SPI value is 1.61 and this value was yielded by base period 8. Columns 4 and 8 provide the absolute value of the difference between the maximum and minimum SPI values, and columns 5 and 9 provide the year associated with the maximum range in value.

	3-month July				3-month October			
Region	**Max SPI | mW**	**Min SPI | mW**	**Range**	**Year**	**Max SPI | mW**	**Min SPI | mW**	**Range**	**Year**
HP	2.37 | mW1	1.61 | mW8	0.75	2015	-1.59 | mW2	-3.09 | mW7	1.5	2012
MW	3.09 | mW4	1.55 | mW8	1.53	2015	-0.30 | mW2	-1.39 | mW7	1.08	2011
NE	2.51 | mW1, 2, 4	1.60 | mW8	0.91	2006	2.88 | mW1	1.62 | mW8	1.25	2018
SE	-1.29 | mW7	-2.75 | mW3	1.46	2007	-0.84 | mW4	-1.49 |mW8	0.65	2007
S	2.88 | mW1	2.05 | mW8	0.82	2015	-0.99 | mW2	-1.94 | mW5	0.95	2000
W	-1.87 | mW1	-2.74 | mW4, 5	0.88	2003	-1.25 | mW2	-2.05 | mW5	0.80	2003
	6-month July				**6-month October**			
Region	**Max SPI | mW**	**Min SPI | mW**	**Range**	**Year**	**Max SPI | mW**	**Min SPI | mW**	**Range**	**Year**
HP	-2.14 | mW2	-3.09 | mW5, 6	0.95	2003	-0.80 | mW2	-1.73 | mW7	0.94	2020
MW	3.09 | mW4	1.43 | mW8	1.66	2011	-0.71 | mW2	-1.91 | mW8	1.12	2012
NE	2.58 | mW1	1.52 | mW8	1.05	2011	3.09 | mW1	1.52 | mW8	1.57	2003
SE	-1.33 | mW7	-2.88 | mW3	1.54	2006	2.58 | mW5	1.80 | mW8	0.78	2003
S	-1.91 | mW4	-2.51 | mW7	0.60	2011	-1.60 | mW2	-3.09 | mW5-7	1.50	2011
W	2.07 | mW4	1.24 | mW6	0.83	2011	-2.07 | mW1, 8	-3.09 | mW6	1.02	2003
	12-month July				**12-month October**			
Region	**Max SPI | mW**	**Min SPI | mW**	**Range**	**Year**	**Max SPI | mW**	**Min SPI | mW**	**Range**	**Year**
HP	2.51 | mW4	1.36 | mW8	1.15	2019	-1.60 | mW2	-2.75 | mW6	1.15	2012
MW	-0.35 | mW2	-1.81 | mW8	1.46	2000	-0.32 | mW2	-1.75 | mW8	1.43	2003
NE	2.66 | mW1	1.16 | mW8	1.50	2004	3.09 | mW1	1.48 | mW8	1.61	2019
SE	3.09 | mW1-4	2.07 | mW7	1.02	2003	2.46 | mW2	1.99 | mW8	0.46	2020
S	3.09 | mW1-3	2.17 | mW8	0.92	2019	-1.17 | mW2	-2.51 | mW7	1.34	2000
W	2.58 | mW3	1.45 | mW6	1.13	2017	-2.01 | mW1	-3.09 | mW3	1.08	2001

Figure 2: 6-month SPI timeseries associated with climate division 0501 (CO) and 1405 (KS) for January, April, July, and October over the 2000-2020 timeframe.

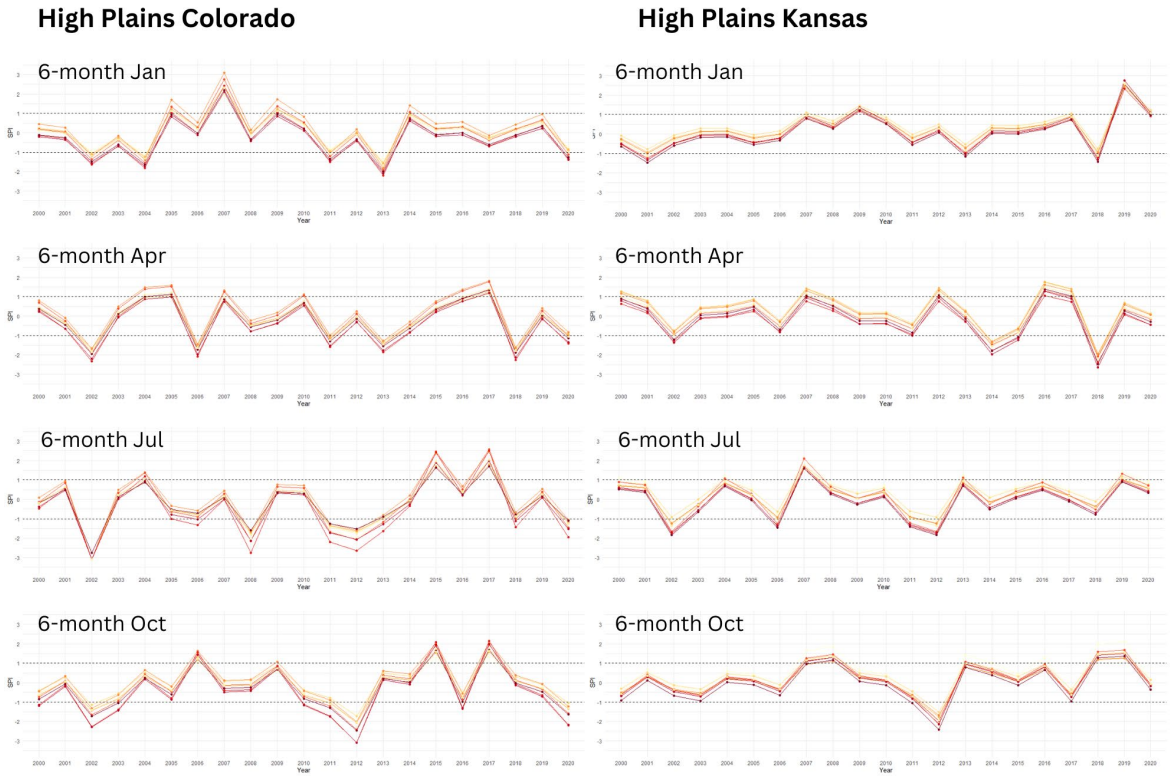

Figure 3: 6-month SPI timeseries in the Midwest region for January, April, July, and October over the 2000-2020 timeframe.

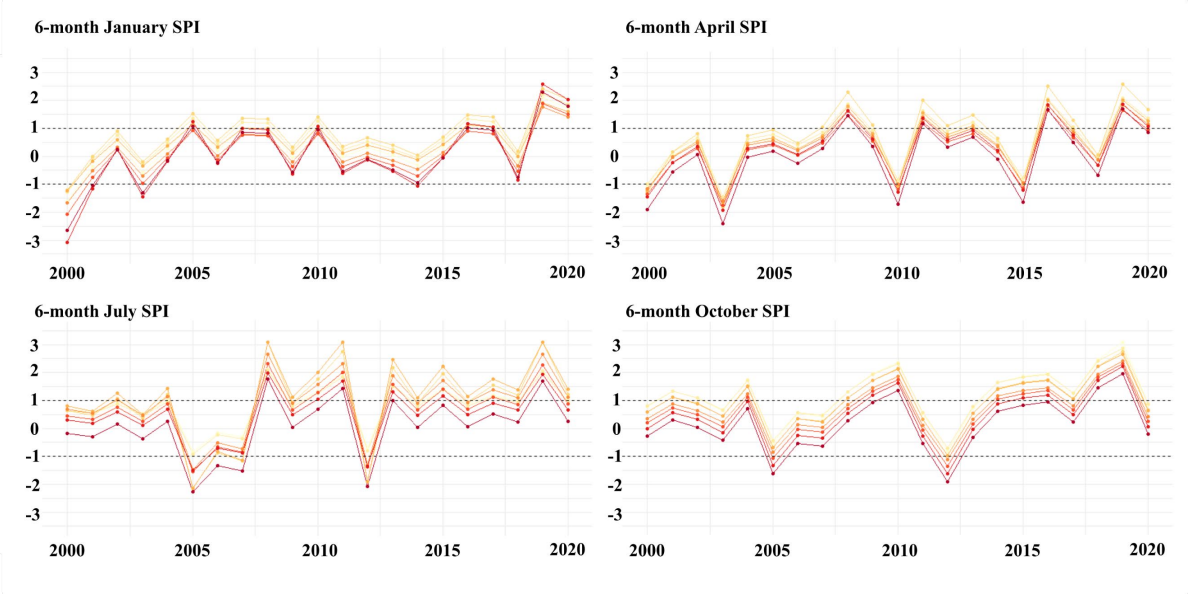

Figure 4: 6-month SPI timeseries associated with climate division 1503 (KY) and 2102 (MN) for January, April, July, and October over the 2000-2020 timeframe.

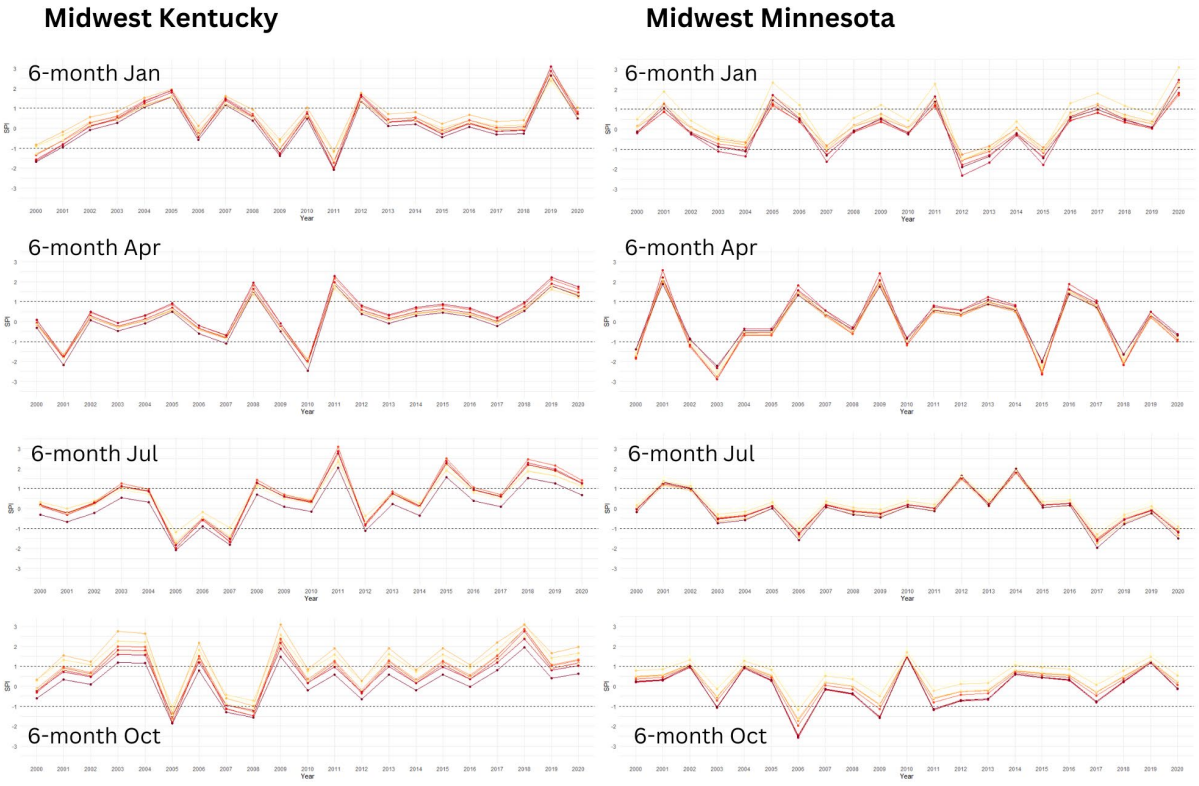

Figure 5: 6-month SPI timeseries associated with climate division 3605 (PA) and 4602 (WV) for January, April, July, and October over the 2000-2020 timeframe.

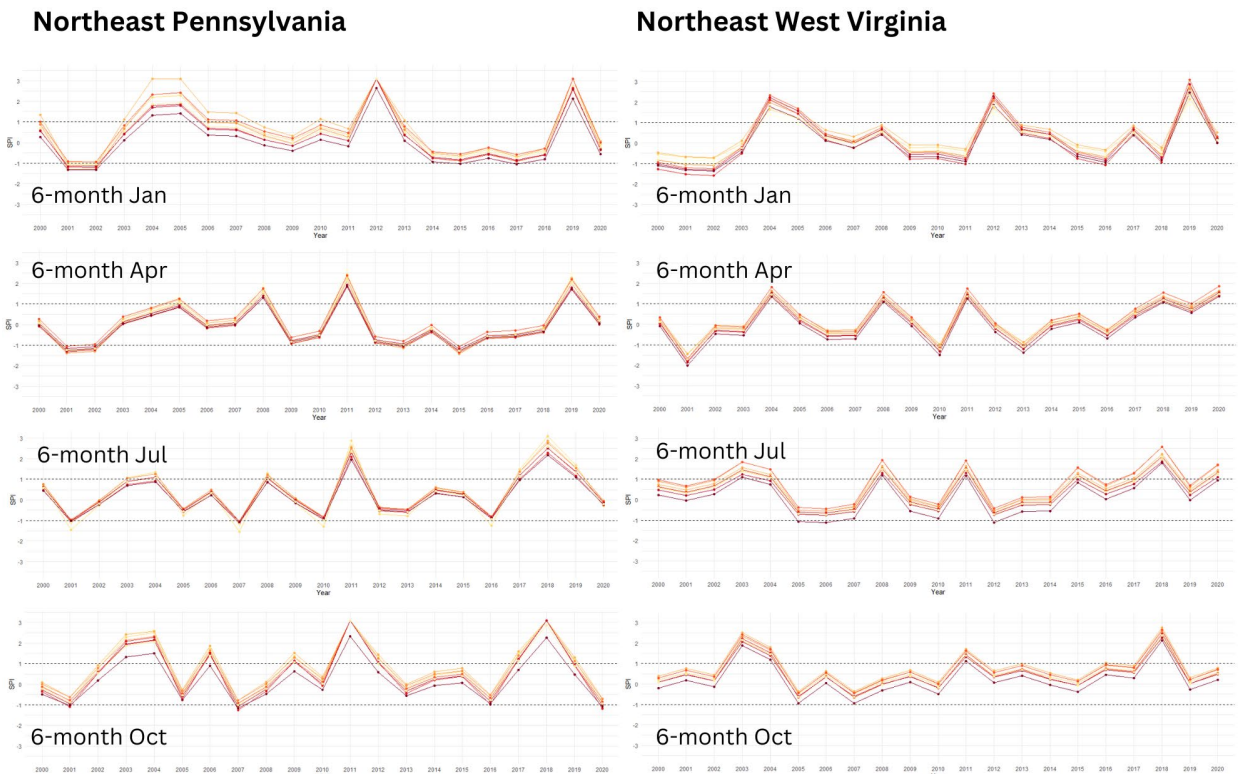

Figure 6: 6-month SPI timeseries in the Southeast region for January, April, July, and October over the 2000-2020 timeframe.

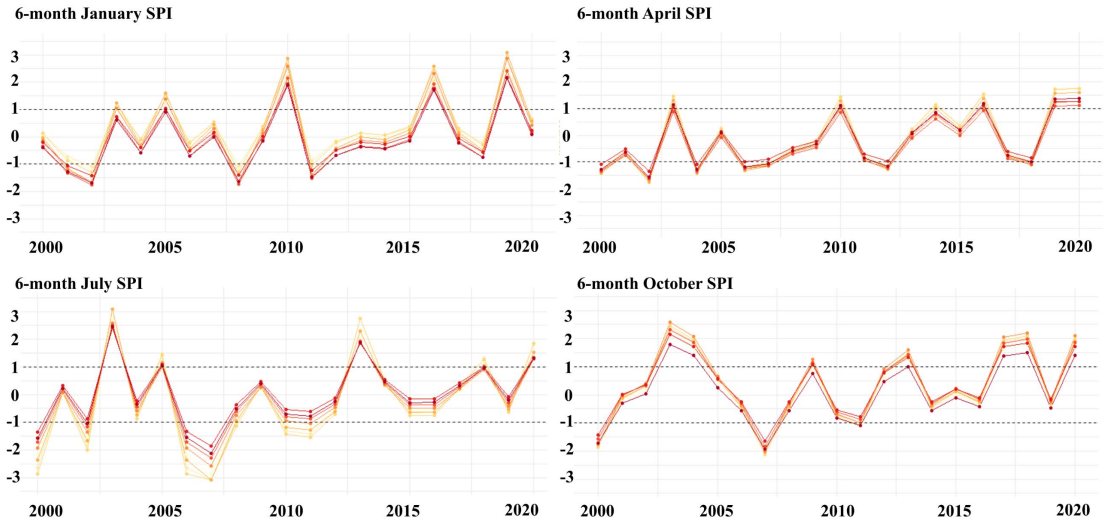

Figure 7: 6-month SPI timeseries associated with climate division 0804 (FL) and 0905 (GA) for January, April, July, and October over the 2000-2020 timeframe.

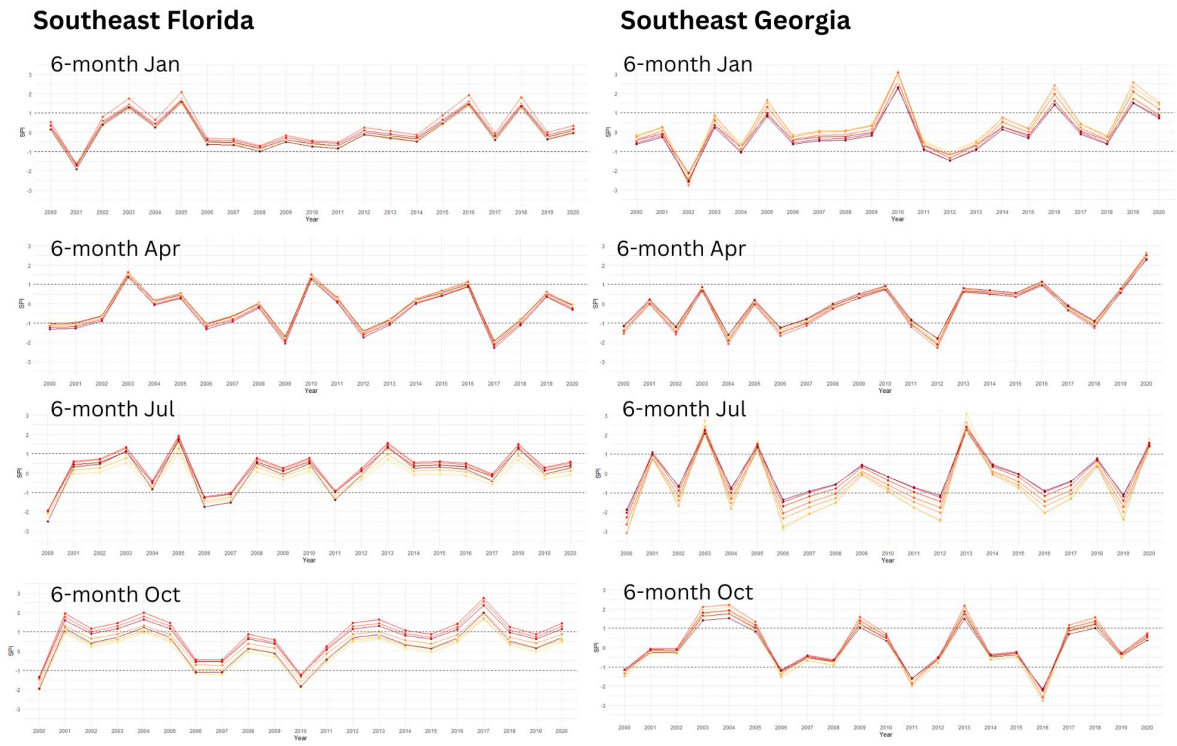

Figure 8: 6-month SPI timeseries associated with climate division 1609 (LA) for January, April, July, and October over the 2000-2020 timeframe.

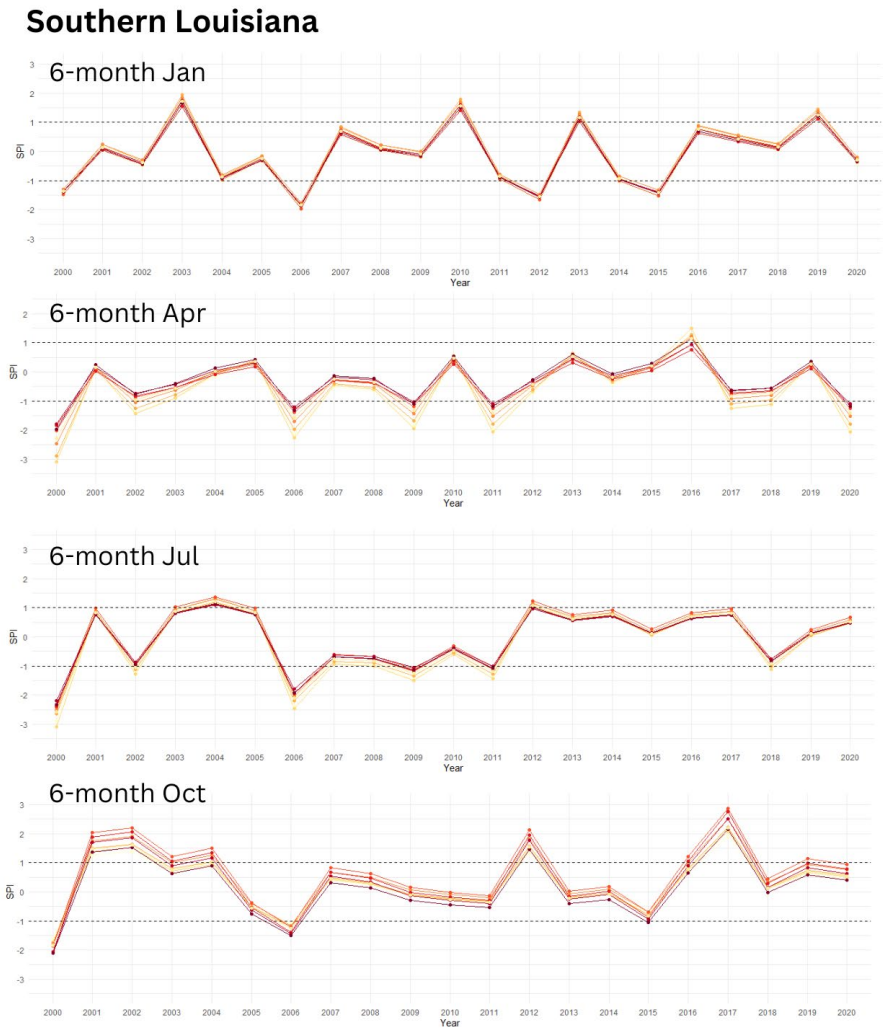

Figure 9: 6-month SPI timeseries associated with climate division 4103 (North TX) and 4109 (South TX) for January, April, July, and October over the 2000-2020 timeframe.

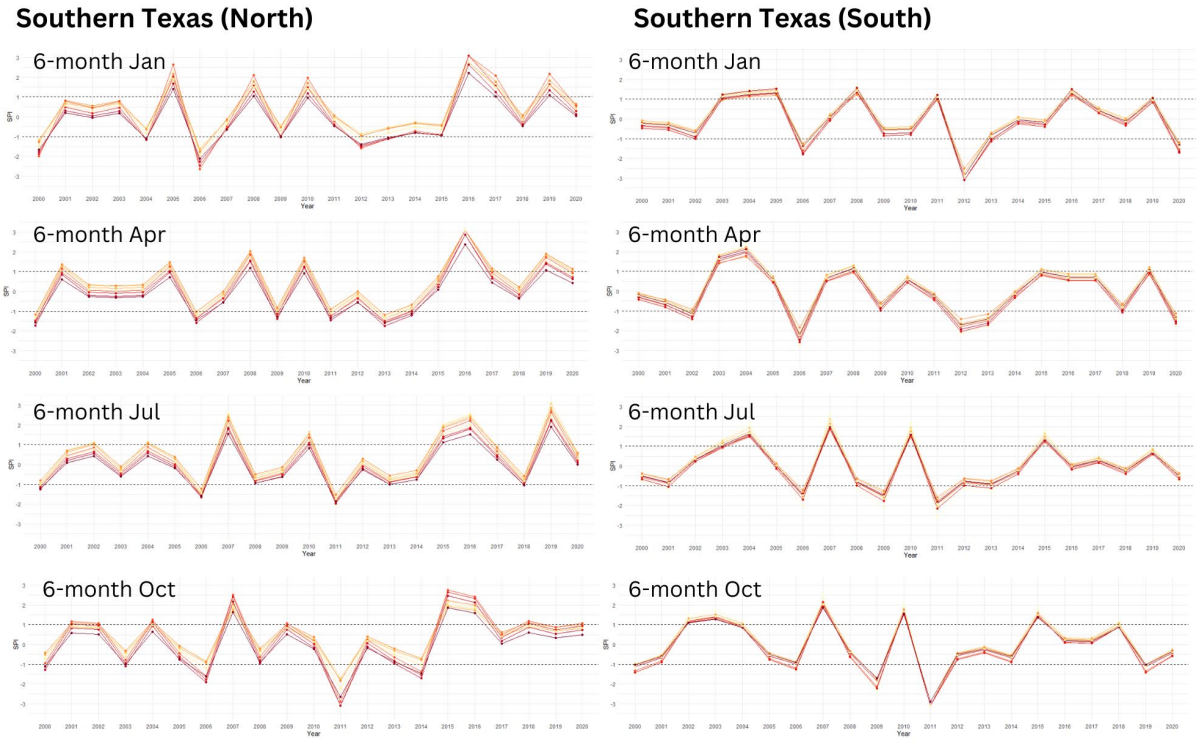

Figure 10: 6-month SPI timeseries in the Western region for January, April, July, and October over the 2000-2020 timeframe.

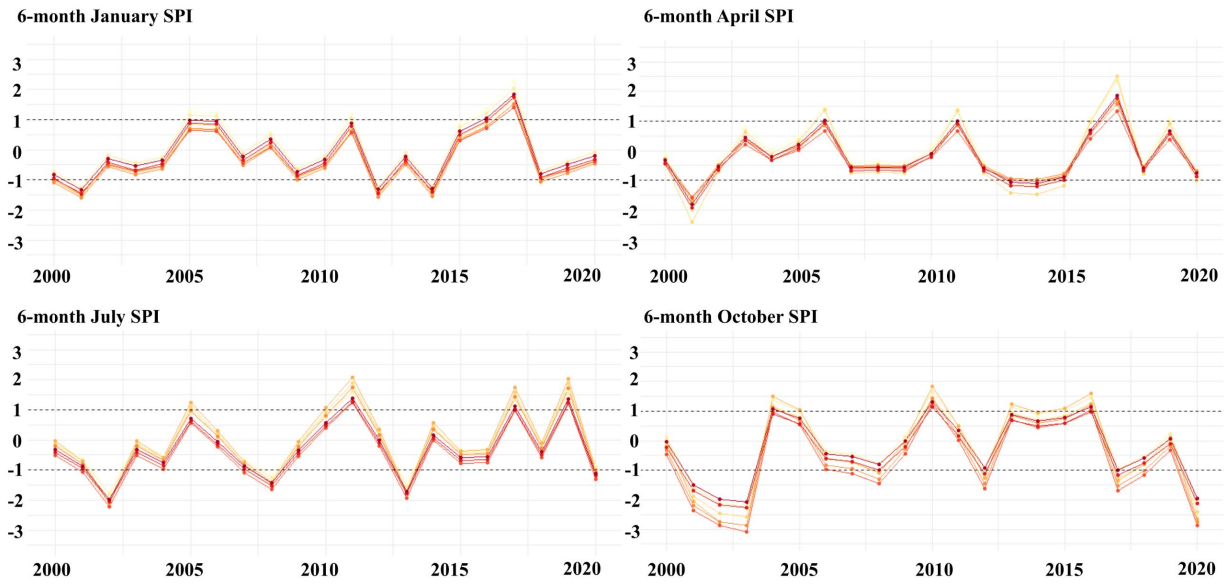

Figure 11: 6-month SPI timeseries associated with climate division 4508 (WA) and 2906 (NM) for January, April, July, and October over the 2000-2020 timeframe.

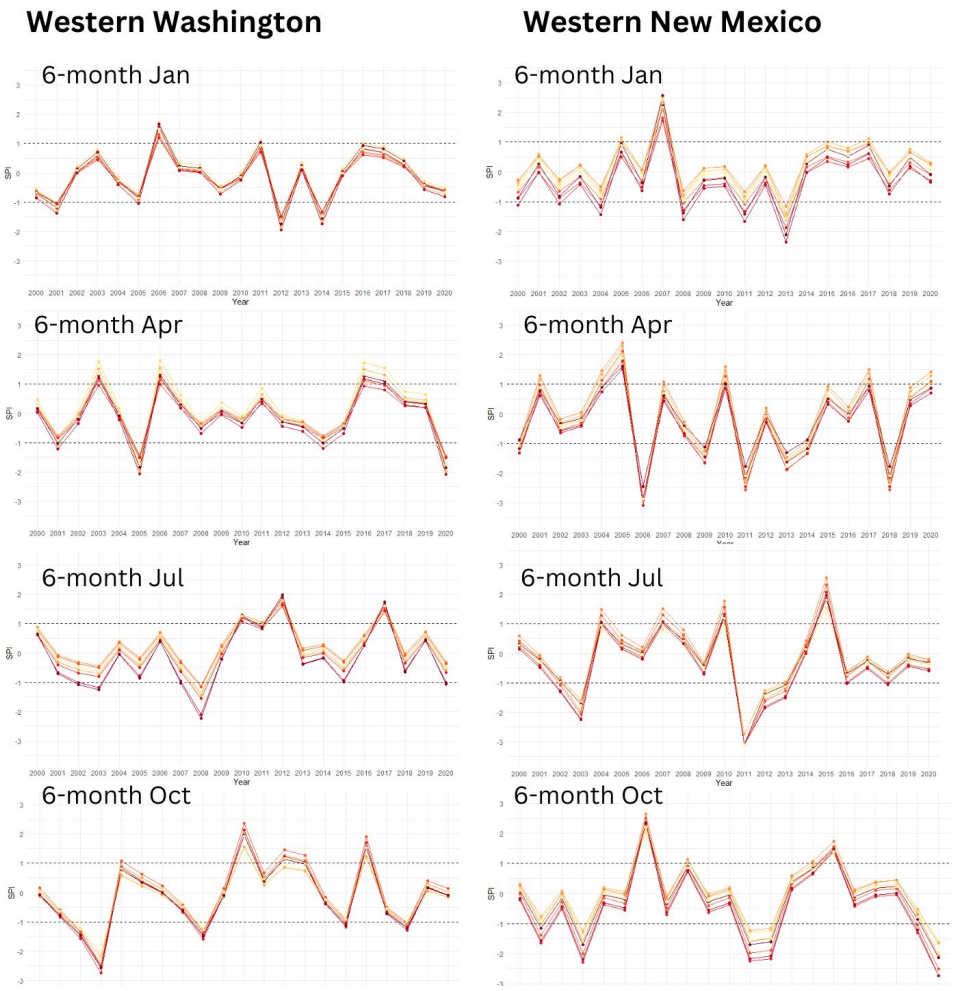

Figure 12: 6-month SPI timeseries associated with climate division 402 (CA) for January, April, July, and October over the 2000-2020 timeframe.

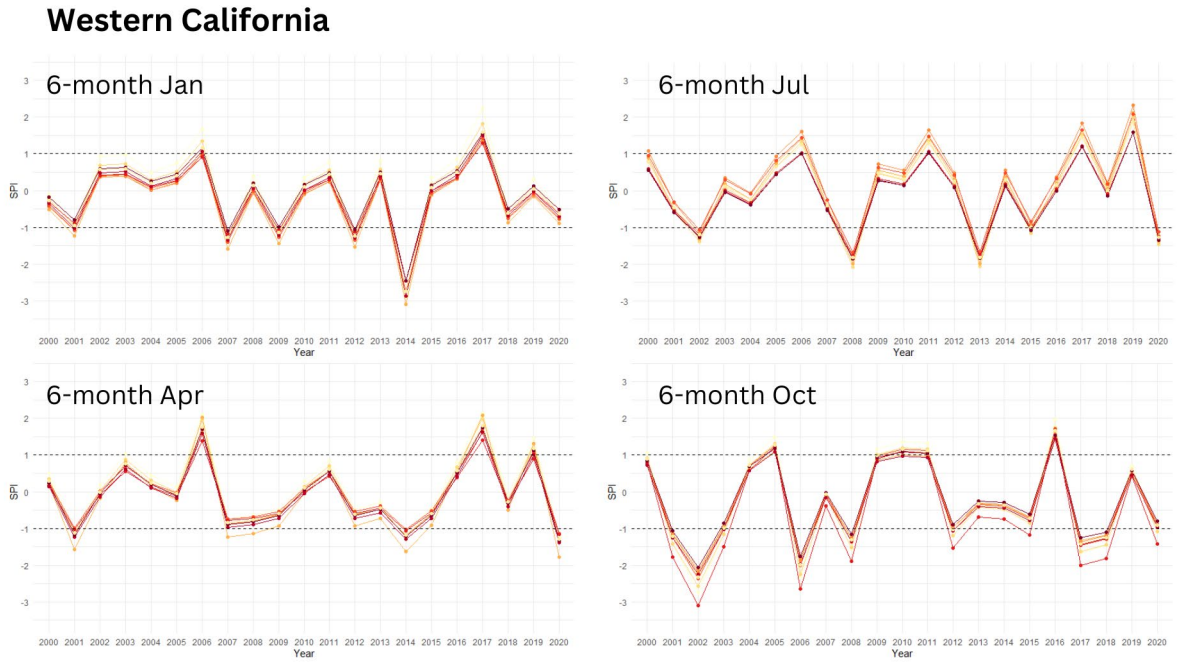

Figure 13: Precipitation frequency distribution (A), fitted Gamma curves (B), and cumulative distribution functions (C) associated with each base period at the 3-month July timescale for the Southern region.

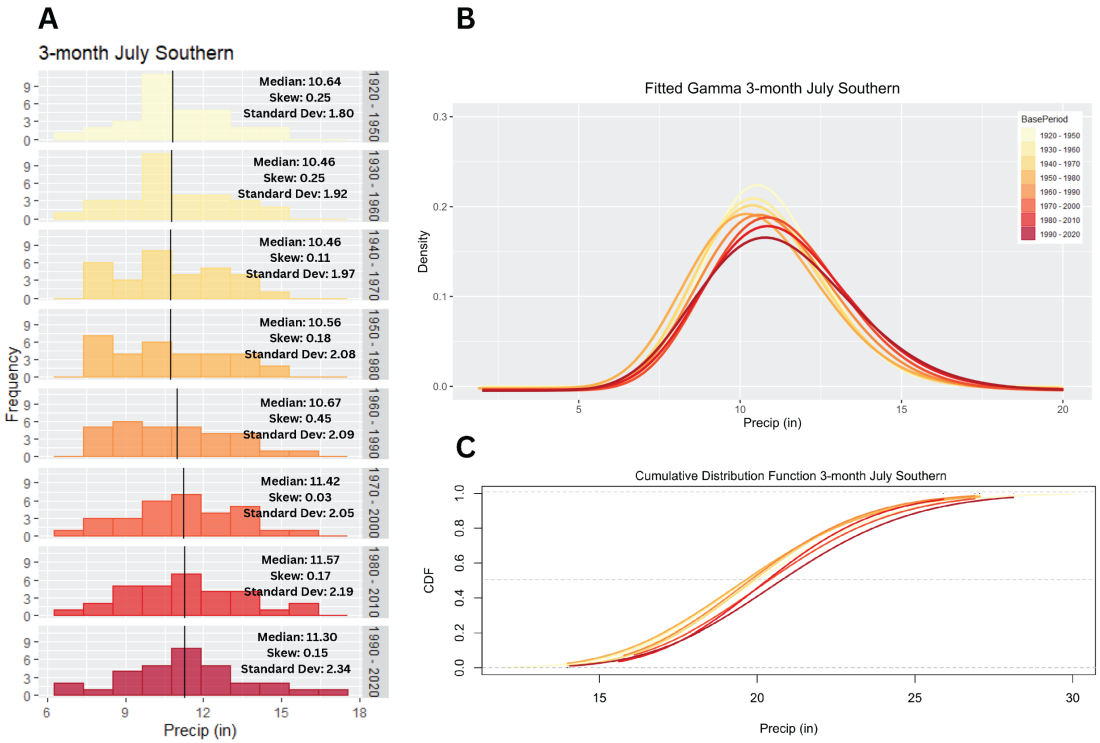

Figure 14: Precipitation frequency distribution (A), fitted Gamma curves (B), and cumulative distribution functions (C) associated with each base period at the 12-month July timescale for the Southern region.

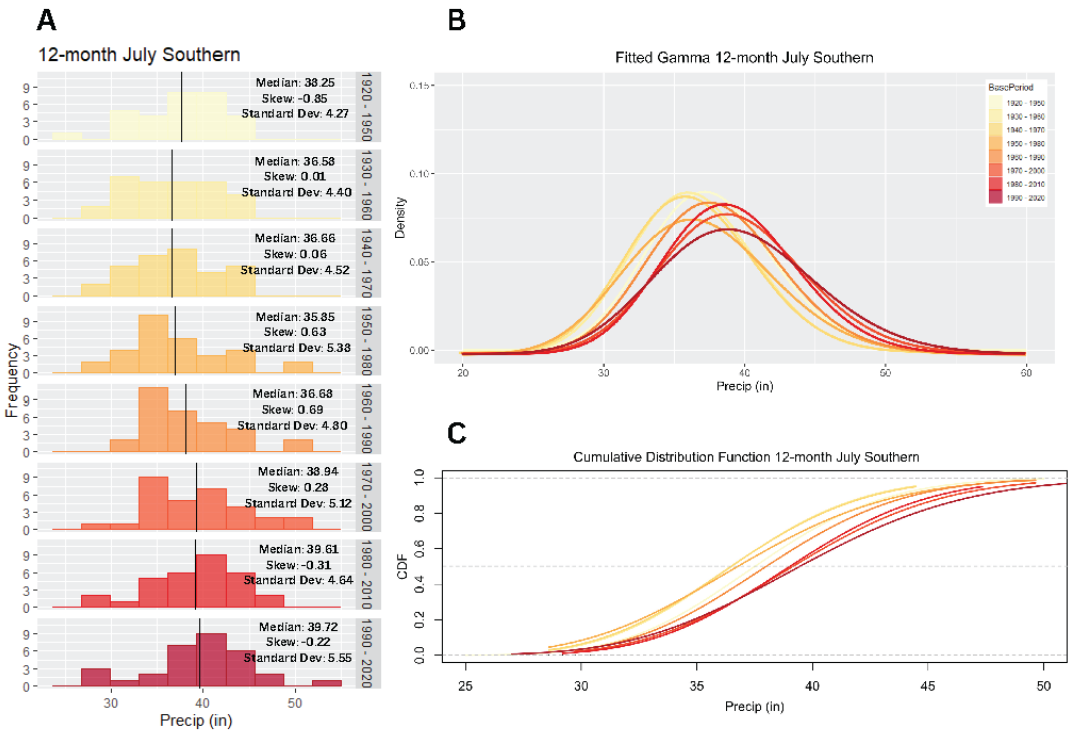

Table 6: Median, standard deviation, and percentile values for base periods 1 and 8 at the 6-month time scale.

Region	Base Period	Median	Standard Deviation	Percentiles (25, 75)
	January			
High Plains	1	7.78	1.28	6.61, 8.43
	8	**8.52**	**1.33**	**7.37, 9.23**
Midwest	1	15.91	2.85	13.91, 17.71
	8	**16.52**	**2.21**	**15.58, 18.55**
Northeast	1	20.45	2.75	18.92, 21,77
	8	**22.39**	**3.46**	**20.69, 24.73**
Southeast	1	22.23	3.80	20.74, 26.62
	8	**24.14**	**3.95**	**22.39, 26.93**
Southern	1	18.48	2.97	15.24, 19.46
	8	**18.51**	**3.52**	**17.06, 21.26**
Western	1	**10.12**	1.58	9.05, 11.54
	8	9.98	**1.88**	**9.08**, **11.97**
	April			
High Plains	1	6.29	**1.14**	5.63, **7.58**
	8	**6.55**	1.10	**5.94,** 7.56
Midwest	1	14.00	**2.26**	11.70, 15.67
	8	**14.78**	1.91	**13.75, 15.84**
Northeast	1	18.81	2.25	17.56, 20.62
	8	**20.41**	**2.67**	**18.22, 22.27**
Southeast	1	22.54	3.69	**19.57**, 24.97
	8	**23.21**	**4.48**	19.38, **26.74**
Southern	1	18.56	3.06	16.39, 20.00
	8	**18.91**	**3.16**	**16.54, 20.92**

Western	1	**11.90**	1.82	10.44, 12.92
	8	11.56	**2.21**	**11.05, 14.29**
	July			
High Plains	1	11.72	1.95	10.50, 13.10
	8	**12.69**	**2.04**	**11.81, 13.55**
Midwest	1	18.96	**3.09**	16.56, 20.62
	8	**21.21**	2.56	**19.86, 23.07**
Northeast	1	21.34	2.21	19.91, 22.86
	8	**22.82**	**2.92**	**21.15, 25.15**
Southeast	**1**	**27.13**	3.55	**25.19, 29.50**
	8	25.36	**4.42**	23.57, 28.69
Southern	1	19.86	3.22	17.77, 22.68
	8	**20.54**	**3.35**	**19.20, 23.27**
Western	1	8.87	1.51	7.99, 9.84
	8	**9.01**	**1.58**	**8.28, 10.38**
	October			
High Plains	1	13.19	2.13	11.53, 14.02
	8	**14.56**	**2.29**	**12.80, 15.62**
Midwest	1	20.99	2.43	19.34, 22.06
	8	**23.29**	**2.62**	**21.70, 25.20**
Northeast	1	22.59	2.42	20.94, 24.02
	8	**24.88**	**3.69**	**22.23, 27.72**
Southeast	1	27.72	3.48	25.36, 30.21
	8	**27.86**	**3.90**	**25.91, 31.51**
Southern	1	19.48	**3.28**	16.68, 21.74
	8	**21.12**	3.10	**19.25, 23.99**
Western	1	7.08	**1.18**	**6.67**, 7.96

	8	**7.44**	1.15	6.64, **8.27**

Figure 15: Average number of drought and pluvial events, respectively, per base period and accumulation period.

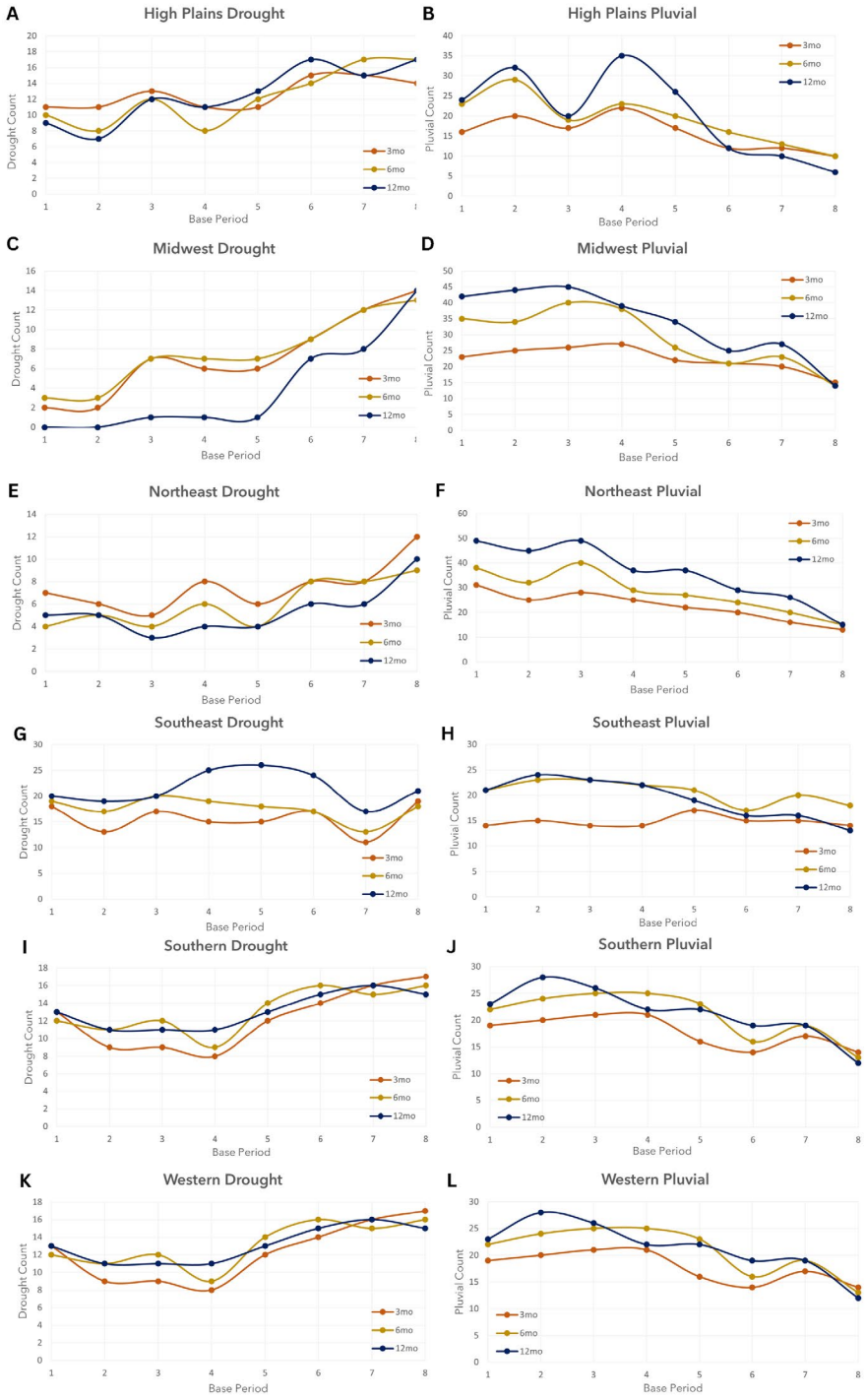

CHAPTER 4: THE EFFECTS OF NONSTATIONARY PRECIPITATION REGIMES ON THE CHARACTERIZATION OF PRECIPITATION EXTREMES BY THE STANDARDIZED PRECIPITATION INDEX

Abstract: With climate change introducing nonstationarity in climatic variables such as precipitation, traditional drought monitoring tools like the Standardized Precipitation Index (SPI), which rely on fixed, climatically representative base periods for reference, may not accurately reflect current precipitation extremes. In this study, climate divisional monthly precipitation data is used to calculate the 3- and 12-month SPI using a series of base periods to evaluate the extent to which the value of the SPI is influenced by its underlying base period. Results indicate that the choice of base period influences the characterization of drought and pluvial values yielded by the SPI, with the more recent base periods showing a shift towards drier conditions in the West, Southwest, and parts of the Southern U.S., and wetter conditions in the Northeast. Additionally, updating the base period from 1980- 2010 to 1990-2020 resulted in changes in drought and pluvial severity levels across climate divisions, indicating a shift toward drier or wetter conditions depending on the region.

4.1 Introduction

The concept of drought is a simple one, occurring when a region's precipitation falls below average for a sustained period of time, yet droughts are among the most complex of natural hazards, notably when it comes to operational drought monitoring. Unlike other natural hazards such as hurricanes, wildfires, or tornadoes, droughts do not have a definitive onset or ending, they are slow to progress, their effects manifest in a multitude of ways (soil moisture deficits, decrease in water level, etc.), and they are regionally dependent – a drought in the northeastern U.S. would likely be considered above average precipitation in the desert southwest. Hence, drought occurrence and severity are dependent on the local climatology, which is often condensed into a climatologically representative base period for monitoring purposes. The Standardized Precipitation Index (SPI) capitalizes on the concept of representative base periods by measuring meteorological drought severity relative to a reference climate, and since its inception in the early 1990s, the SPI has become one of the most widely used operational drought monitoring tools (Svoboda et al., 2002; NOAA NCEI, 2023).

Because the SPI is so widely used, several studies have investigated factors that impact the SPI and its reliability, such as the climatology of the region being studied (Wu et al., 2007), the length of record of the underlying base period (Wu et al., 2005, Spade et al., 2020), and the effect that the probability density function used for normalizing precipitation has on the SPI (Guttman, 1999; Quiring, 2009). More recently, the impact that the underlying base period has on the characterization of drought has been investigated. Thomas et al. (2023) found that updating the base period from 1981-2010 to 1991-2020 resulted in fewer but more severe precipitation extremes in the southern and central United States. Cammalleri et al. (2022) evaluated the impact of transitioning between the two most recent base periods used by the World Meteorological

Organization on the SPI, finding that the effect was more pronounced at longer accumulation periods (9- and 12-month) than for shorter accumulation periods. The authors also found that changing base periods resulted in drought classification shifting from extremely dry to moderately dry.

Other studies have addressed the impact of a nonstationary climate on drought monitoring through adjusting the computational approach of the SPI. Stagge and Sung (2022), for example, used Bayesian splines to develop a nonstationary SPI model that could measure drought relative to a changing climate. The authors found that the model was able to reproduce nonstationary climate patterns identified in other studies, emphasizing that the nonlinear model improved upon other SPI models by reducing uncertainties in several key areas. However, as noted by Hoylman et al. (2022), novel approaches such as that suggested by Stagge and Sung (2022) present a challenge in that they would necessitate a significant change in the established drought monitoring practices. Hoylman et al (2022) instead favor the 30-year moving window approach as it simultaneously captures climate non-stationarity while also leveraging the existing infrastructure for drought monitoring.

In recognizing the prevalence of the 30-year moving window approach for operational drought monitoring, the objective of this study is to evaluate how transitioning between base periods impacts present-day drought characterization according to the 3- and 12-month SPI. The purpose of this analysis is to determine the differential impacts on operational drought monitoring of transitioning between base periods for areas that are trending toward drier or wetter conditions. The analysis is performed at the climate divisional scale over the contiguous U.S., and present-day is represented by the 2021-2023 time period. This study's Data and Methods are detailed in Sections 2 and 3, respectively. The Results, Discussion and Conclusions are provided in Sections

4 through 6.

4.2 Data

4.2.1 Climate Divisional Precipitation

For this study, the SPI is calculated at the 3- and 12-month timescales using climate divisional monthly precipitation data for each of the 344 climate divisions in the contiguous U.S. The divisional precipitation data is available for download through the U.S. Climate Divisional database (nClimDiv; Vose et al., 2014a). Divisional values of precipitation are derived from area-weighted averages of grid-point estimates interpolated from station data (Vose et al., 2014b). These datasets are available for download in TXT, MAP and KMZ file formats.

4.2.2 U.S. Drought Monitor

The U.S. Drought Monitor (USDM) consists of a weekly map of the U.S. displaying the severity of drought conditions using a scale ranging from D1 (moderate drought) to D4 (exceptional drought). A fifth category, D0, indicates abnormally dry conditions, which commonly either precede a drought or depict lingering impacts after a drought. As shown by Table 1, each of the USDM's drought severity categories are associated with a specific range of SPI values.

[Table 1]

The USDM is jointly produced by the National Drought Mitigation Center at the University of Nebraska-Lincoln, the United States Department of Agriculture, and the National Oceanic and Atmospheric Administration (NOAA). The product became operational in 1999 and has since become the standard for operational drought monitoring, due in large part to the product providing a weekly snapshot of both short- and long-term drought conditions across the U.S. in a single map. This is accomplished through blending the results of several drought indicators and indices, including soil moisture, hydrological inputs, climatological inputs, modelled inputs, and remotely sensed inputs (Svoboda et al., 2016). The 2021 – 2023 USDM dataset is used as a

reference in this study because it depicts the operationally established drought conditions. Weekly USDM data over the product's entire period of record are available for download in KMZ, Shapefile, GML, WMS, GeoJSON, and IMG format. For this study, USDM data for January, April, July, and October of 2021 – 2023 were downloaded in shapefile format.

4.3 Methods

4.3.1 Location and Period of Interest

This study's analysis and results focus on January, April, July, and October of 2021 through 2023 in the contiguous U.S. This region was selected for study because of the wide array of precipitation regimes available for study as well as the prevalence of long- term, freely available, and serially complete precipitation datasets such as the climate divisional precipitation dataset. The 2021 through 2023 study period was selected so that the ability of each base period to capture modern day drought and pluvial conditions could be analyzed for a set of years not incorporated in any of the base periods used in this study.

4.3.2 Statistical Analysis

This study fits the 2-parameter Gamma probability distribution (Edwards and McKee, 1997) to a precipitation time series that is aggregated over 3- and 12-months, respectively, using four different months of interest (January, April, July, and October). These months and aggregation periods were selected so that both short- and long-term drought and pluvial events could be assessed across all seasons. This study uses the *fitdistrplus* package and the associated functions in R to fit the Gamma probability distribution to the eight precipitation time series associated with each base period studied (Table 2; Delignette-Muller and Dutang, 2015; R Core Team, 2023).

[Table 2]

Each base period shown in Table 2 is associated with a unique set of Gamma distribution

parameters, the shape and rate parameters, which are retrieved after the precipitation time series has been fitted to the Gamma probability distribution. The shape parameter controls the skewness of the distribution, with lower values indicating a more skewed distribution and higher absolute values indicating a more symmetrical distribution. A distribution with a positive skew indicates that there are more frequent low precipitation events and fewer but more intense high precipitation events, while a distribution with a negative skew suggests that high precipitation events are more frequent than low ones. In contrast, a distribution with a skew value equal to or approaching zero is symmetrical, reflective of a climate with more consistent rainfall patterns. Previous studies by Guo (2022) and Shen et al. (2016) provide additional insights on the relationship between skewness and other higher order statistics with precipitation frequency distributions.

The rate parameter influences the peak of the distribution, with higher absolute values indicating a narrower, more peaked distribution and lower values indicating a wider, and therefore more flat distribution. Changes in the shape and rate parameters amongst base periods are reflective of differing precipitation regimes amongst base periods, which in turn result in differing SPI values yielded by each.

4.3.3 Differential Drought Severity

This study explores the impact of variable precipitation regimes on the characterization drought and pluvial events in two ways: First, after calculating the SPI for the 2021 – 2023 study period, the values were categorized into the same drought severity levels used by the USDM (Table 1). Note that the same severity levels were applied to positive values of the SPI in order to categorize the pluvial values (Table 1). This process was repeated for each study period year and month of interest. The USDM maps associated with the same month and year of interest were

used as a reference, although this was done with caution, as the USDM product depicts both short- and long-term drought and uses several indicators to characterize drought beyond just the SPI.

Second, the effect of transitioning from base period 7 to base period 8 (Table 2) on drought and pluvial severity was analyzed by identifying climate divisions whose SPI values changed by showing a decrease in severity or switching from drought (pluvial) to neutral conditions, increased in severity or switched from neutral to drought (pluvial) conditions, or were equivalent between the two base periods. For the purposes of this study, SPI values that fell within the same drought or pluvial severity group shown in Table 1 were considered equivalent. This analysis was performed for both the 3- and 12- month SPI values for 2021 – 2023.

4.4 Results

4.4.1 Statistical Analysis

4.4.11 Changes in Precipitation Frequency Distributions

Figures 1 – 3 illustrate the 3- and 12-month July precipitation frequency distributions for climate divisions in California (Figure 1A and 1C), Texas (Figure 1B and 1D; Figure 2A and 2C), New York (Figure 2B and 2D), South Dakota (Figure 3A and 3C), and Ohio (Figure 3B and 3D). The vertical lines in each figure mark the average value of each distribution. The associated 3- and 12-month skew, standard deviation, and median values of each distribution are shown in Tables 3 and 4, respectively. These climate divisions were selected because the changes observed in their precipitation regimes amongst base periods and the resultant impact on drought and pluvial characterization (discussed below) are representative of the changes observed for other climate divisions across the U.S.

[Figure 1]
[Figure 2]
[Figure 3]

Distinct differences in the precipitation regimes associated with each base period are illustrated in Figures 1 – 3. For instance, in central California (Figure 1C) the 12-month results indicate that the frequency of above average precipitation has decreased from base period 1 to base period 8, and Table 4 shows that the median precipitation value has decreased as well (note that the vertical black lines in the figure denote the average value rather than the median). Additionally, the skew of each base period's distribution has steadily increased from base period 1 to base period 8, indicating that the frequency distributions are becoming increasingly more asymmetric (Table 4). In comparing the distribution of base period 8 with that of base period 1, it is apparent that the frequency of precipitation extremes on either end of the moisture spectrum have increased. This is also apparent at the 3-month scale (Figure 1A). Also evident at the 3-month scale is that the median precipitation magnitude has decreased from base period 1 to base period 8 (Table 3) while the skew has increased in accordance with the longer tail on the right side of the latter base periods. These longer tails to the right of the average value are indicative of a higher frequency of large magnitude precipitation events. Unlike at the 12-month scale, however, the frequency of the smallest precipitation magnitudes decreased for the latter base periods.

[Table 3]
[Table 4]

In the Texas Panhandle (Figure 1D) the 12-month results indicate that median precipitation value oscillates between 16.40 inches and 18.13 inches, and the skew of each distribution also varies amongst base periods, ranging between 0.71 and 0.15 (Table 4). In the context of precipitation extremes, distributions with a larger positive skew are more asymmetric in accordance with the longer tail on the right side, which is indicative of a higher frequency of large magnitude precipitation events. Still, base period 8 shows an increase in the frequency of the smallest

magnitude precipitation values. At the 3- month scale (Figure 1B), the frequency of below average precipitation magnitudes increased from base period 1 to base period 8, and the median value also decreased (Table 3). In contrast, the frequency of large magnitude precipitation events increased from base period 1 to base period 8, indicating that although the precipitation is decreasing overall, the occurrence of heavy precipitation events has increased.

In eastern Texas and Southeastern New York (Figure 2), the skewness of each distribution oscillates between negative and positive values amongst base periods (Table 4). For instance, at the 12-month scale base period 1 in New York has a skew of 0.87 while the skew of base period 8 is -0.11. This indicates that base period 1 had a higher frequency of small magnitude precipitation events and a lower frequency of large magnitude precipitation events relative to base period 8. This is also reflected by the larger median value of precipitation for base period 8 compared with base period 1, which increased from 40.65 to 46.52 inches (Table 4). Further, the negative skew of base period 8's distribution is indicative of a higher frequency of large magnitude precipitation events. At the 3-month scale the median precipitation magnitude has also increased from base period 1 to base period 8 (Table 3) and Figure 2B illustrates that the frequency of large magnitude precipitation events increased as well. In contrast, the frequency of the lowest magnitude precipitation events has decreased for the latter base periods.

In South Dakota, the distributions have widened for the latter base periods at both timescales, as is evident from the increase in standard deviation (Tables 3 and 4). At the 12-month timescale, the median precipitation increased from base period 1 to base period 8 and the distribution itself has become more symmetrical for the latter base periods (Figure 3C), indicative of more consistent rainfall patterns rather than a higher frequency of extremes on either end of the moisture spectrum. At the 3-month timescale, less variability is seen in the median precipitation

value from base period 1 to base period 8 (Table 3), although the latter base periods have become increasingly asymmetric over time and the frequency of both large and small precipitation magnitudes have increased (Figure 3A).

In central Ohio at the 12-month scale, a slight decrease in the median precipitation magnitude occurs from base period 1 to base period 8, the distribution has narrowed and has become more asymmetric as is evident by the changes in standard deviation and skewness values (Table 4). Figure 3D shows that the frequency of the largest magnitude precipitation events increased in base period 8 and the frequency of the lowest magnitude precipitation events decreased. At the 3-month timescale, the distribution has widened from base period 1 to base period 8 and the median precipitation magnitude has increased (Table 3). The increasingly negative skew values associated with the latter base periods are indicative of a higher frequency of large magnitude precipitation events and lower frequency of small magnitude precipitation events. This suggests a shift toward wetter conditions with fewer dry periods (Figure 3B).

4.4.12 Changes in Gamma Parameters

Tables 3 and 4 also provide the alpha and rate parameters associated with the precipitation frequency distributions shown in Figures 1 – 3. While the skew, standard deviation, and median values discussed above describe the shape of the precipitation frequency distributions, the alpha (also referred to as shape) and rate parameters describe the shape of each distribution after they have been fitted to the Gamma distribution.

Variability in the shape and rate parameters is therefore more directly relevant to the value of the SPI because the cumulative probability derived from the fitted Gamma distribution is what is transformed to the standard normal random variable (equivalent to the SPI).

[Figure 4]

Figure 4 illustrates the Gamma curves fit to the 3- and 12-month July precipitation frequency distributions, respectively, for climate division in 405 in central California and 3002 in southeast New York. Curves are plotted for all eight base periods. In California (Figure 4A and 4C) the fitted distributions have widened from base period 1 to base period 8 at both the 3- and 12-month timescale. Figure 4C illustrates a shift to the left from base period 1 to base period 8, indicating a shift toward lower precipitation values. In New York (Figure 4B and 4D), the distributions at both timescales also widened from base period 1 to 8. In contrast to the California curves, the latter base periods in New York shift to the right, indicating a shift toward higher precipitation values.

Figure 5 illustrates the Gamma curves fit to the 3- and 12-month July precipitation frequency distributions, respectively, for climate division 3905 in southwest South Dakota and 4101 in the Texas Panhandle. Curves are plotted for all eight base periods. In South Dakota at the 12-month timescale (Figure 5C), the fitted curve widened and shifted to the right when moving from base period 1 to base period 8, indicative of a shift toward larger precipitation values. At the 3-month timescale (Figure 5A), the distribution widened from base period 1 to base period 8 and shifted to the right, although to a lesser degree than what was seen at the 12-month timescale. In Texas (Figure 5B and 5D), the fitted Gamma curves maintained their shape from base period 1 to 8 at both timescales, although there is a shift to the left toward lower precipitation values when moving from base period 1 to 8 at both timescales.

[Figure 5]

4.4.2 Differential Drought Severity

4.4.21 Drought and Pluvial Severity by Base Period

Figure 6 illustrates the 3-month July drought and pluvial severity results yielded by each base

period for 2021 precipitation values. Also shown in Figure 6 is the July 2021 USDM drought map. Figure 6 shows that climate divisions in the Pacific Northwest have a lower drought severity for the later base periods, for instance from base period 6 to 8. In California, climate divisions yield a lower drought severity from base period 7 to 8. Drought severity increased in the eastern Dakotas for the later base periods. In the Southeast, pluvial severity decreased from base period 1 to 8. In comparing the drought severity maps yielded by base periods 7 and 8 with the USDM map for July 2021, areas of disagreement are seen in New Mexico, Arizona, and southern California wherein base periods 7 and 8 indicate above average precipitation where the USDM indicates extreme and exceptional drought. This is likely due to shorter term precipitation events ameliorating the longer-term drought conditions depicted by the USDM. Other areas of disagreement in terms of differing drought severities are seen in Minnesota, the eastern Dakotas, southern Nevada, western Colorado, and Utah.

[Figure 6]

Figure 7 illustrates the 12-month July drought and pluvial severity results yielded by each base period for 2021 precipitation values. Also shown in Figure 7 is the July 2021 USDM drought map. Base period 8 shows higher drought severities in the northern Midwest and High Plains as well as the New England area. Lower drought severities are seen in the results of base period 8 in southern California, Arizona, New Mexico, Colorado, and Texas. In comparing the drought severity maps yielded by base periods 7 and 8 with the USDM map for July 2021, areas of disagreement in terms of severity are seen in Arizona, the eastern Dakotas, western Minnesota, and northern Montana for base period 8. For base period 7, disagreement is seen in southwest New Mexico southern and eastern Montana, the eastern Dakotas, Minnesota, and northern Iowa.

[Figure 7]

4.4.22 Differing Drought and Pluvial Severity

Figures 8 and 9 illustrate changes in drought and pluvial severity levels when transitioning from the SPI results yielded by base period 7 to the results yielded by base period 8. Figure 8 provides the 3-month timescale results and Figure 9 the 12-month timescale results. Figure 8 shows that at the 3-month timescale in January and October, many climate divisions in the western U.S. transitioned from either neutral to pluvial conditions or transitioned to a higher pluvial severity value when switching from base period 7 to base period 8. This means that for these areas, the 3-month precipitation regimes of base period 8 were shifted toward smaller precipitation magnitudes as was demonstrated for representative climate division 405 in central California (Figure 1). Furthermore, in April, many climate divisions in the western and southwest part of the country transitioned either from drought to neutral or to lower severity drought values when transitioning from base period 7 to base period 8, which is also indicative of a shift toward lower precipitation magnitudes.

Also evident from Figure 8 is that in January, April, and July, many climate divisions in the High Plains either moved from neutral to drought conditions or transitioned to higher severity drought values when transitioning from base period 7 to base period 8. This suggests that these areas have precipitation regimes that shifted toward wetter conditions.

Representative climate division 3905 in southwest South Dakota (Figure 3A and 3C; Tables 3 and 4) demonstrated changes in the precipitation frequency supporting the results of Figure 8 such as the increase in median precipitation value for the latter base periods and a widening of the distribution.

[Figure 8]

In April and July, climate divisions in parts of the Northeast, Midwest, and Southeast indicated a shift toward either lower severity pluvial or pluvial to neutral conditions. This suggests that these divisions shifted toward wetter conditions from base period 7 to base period 8. Representative climate division 3002 in southeast New York (Figure 2B and 2D; Tables 3 and 4) demonstrated changes in the precipitation frequency supporting the results of Figure 8 such as the increase in median precipitation value for the latter base periods, the negative skew value for the latter base periods, and the decreasing frequency of the lowest magnitude precipitation events.

[Figure 9]

At the 12-month timescale (Figure 9), the results for July and October indicate that many climate divisions in the western part of the country transitioned either from drought to neutral conditions or decreased in drought severity. This is indicative of drier conditions in base period 8 relative to base period 7. For April, July, and October, climate divisions in the High Plains, Midwest, and parts of the southeast transitioned either from neutral to drought or to higher severity drought conditions from base period 7 to base period 8. This is indicative of wetter conditions in base period 8 relative to base period 7 for these climate divisions. Also for these months, climate divisions in the Northeast shifted toward either lower severity pluvial or from pluvial to neutral conditions, indicating that the 12- month precipitation frequency distributions of these areas were wetter in base period 8 than in base period 7.

4.5 Discussion

The results of this study revealed that the variability in the precipitation regimes amongst the eight 30-year base periods analyzed had an impact on modern-day drought and pluvial values, despite each of these base periods having 20 years of precipitation data in common. In the parts of the country that became drier (wetter) from base period 7 to base period 8, drought was

characterized as less (more) severe. These results are supported by similar studies investigating the impact of base period selection on the quantification of precipitation extremes. For instance, Thomas et al. (2023) found that updating the base period from 1981-2010 to 1991-2020 resulted in the detection of fewer very wet days in the southwestern U.S. Likewise in Europe, Cammalleri et al. (2022) found that the 1981 – 2010 base period yielded differing drought classifications than those yielded by the 1991 – 2020 base period.

These findings call into question the reliability of the SPI for drought assessment in the context of a changing climate.

4.6 Conclusion

In the operational drought monitoring setting, the current practice of accounting for nonstationarity in our climate is the use of 30-year moving windows that are updated every 10 years. In recognizing the prevalence of this approach, this study evaluated the extent to which the assessment of modern-day drought and pluvial conditions in the U.S. are impacted by the choice of base period used in calculating the SPI at the climate divisional scale. The approach involved using a series of eight 30-year moving windows as base periods, ranging from 1920-1950 to 1990 – 2020 to calculate the SPI over the 2021 – 2023 timeframe. It was found that climate divisions in the West, Southwest, and parts of the Southern U.S. have shifted toward drier conditions, divisions in the northeast toward wetter conditions. These changes were observed by analyzing the underlying precipitation frequency distributions and the associated median values, standard deviations, and skew values. Changes in the underlying frequency distributions were found to impact modern-day drought characterization by evaluating differences in drought/pluvial severity values yielded by base period 7 and base period 8. Results indicated that when transitioning from base period 7 to 8, drought in the western, southwestern, and parts of the

Midwest was characterized as either lower severity drought or even neutral conditions. Climate divisions in parts of the Northeast, Midwest, and Southeast indicated a shift toward either lower severity pluvial conditions or from pluvial conditions to neutral conditions. Climate divisions in the High Plains, Midwest, and parts of the southeast transitioned either from neutral to drought or to higher severity drought conditions from base period 7 to base period 8. Climate divisions in the Northeast shifted toward either lower severity pluvial conditions or from pluvial conditions to neutral conditions.

4.7 References

Cammalleri, C., J. Spinoni, P. Barbosa, A. Toreti, and J. V. Vogt, 2022: The effects of non-stationarity on SPI for operational drought monitoring in Europe. Int. J. Climatol., 42, 3418–3430, https://doi.org/10.1002/joc.7424.

Delignette-Muller, M.L. and Dutang, C., 2015: fitdistrplus: An R Package for Fitting Distributions. Journal of Statistical Software, 64(4), 1-34. URL: http://www.jstatsoft.org/v64/i04/.

Edwards, D.C. and McKee, T.B., 1997: Characteristics of 20th Century Drought in the United States at Multiple Time Scales. Climatology Report 97-2, Department of Atmospheric Science, Colorado State University, Fort Collins, CO, 155pp.

Guo T., 2022: Extreme Precipitation Strongly Impacts the Interaction of Skewness and Kurtosis of Annual Precipitation Distribution on the Qinghai–Tibetan Plateau. Atmosphere. 13(11):1857. https://doi.org/10.3390/atmos13111857

Guttman N.B., 1999. Accepting the standardized precipitation index: a calculation algorithm. *JAWRA* **35** (2): 311–322.

Hoylman, Z.H., R.K. Bocinsky, K.G. Jencso, 2022: Drought assessment has been outpaced by climate change: Empirical arguments for a paradigm shift. Nature Communications, 13, p. 2715

McKee, T. B., N. J. Doesken, and J. Kleist, 1993: The relationship of drought frequency and duration to time scales. Eighth Conf. on Applied Climatology, Anaheim, CA, Amer. Meteor. Soc., 179–183.

NOAA National Centers for Environmental Information, Monthly Drought Report for July 2023, published online August 2023, retrieved on March 18, 2024 from https://www.ncei.noaa.gov/access/monitoring/monthly-report/drought/202307

Quiring SM., 2009: Developing objective operational definitions for monitoring drought. J Appl Meteorol Climatol. 48: 1217–29. http://journals.ametsoc.org/doi/abs/10.1175/2009JAMC2088.1.

R Core Team, 2022: _R: A Language and Environment for Statistical Computing_. R Foundation for Statistical Computing, Vienna, Austria. <https://www.R-project.org/>.

Shen, S.S.P., Wied, O., Weithmann, A. et al., 2016: Six temperature and precipitation regimes of the contiguous United States between 1895 and 2010: a statistical inference study. Theor Appl Climatol 125, 197–211. https://doi.org/10.1007/s00704-015-1502-2

Spade D., Beurs K., Shafer M., 2020: Major over- and underestimation of drought found in NOAA's climate divisional SPI dataset. J Appl Meteorol Climatol 59:1469–1480

Stagge, J. H., and K. Sung, 2022: A Nonstationary Standardized Precipitation Index (NSPI) Using Bayesian Splines. J. Appl. Meteor. Climatol., 61, 761–779, https://doi.org/10.1175/JAMC-

D-21-0244.1.

Svoboda, M., D. Lecomte, M. Hayes, R. Heim, K. Gleason, J. Angel, B. Rippey, R. Tinker, M. Palecki, D. Stooksbury, D. Miskus and S. Stephens, 2002: The drought monitor. Bulletin of the American Meteorological Society, 83(8):1181–1190

Svoboda, M., Fuchs, B., and Integrated Drought Management Programme (IDMP), 2016: Handbook of Drought Indicators and Indices. Drought Mitigation Center Faculty Publications. 117. http://digitalcommons.unl.edu/droughtfacpub/117

Thomas, N. P., Marquardt Collow, A. B., Bosilovich, M. G., & Dezfuli, A., 2023: Effect of baseline period on quantification of climate extremes over the United States. Geophysical Research Letters, 50, e2023GL105204. https://doi.org/10.1029/2023GL105204

Vose, R.S., Applequist, S., Squires, M., Durre, I., Menne, M.J., Williams, C.N., Jr., Fenimore, C., Gleason, K., Arndt, D., 2014a. NOAA's Gridded Climate Divisional Dataset (CLIMDIV). NOAA National Climatic Data Center. doi:10.7289/V5M32STR

Vose, R.S., Applequist, S., Squires, M., Durre, I., Menne, M.J., and Coauthors, 2014b: Improved historical temperature and precipitation time series for U.S. climate divisions. J. Appl. Meteor. Climatol., 53, 1232-1251. doi: 10.1175/JAMC-D-13-0248.1

Wu, H., Hayes, M.J., Wilhite, D.A. and Svoboda, M.D., 2005: The Effect of Length of Record on the Standardized Precipitation Index. Int. J. Climatol. 25, 505-520. doi: 10.1002/joc.1142

Wu, H., Svoboda, M.D., Hayes, M.J., Wilhite, D.A., and Wen, F., 2007. Appropriate application of the Standardized Precipitation Index in arid locations and dry seasons. Int. J. Climatol. 27, 65-79. doi: 10.1002/joc.1371

4.8 Figures and Tables

Table 1: U.S. Drought Monitor severity levels and associated SPI values. Note that P0 through P4 are not utilized by the Drought Monitor and these pluvial categories were created for the purposes of this study.

USDM Category	Values for SPI
D0	-0.5 to -0.79
D1	-0.8 to -1.29
D2	-1.3 to -1.59
D3	-1.6 to -1.99
D4	-2.0 or less
P0	0.5 to 0.79
P1	0.8 to 1.29
P2	1.3 to 1.59
P3	1.6 to 1.99
P4	2.0 or greater

Table 2: Base periods used in calculating the SPI.

Base Period	Year Range
1	1920-1950
2	1930-1960
3	1940-1970
4	1950-1980
5	1960-1990
6	1970-2000
7	1980-2010
8	1990-2020

Figure 1: 3- and 12-month July precipitation frequency distributions for climate divisions 0405 and 4101.

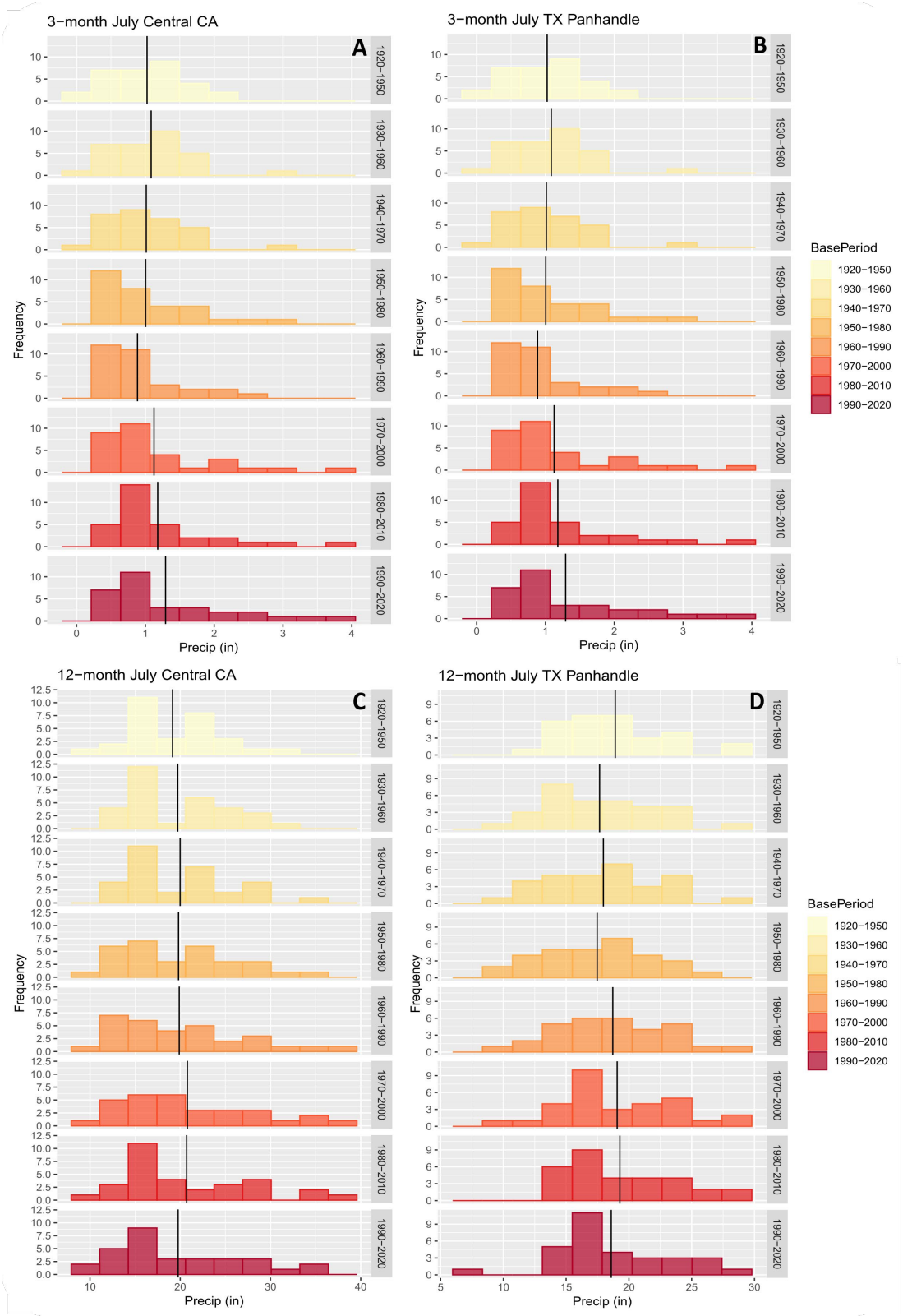

Figure 2: 3- and 12-month July precipitation frequency distributions for climate divisions 4104 and 3002.

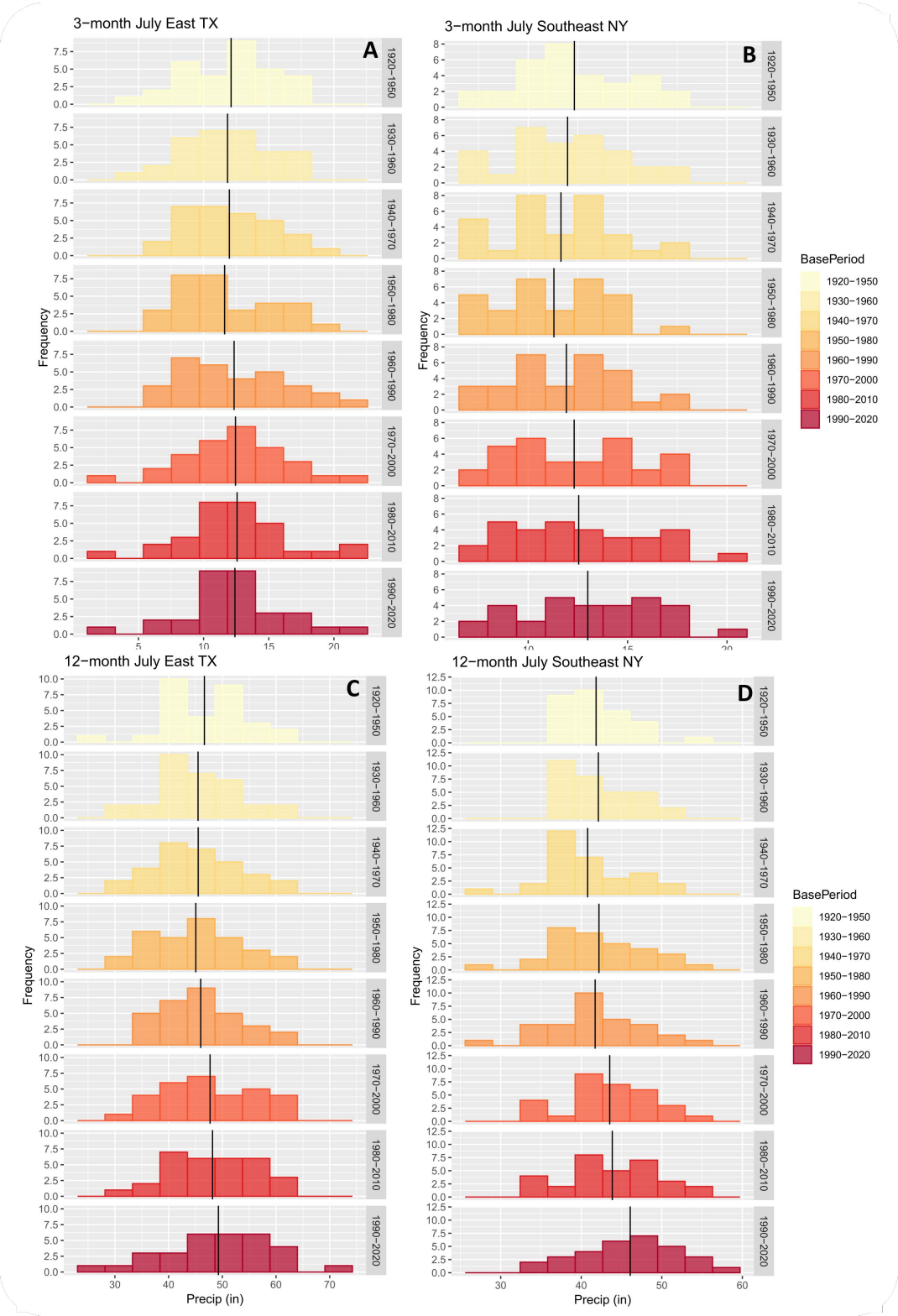

Figure 3: 3- and 12-month July precipitation frequency distributions for climate divisions 4803 and 3305.

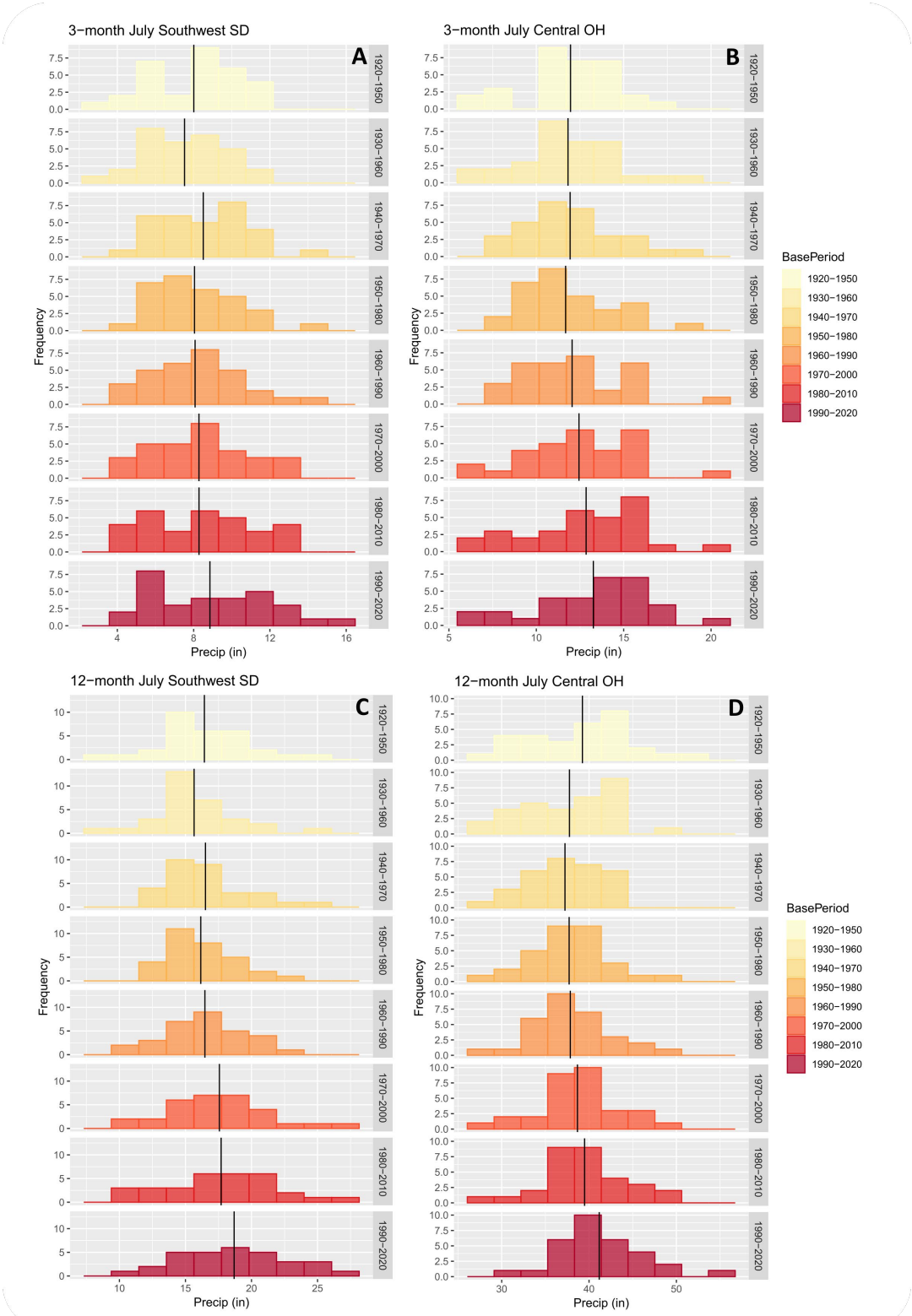

Table 3: Table of 3-month skew, standard deviation, median, alpha and rate parameters associated with the precipitation frequency distributions shown in Figures 1 – 3.

3-month Central CA (405)					
Base Period	**Skew**	**Standard Deviation**	**Median**	**alpha**	**rate**
1	0.01	0.55	1.01	2.55	2.49
2	0.77	0.63	1.12	2.64	2.43
3	1.2	0.61	0.88	2.95	2.91
4	1.25	0.69	0.71	2.53	2.52
5	1.38	0.56	0.71	3.19	3.6
6	1.7	0.85	0.81	2.42	2.15
7	1.7	0.83	0.91	2.65	2.24
8	1.17	0.95	0.86	2.14	1.65
3-month East TX (4104)					
1	-0.2	3.37	13.01	11.71	0.97
2	0.09	3.3	11.32	12.44	1.05
3	0.37	3.26	11.74	13.9	1.16
4	0.51	3.49	10.47	11.84	1.02
5	0.58	4.17	11.74	9.32	0.76
6	0.16	4.06	12.68	8.3	0.67
7	0.38	4.1	12.6	8.56	0.68
8	0.02	3.75	12.49	9.35	0.75
3-month Southwest SD (3905)					
1	-0.24	2.43	8.48	9.6	1.2
2	-0.01	2.16	7.6	11.32	1.51
3	0.4	2.38	8.49	12.93	1.52
4	0.77	2.33	7.79	12.99	1.61
5	0.58	2.51	8.28	10.77	1.33
6	0.23	2.49	8.3	10.91	1.32
7	0.06	2.8	8.39	8.2	0.99
8	0.24	3.1	8.74	7.91	0.89
3-month TX Panhandle (4101)					
1	1.13	2.76	7.52	8.81	1.15
2	0.99	2.75	7.52	8.39	1.11
3	0.63	2.77	8.35	8.38	1.06
4	-0.2	2.25	8.39	10.75	1.4
5	-0.23	2.22	8.66	11.15	1.44
6	-0.23	2.26	8.07	10.25	1.34
7	-0.09	2.09	7.81	12.22	1.61
8	0.32	2.54	7.25	6.72	0.94
3-month East NY (3002)					
1	-0.01	2.79	11.86	18.88	1.53
2	-0.02	2.83	11.86	17.33	1.45
3	0.04	2.85	11.33	16.17	1.39
4	-0.02	2.67	11.23	17.34	1.54
5	0.02	2.85	11.5	16.88	1.42
6	0.18	3.09	11.5	16.15	1.31
7	0.29	3.3	12.03	14.83	1.18
8	-0.01	3.29	13.23	15.23	1.17
3-month Central OH (3305)					
1	-0.62	2.84	12.27	15.27	1.28
2	0	3.01	11.7	14.51	1.23
3	0.53	2.8	11.7	19.21	1.61
4	0.77	2.71	10.87	20.36	1.74
5	0.51	2.96	11.84	17.57	1.46
6	0.01	3.11	12.58	15.39	1.24
7	-0.3	3.36	13.19	13.36	1.04
8	-0.52	3.26	13.72	14.57	1.1

Table 4: Table of 12-month skew, standard deviation, median, alpha and rate parameters for the precipitation frequency distributions shown in Figures 1 – 3.

12-month Central CA (405)					
Base Period	**Skew**	**Standard Deviation**	**Median**	**alpha**	**rate**
1	0.33	5.05	18.65	14.73	0.77
2	0.43	5.53	17.33	13.48	0.68
3	0.77	5.81	17.79	13.17	0.66
4	0.59	6.59	17.79	9.67	0.49
5	0.86	7.37	17.79	8.25	0.41
6	0.7	7.49	19.32	8.43	0.41
7	0.84	7.17	17.65	9.5	0.46
8	0.7	7	16.98	8.78	0.44
12-month East TX (4104)					
1	-0.26	7.92	48.04	32.86	0.7
2	0.45	7.65	44.03	37.25	0.82
3	0.38	8.3	43.99	31.51	0.69
4	0.37	8.65	43.99	28.5	0.63
5	0.46	7.73	44.11	37.46	0.81
6	0.05	8.71	46.12	30.38	0.64
7	-0.16	7.76	48.42	38.24	0.79
8	-0.29	9.76	49.13	23.97	0.49
12-month Southwest SD (3905)					
1	0.21	3.43	16.54	22.89	1.39
2	0.43	3.07	15.4	26.45	1.69
3	0.84	2.91	16.4	35.39	2.14
4	0.5	2.58	15.82	41.55	2.57
5	0.02	3.08	16.4	28.4	1.72
6	0.39	3.8	17.51	21.97	1.25
7	-0.02	4.26	17.75	16.65	0.94
8	0.03	4.21	18.74	19.24	1.03
12-month TX Panhandle (4101)					
1	0.71	4.16	18.13	22.62	1.2
2	0.61	4.33	16.4	17.78	1.01
3	0.37	4.41	17.91	17.07	0.95
4	0.15	4.13	17.57	17.87	1.02
5	0.25	4.34	17.92	18.96	1.01
6	0.38	4.53	17.55	18.44	0.97
7	0.53	4.41	17.88	20.66	1.07
8	0.25	4.65	17.35	15.72	0.85
12-month East NY (3002)					
1	0.87	4.12	40.65	107.79	2.58
2	0.61	4.53	40.91	92.38	2.19
3	0.15	5.49	40.36	56.34	1.38
4	0	6.11	42.27	47.89	1.13
5	-0.03	6.05	41.2	47.62	1.14
6	-0.06	5.66	43.21	59.65	1.37
7	-0.01	6.15	42.94	51.44	1.17
8	-0.11	6.32	46.52	53.23	1.16
12-month Central OH (3305)					
1	0.03	5.88	40.47	44.98	1.15
2	-0.27	5.13	39.09	53.6	1.42
3	-0.45	4.1	37.66	81.46	2.19
4	0.1	4.41	37.93	74.87	1.99
5	0.33	4.6	37.43	70.57	1.86
6	-0.05	4.74	38.73	66.97	1.73
7	0.05	4.99	39.18	63.27	1.6
8	0.63	4.95	39.97	73.33	1.78

Figure 4: 3- and 12-month July probability density distributions for climate divisions 0405 and 3002.

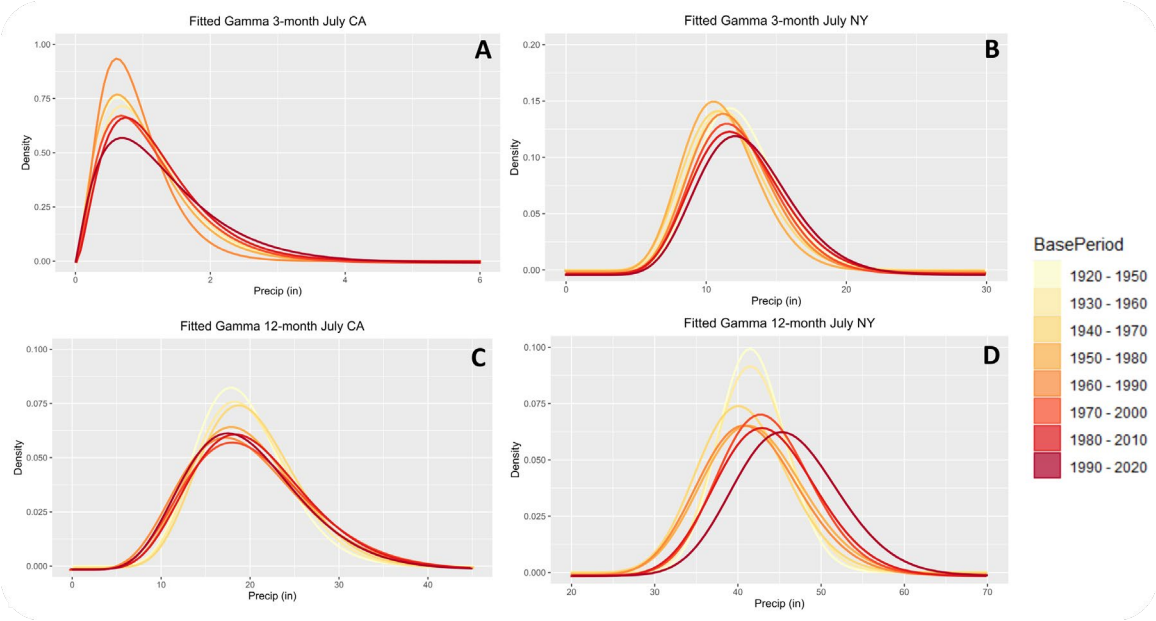

Figure 5: 3- and 12-month July probability density distributions for climate divisions 3905 and 4101.

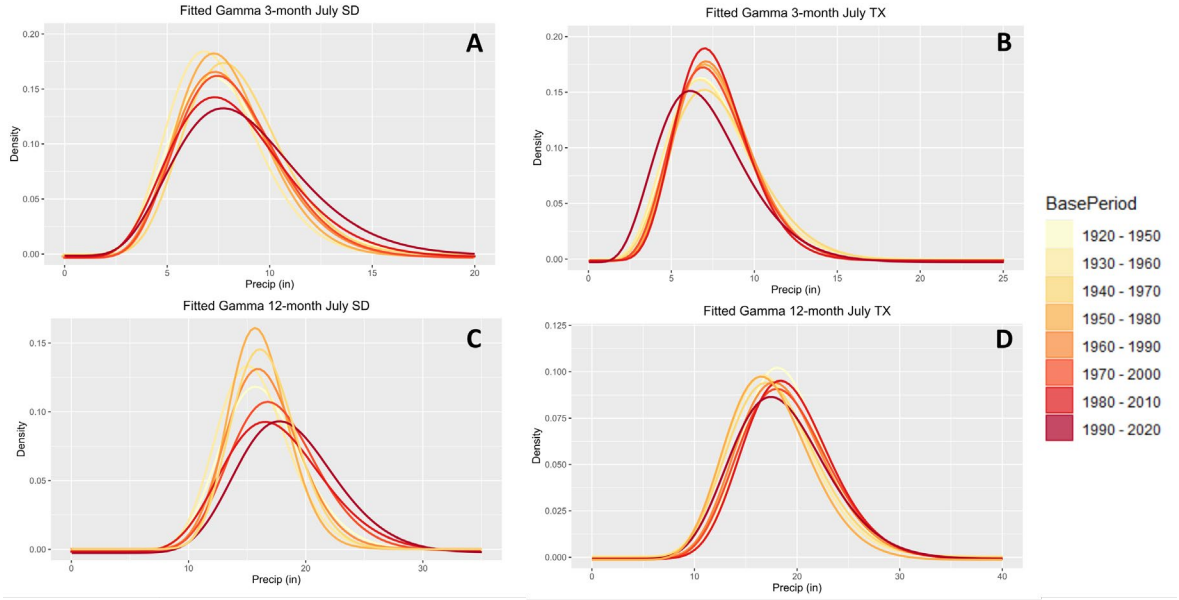

Figure 6: 3-month July drought severity maps for each base period for July 2021. The lowermost panel illustrates the July 2021 USDM map.

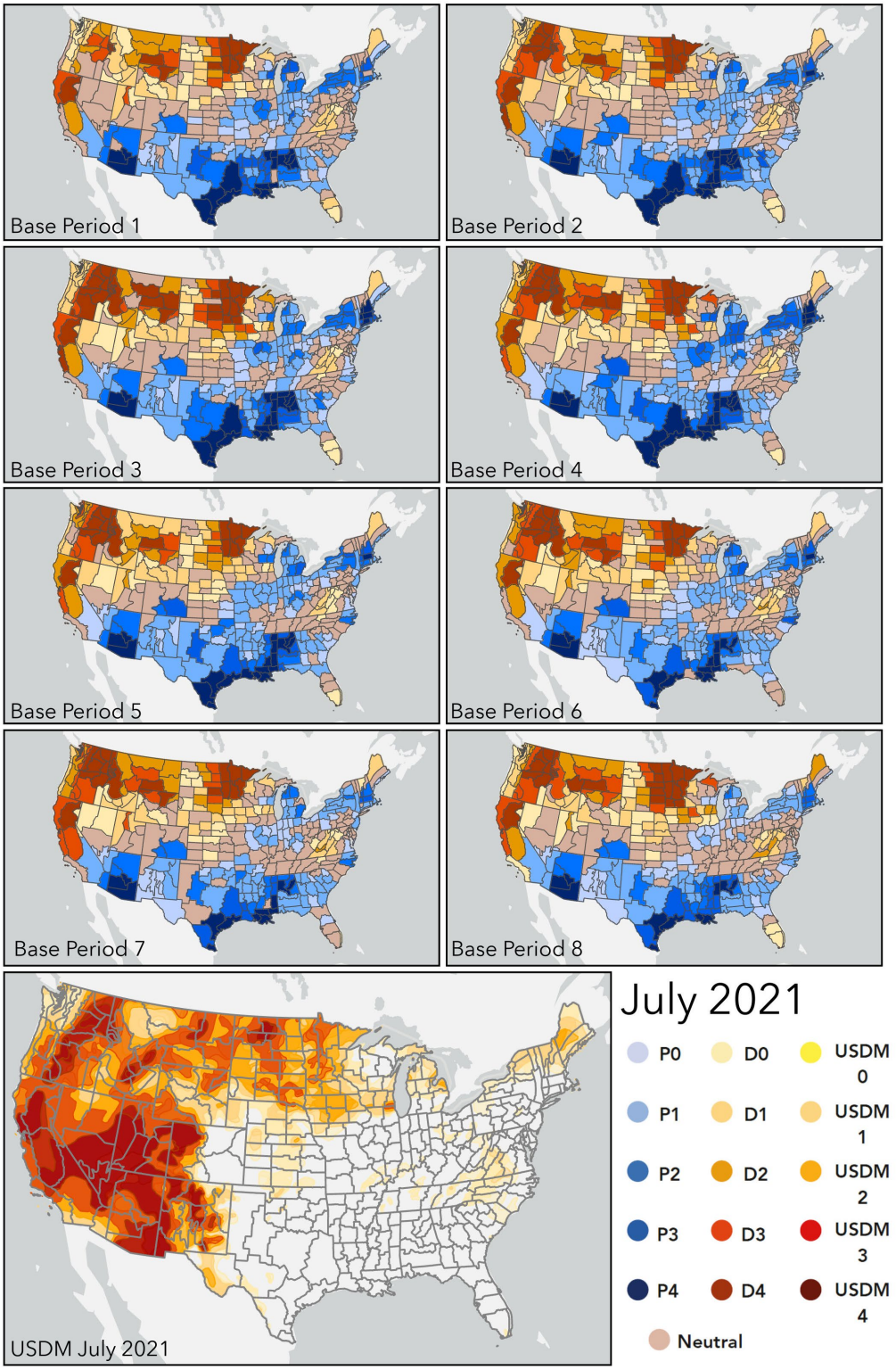

Figure 7: 12-month July drought severity maps for each base period for July 2021. The lowermost panel illustrates the July 2021 USDM map.

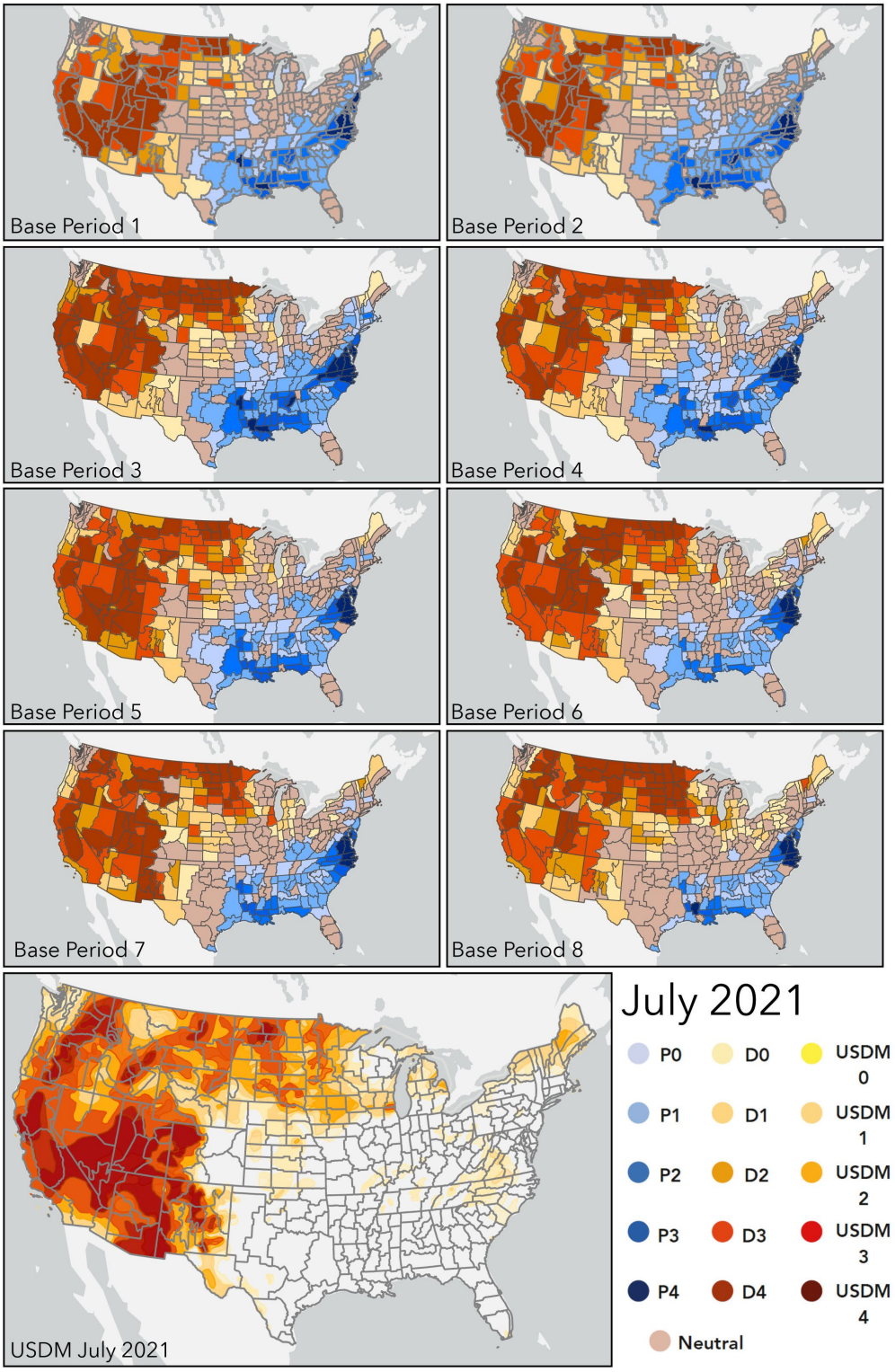

Figure 8: Differential drought severity between base period 7 and base period 8 according to the 3-month SPI.

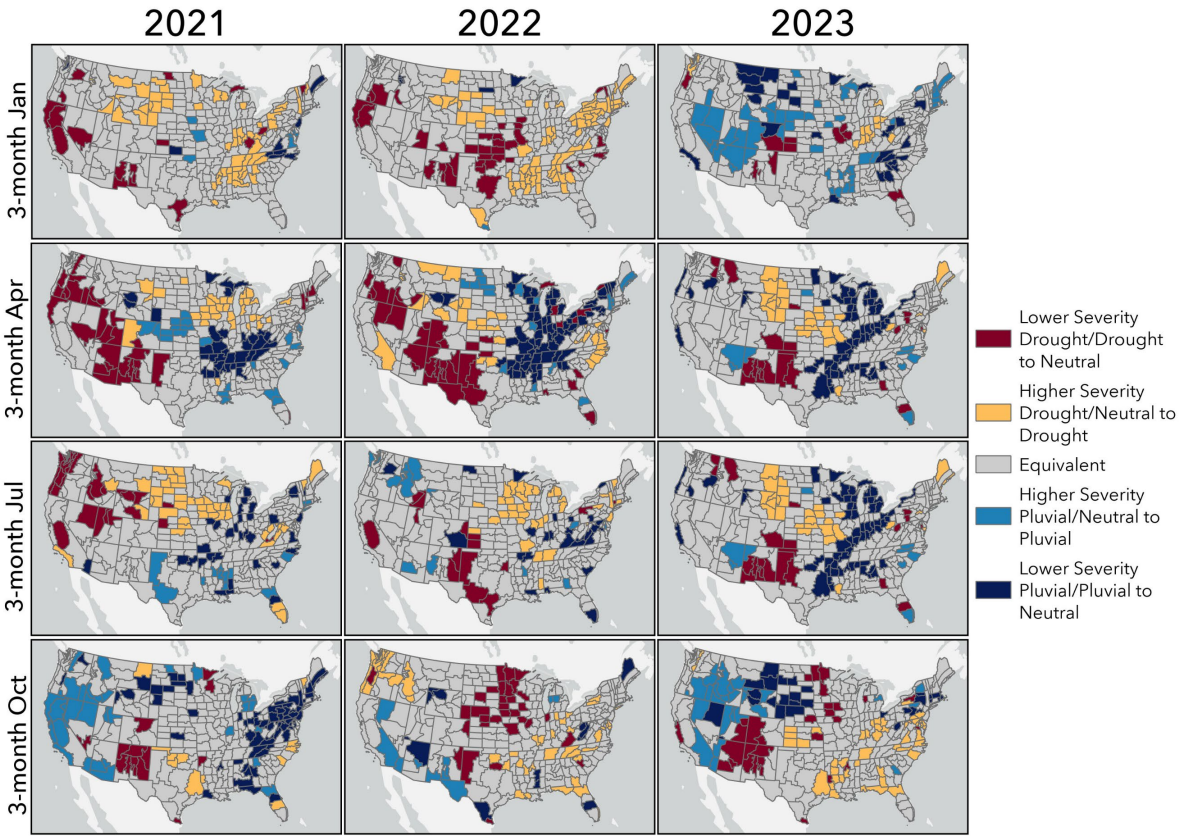

Figure 9: Differential drought severity between base period 7 and base period 8 according to the 12-month SPI.

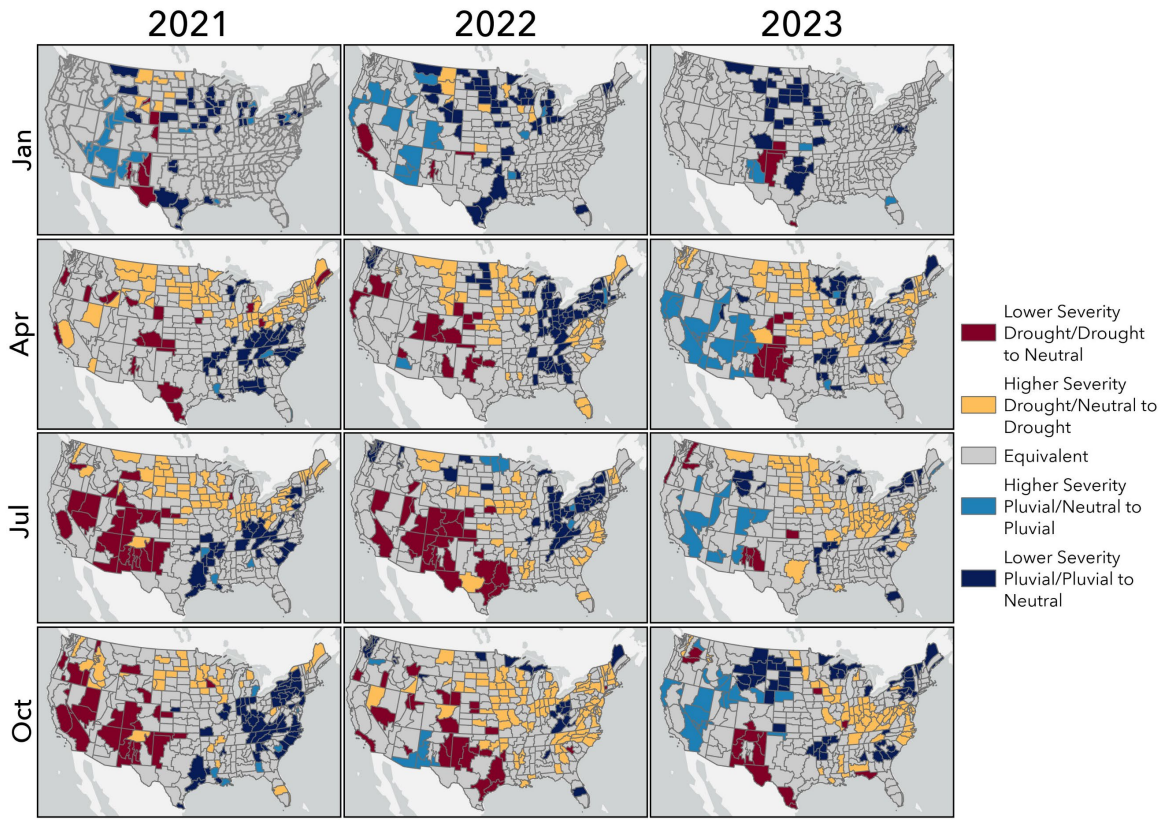

CHAPTER 5: CONCLUSION

The regional subjectivity of drought is perhaps one of its most complicating factors, and is a driving force behind the vast array of indices used to monitor its onset and severity. However, as discussed in Chapter 1, rather than continuing to develop new indices to monitor different aspects of drought, the scientific community should instead focus on improving the monitoring tools already in circulation. The SPI is one of the most prevalent drought indices in circulation both operationally and in the research setting because it requires only precipitation data to be computed, it can be calculated at various time scales, and it is normalized with respect to location, allowing it to be comparable across regions with different climates. Further, the index only requires precipitation data to be computed and the computational procedure is far less complex than other common drought indices such as the Palmer Drought Severity Index (PDSI) or the Standardized Precipitation Evapotranspiration Index (SPEI). Nonetheless, the results of this dissertation shed light on a major weakness of the SPI, especially in the context of a changing climate, and that is its sensitivity to the base period used as a climatologically representative reference frame. The occurrence and apparent severity of a drought event according to the SPI is dependent on this reference frame.

One major factor that the drought monitoring community must contend with is the issue of stationarity, or the lack thereof, in our global climate. Stationarity is the assumption that environmental variables fluctuate within a static envelope of variability and can be modeled with a time-invariant probability density function estimated from the instrumental record. This assumption is pervasive in drought monitoring. Thus, in the context of a changing climate, drought monitoring specialists must use careful consideration when selecting the base period to use as reference. This concept is an emerging area of research in the contemporary drought

monitoring community, as its implications are relevant not only to the field of climatology, but also to water managers, community planners, and to the broader scientific community. The impact of base period selection on the SPI's ability to capture drought occurrence and severity was explored throughout this dissertation through addressing three research questions:

1. How do operational SPI databases, such as those used by the NCEI, compare to research databases?
2. Does the choice of base period impact the severity and frequency of drought events according to the SPI?
3. How does transitioning between base periods impact contemporary drought characterization?

Question 1 is explored in Chapter 2 of this dissertation. The metadata associated with the NCEI-maintained SPI database cites a static base period of 1931 – 1990. A major benefit of the SPI is that its statistical framework serves as a predictor for the anticipated drought frequency over the base period selected for reference. Recalling that the SPI is based on a transformation of the probability distribution function modelling the precipitation regime to the standard normal distribution, abnormally dry and wet conditions are expected roughly 16% of the base period, respectively, and average conditions roughly 68% of the base period. However, the results of Chapter 2 illustrated that the NCEI's SPI database is over-representing drought in certain parts of the U.S. and under-representing drought in other parts of the country. Consultation with the database's point of contact revealed that the reason for the apparent dry and wet biases over the base period was due to a miscommunication in the metadata file. That is, the base period associated with the database is in fact the full period of record, which expands on an annual basis.

This sliding scale approach to calculating the SPI means that there is no fixed baseline associated with the dataset because it is updated every year. The lack of a standard baseline renders the NCEI SPI database unusable as a research tool because the baseline expands annually as new precipitation data is collected; consequently, it is impossible to accurately compare across studies as they each may be comparing against different historical records. Further, it becomes impossible to use the dataset to identify changes in frequency of occurrence or intensity of drought because that necessitates comparing present anomalies with an established baseline to assess change, such as departure from 20th-century average (e.g., IPCC, National Climate Assessment, and NCEI State of the Climate Report).

Based on the analysis of Chapter 2, the NCEI SPI database is not recommended for assessing changes in drought frequency or severity, nor is it recommended for use in research because the SPI values change yearly as their underlying base period is updated. For example, in 1934 climate division 2503 in Nebraska has a 6-month September SPI value of −1.35 based on a 1931–90 base period, −1.62 based on an 1895–2009 base period, and −1.58 based on an 1895–2019 period. Thus, the only way for different studies using this data to be comparable would be if the respective authors happened to download the dataset in the same year. Further, this database is not recommended for operational drought monitoring because the SPI values are being influenced by precipitation regimes from 1895 to present, and in the context of a nonstationary climate, time periods in the late 19th and earlier 20th centuries are not representative of modern-day climate. For example, the values of the SPI might indicate a higher drought severity than what is being experienced by the region impacted. Alternatively, the index might underestimate drought severity, which could result in the impacted region neglecting to take precautions such as water restrictions.

This concept was explored further in Chapter 3 through an evaluation of drought frequency and severity according to eight different SPI timeseries, each associated with a distinct 30-year base period, ranging from 1920 – 1950 to 1990 – 2020. This moving 30-year window approach to investigating the sensitivity of the SPI to its underlying base period illustrated why the SPI's sensitivity to its underlying base period is a distinct weakness of the index. For instance, in the High Plains, Midwest, Northeast, and Southern regions of the U.S., the older base periods tended to yield SPI values that are less severe than the newer base periods during times of drought. In contrast, in the Western and Southeast regions, the older base periods tended to yield SPI values more severe than the newer base periods during times of drought. The results of this chapter further complicate the task of operational drought monitoring because they call into question the appropriate selection of reference frame to use. For instance, a biologist investigating the relationship between land cover change and drought must consider which reference frame is appropriate to use. Unfortunately, the answer to this question based on the results of Chapter 3 is that it depends. If the object of the study is to establish a relationship between recent drought events and land cover change, then a base period coinciding with the current Climate Normal might be ideal. However, if the goal is to investigate land cover changes associated with historic drought events such as the Dust Bowl, this would necessitate a base period incorporating precipitation data from the 1930s. If the goal is to compare land cover changes associated historic drought events to land cover change associated with modern day drought, this would necessitate a longer base period that incorporates both historic and modern precipitation data. However, based on the results of Chapter 3, the modern-day drought severity would either be over- or under-estimated, depending on the region.

Another item for consideration when using the SPI as a research tool is that the ability of the

index to capture drought occurrence is also dependent on the base period selected. In the Midwest region, for example, the climate was found to be trending toward wetter conditions when moving from earlier to more recent base periods, and in this region the lattermost base period analyzed (1990 – 2020) captured 14 drought events at the 12-month SPI timescale over the 2000 – 2020 time period whereas the earliest base period analyzed (1920 – 1950) did not capture any drought events over that time period. In contrast, the climate of the Southeast region is trending toward drier conditions when moving from earlier to more recent base periods. In the Southeast region, one of the newer base periods (1980 – 2010) captured 10 drought events over the 2000 – 2020 time period whereas the 1920 – 1950 base period captured 18 drought events over the same period.

Fundamentally, the results of Chapter 3 demonstrated that in regions where the climate is trending toward drier conditions, the index is less likely to detect drought and in regions where the climate is trending toward wetter conditions, the SPI is more likely to detect drought. Precipitation trends are at the core of any discrepancies observed among SPI values derived using different base periods, and the third and final research question of this dissertation built off of these findings by investigating the impact on drought characterization when transitioning between the two most recent base periods in order to investigate how contemporary precipitation trends are impacting operational drought monitoring. Results demonstrated that drought characterization changes even when transitioning between base periods sharing 20 years of precipitation data, that is base periods 1980 – 2010 and 1990 – 2020. The impact of transitioning to the latter base period on drought and pluvial severity was analyzed by identifying climate divisions whose SPI values changed in any of the following three ways:

- Climate division showed a decrease in severity or switched from drought/pluvial to

neutral conditions.

- Climate division showed an increase in severity or switched from neutral to drought/pluvial conditions.
- Climate division showed equivalent values between the two base periods.

Results indicated that in the Western U.S., a region becoming drier, climate divisions either transitioned to a lower drought severity level or to neutral. In contrast, climate divisions in the northern High Plains and eastern U.S., regions which have become wetter, climate divisions either transitioned to a higher drought severity level or switched from neutral to drought. Thus, even with 20 years of overlapping precipitation data, the SPI's characterization of drought changes considerably between base periods.

Based on the results of the research questions explored in this dissertation, the following questions warrant further discussion in the drought monitoring literature:

1. What base period is recommended for operational drought monitoring? Does this differ from the base period recommended for researching climate change?
2. What update frequency between base periods is recommended?
3. Given the sensitivity of the SPI to the base period selected, should it continue to be used for operational drought monitoring?

Given that the primary goal of operational drought monitoring is to identify drought severity, or the departure from "normal conditions", a base period coinciding with the current Climate Normal is recommended for operational drought monitoring. As demonstrated in Chapters 2 and 3, long-term trends can affect baseline "normal" weather conditions. Furthermore, emergency drought recovery programs offered to farmers and ranchers through the U.S. Department of Agriculture are automatically triggered once a certain level of drought severity according to the

U.S. Drought Monitor (USDM) is maintained for a certain number of weeks. Although the USDM incorporates a blend of multiple drought indices, including the SPI, the point stands that the accurate portrayal of drought severity is paramount.

The purpose of using 30-year normals is to understand present-day conditions rather than long-term trends. In contrast to operational drought monitoring, when studying long-term changes in climate, longer periods are recommended, such as a twentieth century benchmark. Further, using a twentieth century base period offers consistency as conditions change over time and the findings are not subject to updates every 10 years.

Regarding the update frequency between base periods, the findings of Chapter 4 demonstrated that a 10-year update frequency does not keep pace with the rate at which precipitation regimes are changing across the U.S. That is, values of the SPI show a steep change when updating between base periods, including switching from neutral to drought/pluvial and vice versa or increasing/decreasing in severity levels used by the U.S. Drought Monitor. Based on these findings, a 5-year update frequency is recommended in order to mitigate the impacts of non-stationary precipitation regimes.

The results of this dissertation demonstrate that "normal" is nonstationary, and this influences the characterization of drought by the SPI. Should the scientific community continue using the SPI, or should we consider moving away from this tool?

Undoubtedly, the SPI has limitations that require careful consideration before opting to use this index as a tool for research or operational drought monitoring. For instance, the SPI does not account for temperature or evapotranspiration, both of which impact drought occurrence and severity. Given that temperature trends are also changing across the U.S., this shortcoming presents a major blind spot of the SPI in that it is only considering one piece of the puzzle. The

sensitivity of the index to its underlying base period is also a noteworthy shortcoming of the SPI, as this further complicates the nature of drought. Nonetheless, the SPI has several benefits that support its continued use despite its shortcomings, as long as these are taken into consideration. The SPI offers modest data requirements, it is multiscaler, regionally comparative, and it succinctly classifies moisture conditions on a standardized scale. Thus, the overall recommendation based on the findings of this dissertation is that the SPI continue to be used operationally and as a research tool, however a clear understanding of the underlying base period used for reference is critical, as this period controls contemporary drought characterization.